UNIVERSITY OF JORDAN
Faculty of Graduate studies

Testing and Performance of a Locally Manufactured Glassfiber Reinforced Plastic Wind Turbind Blade

By

Isaac Ali Saleh

Supervisor
Dr. Saad Habali

SUBMITTED IN PARTIAL FULFILLMENT OF THE REQUIREMENTS FOR THE DEGREE OF MASTER OF SCIENCE IN MECHANICAL ENGINEERING

Faculty of Graduate Studies
University of Jordan

March 1994

The examining committee unanimously considers this thesis satisfactory for the degree of master of science in mechanical engineering.

COMMITTEE MEMBERS	SIGNATURE
1. Dr. Saad Habali Mechanical Engineering Department University of Jordan	Committee Chairman J. Habali 04/13/94
2. Dr. Bassam Jubran Mechanical Engineering Department University of Jordan	Committee Member B. Jubran 04/13/94
3. Dr. Mohammad Dado Mechanical Engineering Department University of Jordan	Committee Member Mohd H. Dado 04/13/94

Acknowledgments

I would like to thank the Mechanical Engineering Department at the University of Jordan , especially my supervisor Dr. Saad Habali for his valuable assistance and patients and the much needed instructions throughout this study.

The author would like to acknowledge with greate appreciation the support and encouragement from the Royal Scientific Society represented by its president Dr. Hani El-Mulki and the director of the Renewable Energy Research Center Dr. Rizeq Ta'ani where all of this work had taken place.

Also my great gratitude is due to my colleagues at the wind energy section Dr. Mohammad Amr (section head), Eng. Farid Samara, Eng. Sultan El-Hayek, Eng. Khaled Dawoud, and special thanks to Mr. Jafar Aliyan who made the illustrations so beautiful, Mr.Younis Smadi, and Mr. Yahya Al-Ali. My sincere thanks and appreciations to Miss. Sana Mouasher from SMS for her efforts in producing the color prints . The author is also in debt to great many people who helped in making this work a reality.

Contents

Committee Decision ii

Dedication iii

Acknowledgments iv

Contents v

List of Tables.....vii

List of Figurs.....viii

Nomenclature.....xi

Abstract.....xiiii

Chapter 1 Introduction.....1

1.1 General.....1

1.2 Scope and Objectives.....2

1.3 Literature Review.....4

Chapter 2 Rotor Design.....8

2.1 Overview of Rotorblade Aerodynamics,

(Theory and Definitions).....8

2.1 The axial Momentum Theory.....9

2.3 Blade Element Theory.....12

2.4 Airfoil Selection.....15

2.5 Determination of Blade Data.....18

2.5.1 Rated Power.....19

2.5.2 Rotor Dimensions.....20

2.5.3 Blade Root.....21

2.5.4 Blade Taper (Flapwise).....25

2.5.5 Blade Thickness (Edgewise).....27

2.5.6 Profile Matching.....30
2.5.7 Blade Twist.....31
2.6 Aerodynamic Loads.....38
Chapter 3 Strength and Stress Analysis.....44
3.1 General.....44
3.2 Geometric Solid Modeling.....44
3.3 Section and Mass Properties.....47
3.4 Finite Element Modeling.....50
3.5 Post Solution Analysis.....56
Chapter 4 Manufacturing the GRP Blades.....60
4.1 Stage 1 : Manufacturing the Model.....60
4.2 Stage 2 : Manufacturing the Mold.....63
4.3 Stage 3 : Manufacturing the Prototype Blade.....65
Chapter 5 Performance Testing.....70
5.1 Introduction.....70
5.2 Testing Strategy.....75
5.3 Description of the Measuring System.....75
5.4 Results of the Measuring Program.....78
Chaptetr 6 Conclusions and Recommendations.....84
References.....87
Appendix.....91
Abstract in Arabic 120

List of Tables

Table 2.1 Blade Parameters and Profile Matching.....31

Table 2.2 Input Data to the AERODYN™ Program.....36

Table 2.3 P(4),P(10),and P(16) for the 4-Twist Distibutions.....36

Table 2.4 Complete Blade Data.....37

Table 2.5 Blade Loads and Moments Along the Blade During Normal Operation at A Maximum Wind Speed of 25m/s and Zero Pitch Angle.....39

Table 2.6 Input Data for Blade Loads Calculations.....40

Table 2.7 Maximum Shear Force for Different Pitch Angles.....41

Table 2.8 Maximum Bending Moment for Different Pitch Angles.....42

Table 2.9 Blade Loads FY(N/m) and FX(N/m) Distibution for 25 and 42m/s Wind Speeds Respectively and 30-Degree Yaw and Zero pitch Angle.....43

Table 3.1 GRP Mechanical Properties.....48

Table 3.2 Blade Mass Properties.....49

Table 5.1 Technical Specifications of the RSS WEC.....72

Table 5.2 Ranges for Measured Values.....77

List of Figures

Fig. 2.1 Axial Flow Model....9
Fig. 2.2 Power Coefficient - Axial Interference Factor....10
Fig. 2.3 Rotor Annulus at Radius r....11
Fig. 2.4 Three - Bladed Propeller Type Wind Turbine With Annulus Element Representation....12
Fig. 2.5 Velocity and Forces at A Blade Element at Radius r....13
Fig. 2.6 Profiles Acceptable for Use on The Inboard Region of Wind Turbine Blades....16
Fig. 2.7 Profiles Acceptable for Use on the Outboard Region of Wind Turbine Blades....16
Fig. 2.8 FX 66 Profile Data From Ref. [15]....17
Fig. 2.9 NACA 63-621 Profile Data From Ref. [15]....18
Fig. 2.10 Three Blade Rotor Assembly Showing the Hub and Blades....20
Fig. 2.11 Load Case 1 and Associated Moments....22
Fig. 2.12 Determination of Outside and Inside Root Diameters....24
Fig. 2.13 Blade Root Design....25
Fig. 2.14 Chord Length Distribution Along the Blade in Millimeters....26
Fig. 2.15 Efficiency Losses Related to Ideal Shape Rotor Blade....27
Fig. 2.16 Viewing Rotor Blade Geometry....28
Fig. 2.17 Blade Thickness Envelope....29
Fig. 2.18 Blade Thickness Distribution....29
Fig. 2.19 Graph of Zero Lift Line....33
Fig. 2.20 Aerodynamic Loads and Moments....38
Fig. 2.21 Load Distribution Configuration (N/m) for 25 and 42 m/s....43

Fig. 3.1 Minimum Number of Section Curves for the Blade.....45
Fig. 3.2 Solid Skin for the Two Inner Cavities of the Blade.....46
Fig. 3.3 Solid Skin for the Outer Blade Surfacse.....47
Fig. 3.4 Completed Solid Geometric Model of the Blade.....48
Fig. 3.5 Second Moment of Inertia Ix , Iy Distributions Along the Blade.....49
Fig. 3.6 Phases of Finite Element Modelling.....50
Fig. 3.7 Tetrahedron Element 52
Fig. 3.8 Complete FE Model of Rotor Blade Root Region by ARIES.....53
Fig. 3.9 FE Results Display After Completing the Finite Element Analysis Using ANSYS™ Module Within ARIES™.....55
Fig. 3.10 Curve Fit Extrapolation of Blade Deflection During Extream Operating Conditions at 42m/s.....56
Fig. 3.11 Blade Root Cross Section With Loads and Moments Imposed.....57
Fig. 3.12 Stress Distribution at the Root Section of the Rotorblade 58
Fig. 4.1 Airfoil Section Cut From Wood and Reduced to Allow for Skin Segments Buildup.....61
Fig. 4.2 Method of Fixing the Airfoil Sections in Their Respective Chord and Twist Distribution Prior to Installing the Skin 15x15 mm Segments.....62
Fig. 4.3 Blade Model 5-meter Long Made From Wood.....63
Fig. 4.4 Fiberglass and Polyester Resin Laminates are Being Layed on the Wooden Model to Get its Shape.....64
Fig. 4.5 The Two Mold Halvs After Finishing are Being Strengthened by Lateral Ribs and Steel Frame.....64
Fig. 4.6 Cross Section of the Upper and Lower Shell Construction and Area for Adhesion Allowance.....66
Fig. 4.7 Steel Flange Configuration for the Blade Root.....67
Fig. 4.8 Photograph of the First Prototype GRP Blade.....68

Fig. 4.9 Load Testing of the Prototype Blade After Manufacturing.....69

Fig. 4.10 Blade Load - Tip Deflection Curve.....69

Fig. 5.1 Photograph of the RSS 15 kW Type - 1 Prototype Wind Turbine.....71

Fig. 5.2 Block Diagram of the Measuring System.....76

Fig. 5.3 Block Diagram of the Data Acquisition System.....77

Fig. 5.4 P - V Curve of the RSS - 1 WEC.....79

Fig. 5.5 Line Voltage vs. Wind Speed for RSS - 1 WEC.....80

Fig. 5.6 Line Frequency vs. Wind Speed for RSS - 1 WEC.....81

Fig. 5.7 Cp - λ Curve for RSS - 1 WEC.....82

Fig. 5.8 Instantaneous Measurements of WEC's Data.....83

F_x : force in the x-direction.

F_y : force in the y-direction.

F_z :force in the z-direction.

F_t : tangential force.

f : tip losses factor, line frequency.

G : shear modulus.

I_x : area moment of inertia around the x-axis.

I_y : area moment of inertia around the y-axis.

I_z : area moment of inertia around the z-axis.

L : lift force.

$M_{x,y,z}$: moment of force around the respective axis.

$\dot{m}$: time rate of change of air mass.

P : power.

p : ambient pressure.

Q : torque.

R : total radius.

r : local radius.

T : thrust force, (momentum).

U : local wind velocity.

V : wind speed, wind velocity.

W : relative wind speed.

α : angle of attack.

α_t : blade tip angle of attack.

β : blade twist angle.

η : efficiency.

λ : tip speed ratio of the rotor blade.

Γ : circulation of one blade at radius r.

Γ_{∞} : circulation of rotor with infinite number of blades.

Φ : flow angle of relative wind speed to the airfoil.

Ω : rotor angular speed.

ω : wake angular speed.

ρ : air density.

σ : magnitude of stress.

ε : magnitude of strain.

Abstract

TESTING AND PERFORMANCE OF A LOCALLY MANUFACTURED GLASSFIBER REINFORCED PLASTIC WIND TURBINE BLADES

by : Isaac Ali Saleh
Supervisor: Dr. Saad Habali

Wind energy has attracted a great deal of attention in recent years in Jordan as one of the possible alternative energy resources. Almost all of the local research and development activities in this field were directed to explore ,develop,and optimally utilize wind energy systems. Given all the previous research work, the time has come to establish a link between local scientific (acadimic) work and local industries to produce a usable technology which will increase the local share in an inevitably emerging wind energy industry in Jordan.

In order for a wnid energy industry to be established in Jordan, a well founded manufacturing base is required. Jordan has virtually hundreds of different kinds of industries, but no one is specialized in manufacturing wind system components. Thus, a problem exists which will be addressed in this thesis to establish a local manufacturing procedure and capability for Glassfiber Re-inforced Plastic (GRP) wind turbine blades and to identify the basic components of this technology which are required from the local market.

A brief summary of rotorblade aerodynamics is given to define the varios parameters governing blade design and with the help of a special software, a complete aerodynamic analysis was performed. A 3-D solid model is then created and a FEM analysis was performed using a powerful computer which yielded a real simulation to the actual blade operating under loads. A final blade geometry was verified and a full-scale model was made.

During the course of this work, one Jordanian company was identified and has succeeded in adapting to this new technology, and according to the procedure set forth had produced a high quality 5-meter GRP blade. The blade had also passed successfully the pre-assigned stress test, and when installed on a functional wind turbine, performed satisfactorly with a favorable power coefficient of 41.2%.

Chapter 1

INTRODUCTION

1.1 General

Wind energy technology is fairly new to Jordan. It was first introduced in its modern form by the Royal Scientific Society (RSS) in 1983, when a multi-blade ten killowatt wind turbine was installed to pump water from a desert well. Wind energy technology is also multi-diminsional, it encompases aerodynamics,structural mechanics,machines, and power electronics. One of the most complex and costly parts of modern wind turbines is the rotor blade [1]. It was shown by a pre-feasibility study carried out by the Ministry of Energy and Mineral Resources (MEMR) [2] that rotor blades account for 30% of the total cost of wind turbines. This was done in the framework of the establishment of Jordan's first wind farm in Ibrahimya north west of the country and the attempt to evaluate the share of the local industries in any future developments.

The RSS being a national research and development institution has taken the lead in transferring wind energy technology starting from premetive windpumps to sophisticated electrical grid-connected machines. The latest development was the design and manufacturing of a 15-kW wind turbine where the rotor blades took most of the efforts which will be the subject of this thesis. The role of the Jordanian universities in the wind energy field at this time is characterized by the theoretical

studies and research of conventional and unconventional wind energy systems. For example, at the university of Jordan, many research topics have been treated such as the evaluation of wind data, wind farming, augmentation principles (e.g. vortex augmentation) and the design of new airfoils.

1.2 Scope and Objectives

The bulk of this work will concentrate on the development of the rotor blades. The philosophy underlying the choise of the blade size was that a small blade will be too stiff by nature and unable to exibit the behaviour of full size blades used for electricity generation. On the other hand, a large blade will be over the capabilities of the technical and financial resources. Hence, the desicion was made to experiment with a 5-meter blade which has the characteristics of large blades and the handeling conveniece of small blades. One of the objectives was to test the capabilities of local manufacturers in the execution of such complex designs and to examine their performance in adapting to this new technology.

The blade material was a major challange in its own right where the choice will fall on a material that can be easily adapted to mass production such as fiberglass. This is a composite material which means it has more than one component. Boeing Engineering and Construction [3] proposed 10 different components to be used in the construction of MOD-2 wind turbine blades, where the design was based on stiffness, fatigue, and compression buckling requirements that resulted in a tensile strength less than 69 N/mm^2 which means that the above requirements have been accounted for. The objective of using Glassfiber Re-inforced Plastic (GRP) material can be related to many attributes; one is the availability of the polyester resin which is locally produced. This is important to the economics of the overall system.

Rotor blade design relies heavily on the aerodynamic theory. The blade is an aerodynamic body having a special geometry mainly characterized by an airfoil cross section. Extensive calculations are necessary in order to determine the blade parameters such as chord and thickness distributions, twist distibution and taper that are matched with the selected airfoil sections. For practical purposes, more than one airfoil section must be chosen to fit the thickness distribution where closer to the root a thick section is needed, and thinner sections are applied along the blade to give a smooth transition from root to tip. Another objective of this research work is to develop the basic engineering design of GRP blades and also to establish the procedure for local manufacturing. Ultimately, this work will contribute toward the initiation of a GRP blade test facility which can lead to establishing a local design code.

Wind turbine blades must be designed to operate in one of the most unpredicted environments and still give satisfactory performance for the life time of the system. Since the blade is subjected to variable loading in three-dimensional form, exact calculations of the strength characteristics is unattainable. Many computer softwares have been written to simulate what realy happens during the blade flight and attempted to predict the loads and their variations. For example, Hartin [4] used a software package called LOADS that analyzes blade loads for rigid rotors of simple geometry for the Grumman WS33 wind turbine and concluded that the sensitivity of the load predictions to the phase of the turbulent wind simulation and the length of the simulation record point to the need for improving wind simulation techniques.

This note reveals the fact that the blade is subjected to cyclic loadings of different magnitudes which may cause fatigue failure if not designed properly. It will be shown in the strength analysis treatment that this fact is accounted for in an elegant simplified method which guarantees the safety of the design.

Manufacturing the blade which is one of the prime objectives of this resarch is divided into three integrated parts; The model, the mold, and the prototype. The model is made from soft white wood to simplify shaping the exact geometry of the airfoil, taper, and twist. The model will also facilitate verification and modification to certain parts of the blade especially ensuring streamlining. A mold having the exact imprint of the model is then produced from fiberglass material. The mold will have two cavities; upper and lower, to facilitate ease of extracting the molded blade. The interior surfaces of the mold cavities are carefully treated and highly polished to yield a fine surface finish on the blade surface.

A method that is simple and practicle is developed for the local manufacturer to apply which produces a strong and exact geometry blade. The method also includes a proof-load test procedure, when applied and passed, it will guarantee fatigue strength capabilities.

Four blades were manufactured. One was proof-load tested and three were installed on a grid connected wind turbine having rated power of 15kW with pitch regulation and electohydraulic control. A special measuring system was installed between the turbine and the grid that measure the power, wind speed, voltage, and frequency of the generator. These values will be used to evaluate the performance of the rotor blade after proper accounting for the various efficiencies of the whole turbine system. The treatment of these data can ultimately produce a power curve for the turbine which leads to the calculation of the overall performance and finally leads to the performance of the single rotor blade.

1.3 Literature Review

A comprehensive study of the possibilities for local manufacturing of wind turbine components was performed in the framework of the MEMR "Wind Energy Project in

Jordan" in cooperation with the Jordan Electricity Authority (JEA) and two Danish consulting firms in 1989 [2].

The study of local production identified a significant theoretical potential for local production where local share can be increased from 15% to 60 or 70% over a number of years. The study concluded that the development of this potential requires significant efforts in developing local production with high standard of quality.

In a report to the government of Jordan from UNIDO, Petersen [5] stated that "viewing Jordan as a market, it must be realized that the market is small and hardly appealing to foreign companies establishing a joint venture for production of wind turbines in Jordan unless local finance could be established". Petersen[5] added that "although assembling of machines in Jordan would lower the price, the import of wind turbines would still presuppose that considerable foreign currency would be available. For these reasons (Petersen added) it is most likely that the best approach would be to develop wind turbines in Jordan".

Production of wind turbine blades needs no factory equipment except the mold for the glassfiber blades, and this would apply to any size blades [5]. Blades should be constructed to withstand the loads resulting from normal operation, gust, or turbulences during which major altrnating stresses arise,and all materials used must consequently be capable of withstanding the fatigue resulting from them. A variety of blade designs were suggested by Park [6] but more advanced blades having optimized geometry were introduced by Jackson [7].

In general, the design of a wind turbine rotor consists of two steps as given by Lysen [8]: (1) the choice of basic parameters, such as the number of blades, the radius of the rotor, the type of airfoil, the tip-speed ratio, and (2) the calculations of the blade setting angle and the chord length at each position along the blade.

However, at the core of the problem is the complete aerodynamic and mechanical design of the blade itself.

One of the most recent developments in blade design is the special purpose thin-airfoil family inroduced in 1990 by the Solar Energy Research Institute (SERI) at Golden , Colorado USA. These SERI blades were described by Davidson [9] as "the blades of the future" and could produce 31% more power than the traditional Danish made blades. The design and field test results of the new blades are described by Tangler et. al [10], however, the new design is far noisier then the Danish one.

Petersen [5] argued that the claims of Davidson [9] and Tangler et. al. [10] are invalid and the increase of performance for the new SERI blades is largely due to increased rotor area and partly to enhanced aerodynamic behaviour. Tangler et. al. claimed that the increased rotor area achieved by the longer blades constitutes a part of the improved efficiency because of the characteristics of the new blades that lower the blade loads, thereby admitting the larger blades without other changes to the wind turbine. These characteristics are nevertheless similar to other modern blades with NACA 63-nnn profile series.

Most modern blades have profiles of the NACA 63-nnn series. The profiles have shown excellent properties for wind turbine blades, but some improvements can still be achieved for profiles at the inner portion of the blades in order to make the profile sufficiently thick for structural reasons while still having high lift coefficient. For this reason, developments are taking place to design thick airfoils for the inner parts of the blade. An example of this is the SERI S807 profile. Other examples are the LS(1)-0421, and NACA 63-621 profiles.

It is interesting to know the big difference of these profiles, however all are suited for use. The reason for this development is that the profiles NACA 63-2nn to NACA

63-4nn are well suited for the outboard region of the blades, but having a rather low lift for the inboard portion. Petersen [5] did not expect more than a few percents improvement from this development.

The other side of development is dealing with the mechanical characteristics of wind turbine blades. Blades are often found to have failed under the action of repeating of fluctuating stresses, and yet the most careful analysis reveals that the actual maximum stresses were below the yield strength. The most distinguished characteristic of these failures has been that the stresses were repeated a very large number of times. Hence the failure is called a fatigue failure.

Most wind turbine blades today are made from GRP, and theories involved with the concept of fiber reinforcement were established around 1961 and documented by Holister and Thomas in 1966 [11]. However, the oldest blades were made in the 1970's but actual large scale implementation took place in the early 1980's [5].

Since 1983, a static proof-test for GRP blades was only required and performed by the prominent Test Station for Windmills, Risoe, in Denmark as a part of the certification procedure for windmills. In 1984 a new procedure for fatigue testing of GRP blades was developed as part of the general research and development work, and since then a number of commercially available GRP baldes have been fatigue tested as described by Jensen et. al [12]. The fatigue testing is done by forcing the blade to oscillate with constant amplitude at a natural frequency untill failure ocurrs. Their results showed that the load used for the static proof-load test is sufficient to cover the range of this fatigue testing strategy and therefore will be enough to be used as a design guide.

Chapter 2

ROTOR DESIGN

2.1 Overview of Rotorblade Aerodynamics (Theory & Definitions)

The flight of a rotorblade is a complex phenomenon which cannot be modeled exactly. This complexity arises from the fact that the flow of air around the blade is three-dimensional with various vortex sheddings resulting from variable rotational speed. This is also coupled with the variation of wind speed distribution along the blade caused by the wind shear and the large scale boundary layer on the earth surface.

This phenomenon however can be approximatly described by imposing several assumptions. One of the simplest descriptions of extracting energy from the wind is the one-dimensional, incompressible, non-viscouse flow model using the axial momentum theory developed by Rankine in 1865 and later improved by Froude. The flow is assumed to be entirely axial with no rotational motion. Then came the German scientist Betz in 1924 and included rotational wake effects, and more recently Wilson and Lissaman in 1974 [13] have further analyzed the aerodynamic performance of wind turbines by using computer programming and numerical techniques.

The momentum theory cannot provide the necessary information on how to design the rotor blades; however, the momentum theory when combined with the blade element theory will then yield this kind of information.

In the following section, a brief overview of both the momentum and blade element theories will be outlined in order to establish the necessary terminology and definitions.

2.2 The Axial Momentum Theory

Three principle assumptions are made:

1- The flow is completely axial.

2- The flow is rotationally symmetric.

3- No friction occurs when the air passes the wind turbine rotor.

Using Figure (2.1) with the flow governing equations we obtain:

Continuity $UA = U_1A_1$ .....(2-1)

Momentum(thrust) $T = \dot{m}(V - U_1) = \rho AU(V - U_1)$ .....(2-2)

Bernoulli upwind $p_0+1/2\rho V^2 = p+1/2\rho U^2$ .....(2-3)

Bernoulli downwind $p_0+1/2\rho U_1^2 = p'+1/2\rho U^2$.....(2-4)

thus $p - p' = 1/2\ \rho(V^2 - U_1^2)$.....(2-5)

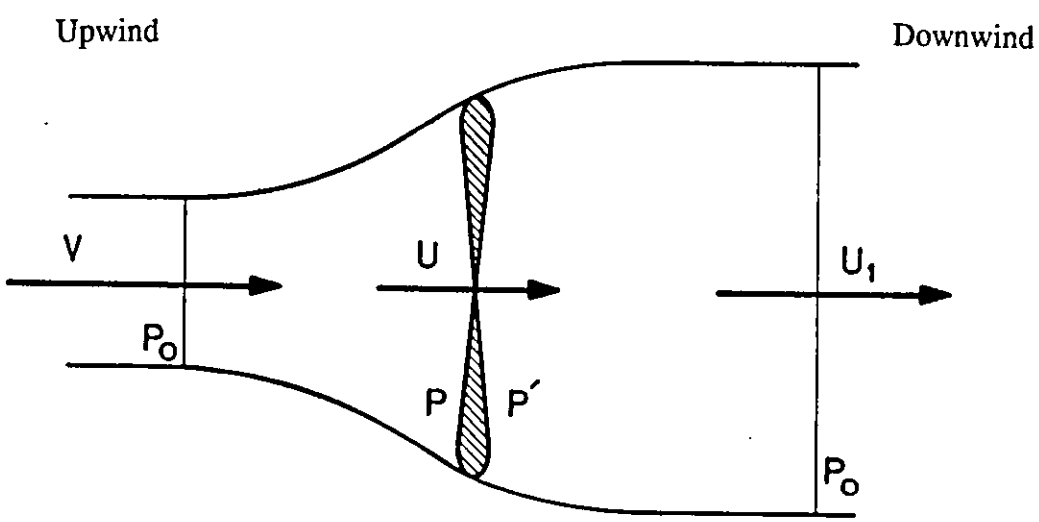

Fig. 2.1: Axial flow Model.

Combining equqtion (2-2) and (2-5) with:

$T = A\Delta p$ .....(2-6)

yields : $U = (V + U_1)/2$ .....(2-7)

The power extracted will then be:

$P = 1/2\dot{m}(V^2 - U_1^2) = 1/2\rho UA(V^2 - U_1^2)$ .....(2-8)

Now denoting a power coefficient $C_p = P/(1/2\rho V^3 A)$ .....(2-9)

and we know that the flow has been interfered with (retarted) at the rotor disc by slowing down a certain amount (a), then we get:

$U = (1-a)V$, and with (2-7) $U_1 = (1-2a)V$.

Using U and U_1 in (2-8) we have:

$C_p = 4a(1-a)^2$ .....(2-10)

which has a maximum when $a = 1/3$ as shown in Figure(2.2).

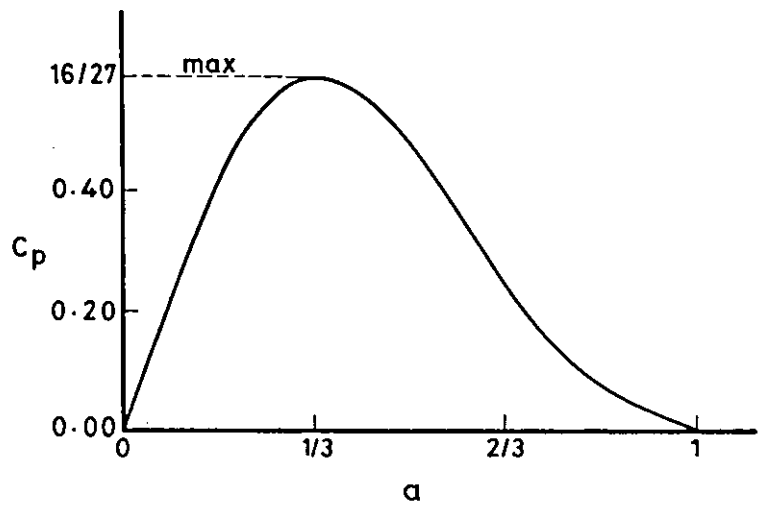

Fig. 2.2 Power Coefficient-Axial Interference Factor Curve.

In order to enhance the results and make them close to reality, the effect of wake rotation will be included. In describing this effect, the assumption is made that upstream of the rotor, the flow is entirely axial and that the flow downstream rotates with an angular velocity $\omega(r)$, but remains irrotational.

Expressions for torque and power may be obtained by considering the flow through an annulus at radius r with area $dA = 2\pi r dr$ as seen in Figure (2.3).

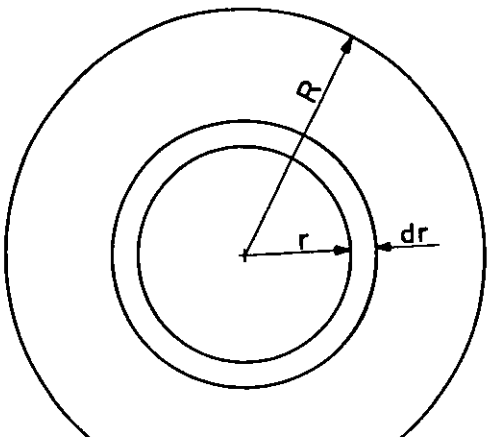

Fig. 2.3: Rotor Annulus at Radius r.

By changing the momentum in the air in the tangential direction, tangential forces act uppon the rotor as:

$$dF_t = \dot{m}dV = \rho U dA \omega r \quad \text{.....(2-11)}$$

$$= 2\pi\rho U \omega r^2 dr \quad \text{.....(2-12)}$$

The torque generated in the annulus dr is:

$$dQ = 2\pi\rho U \omega r^3 dr \quad \text{.....(2-13)}$$

and since power = torque x rotor angular speed, the power extracted is:

$$dP = 2\pi\rho\Omega U \omega r^3 dr \quad \text{.....(2-14)}$$

In integral form, the torque and the rotor power then become:

$$Q = 2\pi\rho \int_o^R U\omega r^3 dr \quad \text{.....(2-15)}$$

$$P = 2\pi\rho\Omega \int_o^R U\omega r^3 dr \quad \text{.....(2-16)}$$

In order to be able to calculate torque and power, one must have the values of the wake's angular velocities $\omega(r)$ by introducing the tangential induction factor (a') [9] :

$$a' = 1/2\ (\omega/\Omega) \quad \text{.....(2-17)}$$

Q and P can then be easily found.

2.3 Blade Element Theory

The blade element theory is governed by two main assumptions:

1- The forces and moments acting on a blade element are solely due to the lift and drag characteristics of the profile section of that blade element.

2- There should be no interference between adjacent blade elements because the forces on each element are calculated with their local wind velocities. The flow at a blade element dr as shown in Figure (2.4) may be regarded as two dimensional.

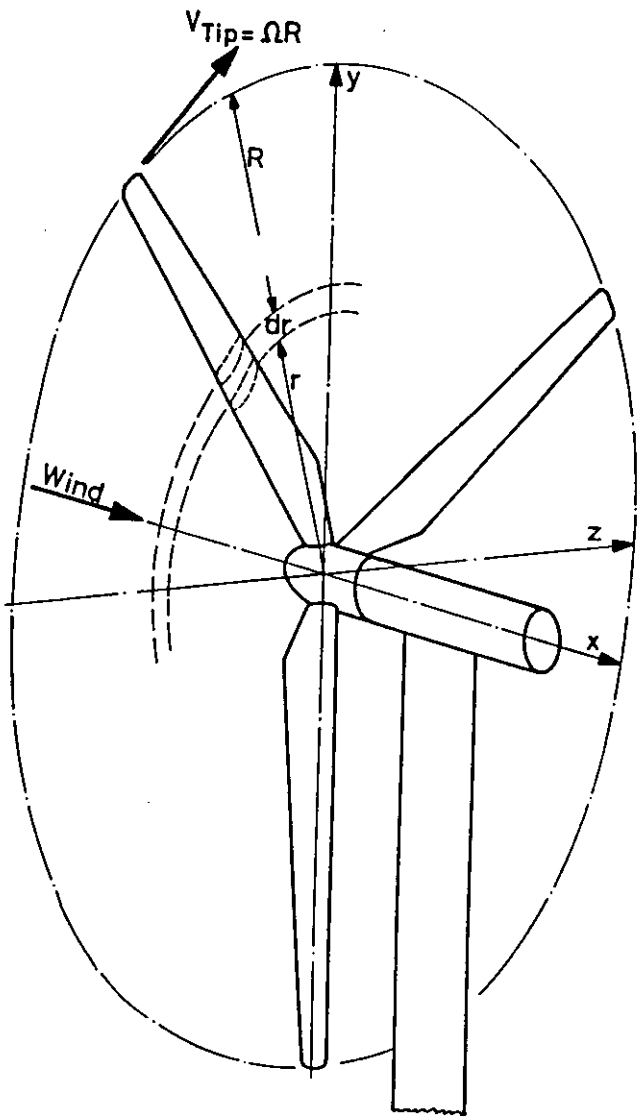

Fig. 2.4: Three-Bladed Propeller Type Wind Turbine With Annulus Element Representation.

A cross section of an element at radius r in Figure(2.4) is shown in Figure(2.5). In this representation, the angular velocity of the rotor Ω is assumed to be half the value of the final rotational velocity in the wake ω [8] which is an approximation to equation (2-17) by setting $a' = 1$.

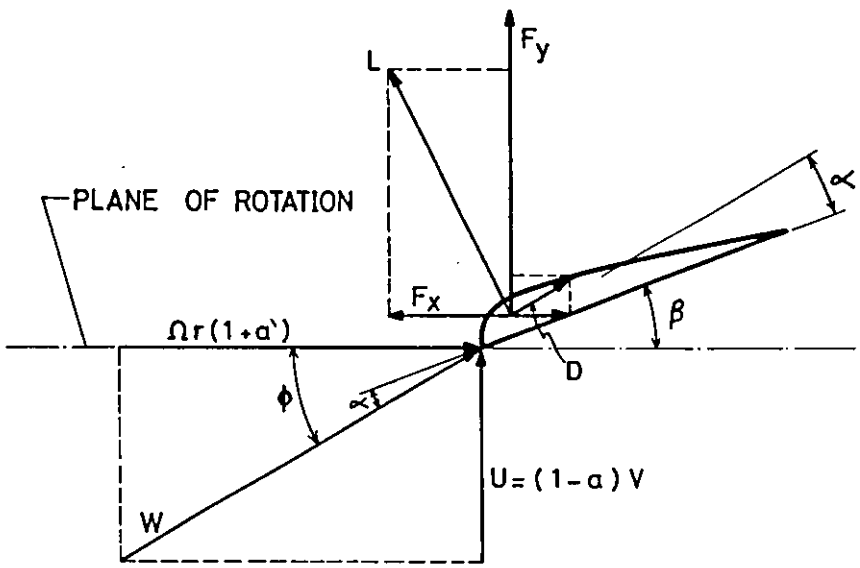

Fig. 2.5: Velocity and Forces at A Blade Element at Radius r.

Defining $dq = 1/2\ \rho\ W^2\ dA = 1/2\ \rho\ W^2\ c\ dr$ gives:

$C_L = dL/dq$ .....(2-18)

$C_D = dD/dq$ .....(2.19)

$C_X = dF_X/dq$ .....(2-20)

$C_Y = dF_Y/dq$ .....(2-21)

The following trigonomotric relations may be obtained from Figure(2.5):

$\alpha = \Phi - \beta$ .....(2-22)

$\tan \Phi = (1-a)/(1+a')\ *\ V/\Omega r$ .....(2-23)

$C_Y = C_L \cos \Phi + C_D \sin \Phi$ .....(2-24)

$C_X = C_L \sin \Phi - C_D \cos \Phi$ .....(2-25)

With $dA = cdr$ and c = blade chord length, expressions may now be derived for the thrust T and torque Q for an element dr at radius r as follows:

$dT = Bc\ 1/2\ \rho W^2 C_Y dr$ .....(2-26)

$dQ = Bc\ 1/2\ \rho W^2 C_X dr$ .....(2-27)

where B is the number of blades.

The thrust and torque equations were also derived using the axial momentum theory, but with the assumption that no friction occurs. Hence, in order to equate the two results we must assume $C_D = 0$, then equating (2-2) and (2-13) to (2-26) and (2-27) gives:

$a/(1-a) = (cBC_Y)/(8\pi r \sin^2 \Phi)$ .....(2-28)

$a'/(1+a') = (cBC_X)/(8\pi r \sin\Phi \cos\Phi)$ .....(2-29)

From figure(2.5) we can conclude that:

$W = V(1-a)/\sin\Phi$ .....(2-30)

or

$W = \Omega r(1+a')/\cos\Phi$ .....(2-31)

The local solidity ratio of the rotor is defined as:

$\sigma = cB/2\pi r$ .....(2-32)

Solving (2-28) and (2-29) for a and a′ gives:

$a = 1/((4 \sin^2 \Phi/\sigma C_Y)+1)$ .....(2-33)

$a' = 1/((4 \sin\Phi \cos\Phi/\sigma C_X)-1)$ .....(2-34)

With a finite number of blades (e.g. B=3), the assumption that the flow through the rotor is rotationally symmetric abviously does not hold, in addition to the two dimensional flow assumption. The effects due to a finite number of blades results in performance losses concentrated near the tip of the blade. This phenomenon was first analyzed by Prandtl [14] , which is known as the tip-losses model. The tip losses are expressed by a circulation-reduction factor defined by:

$F = B\Gamma/\Gamma_\infty = 2/\pi \arccos(e^{-f})$ .....(2-35)

where Γ is the actual circulation of one blade at radius r, and Γ_∞ is the circulation of a rotor with an infinite number of blades as was calculated in the axial momentum theory, and

$$f = B/2 * (R-r)/(r \sin \Phi) \quad \text{.....(2-36)}$$

Prandtl[14] gives as a result, the modified axial and tangential velocity factors:

$$a = 1/[(4 \sin^2 \Phi)F/(\sigma C_Y) + 1] \quad \text{.....(2-37)}$$

$$a' = 1/[(4 \sin \Phi \cos \Phi)F/(\sigma C_X) - 1] \quad \text{.....(2-38)}$$

Noting that the Prandtl factor F does not change the relation between the two factors as previously derived.

2.4 Airfoil Selection

Airfoils chosen for wind turbine applications have focused on the half-century old NACA 23nnn and NACA 44nn series of airfoils. The NACA 23nnn series were found (by Tangler [10]) to experience large drop in maximum lift coefficient (Cl_{max}) as the airfoil becomes soiled (dirty). This problem was also found on the NACA 44nn series however to a lesser extent.

In an effort to solve this blade soiling problem, manufacturers began using the LS - 1 and NACA 63nnn series of airfoils. Both of these airfoil sections have their camber farther back which provides some improvement in reducing the airfoil's Cl_{max} sensitivity to roughness effects. In addition, the NACA 63nnn provided a lower Cl_{max} which helped control peak power; However, this characteristic is desirable only over the tip region of the blade, and when used on the inboard region, a degredation in energy production is expected. The LS - 1 series have the opposite problem; this airfoil provides a desirable high Cl_{max} toward the blade root, but contributes to excessive peak power when used over the outboard portion of the blade. The excessive peak power must then be controlled with undesirable reduction in blade solidity or a less efficient blade operating pitch angle. Figure(2.6) shows the two airfoil profiles.

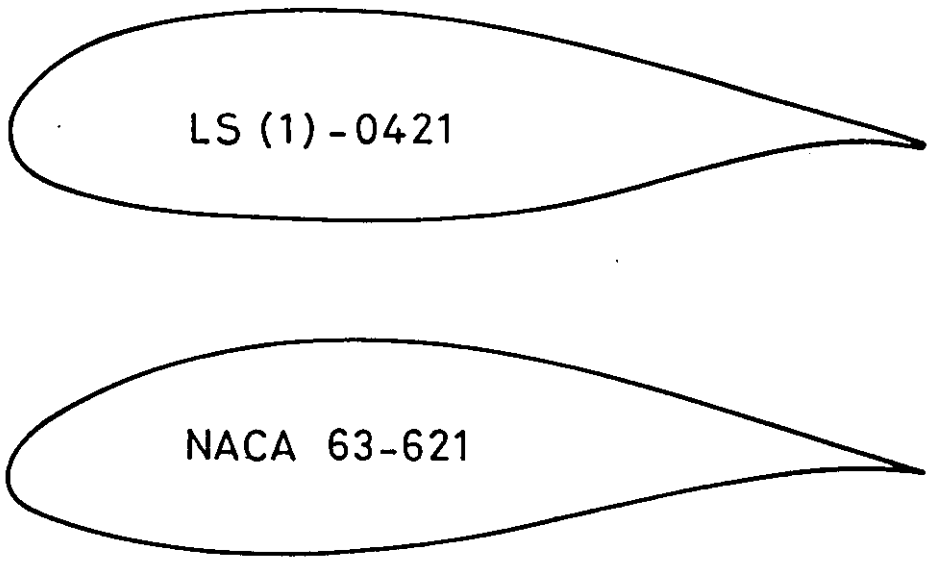

Fig. 2.6: Profiles Acceptable for Use on the Inboard Region of Wind Turbine Blades.

The FX - S airfoil family has in its series the characteristics required for the outboard region and also the tip. They seem to gather the characteristics of both profiles shown in in Figuer(2.6), see Figure(2.7).

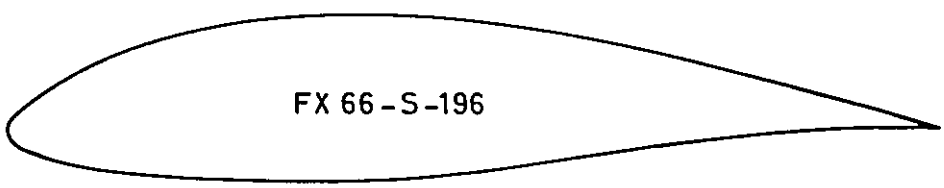

Fig. 2.7: Profile Acceptable for Use on the Outboard Region of Wind Turbine Blades.

This family has a stable Lift coefficient (C_l) at high angles of attack (low wind speeds) and an optimum (C_l) at low angles of attack (high wind speeds). In addition, their moment coefficient (C_m) is smooth and almost constant over the whole range of operating angles of attack and therefore will be selected for the outboard region of our blade. Figure(2.8) shows the profile data depicted from reference [15].

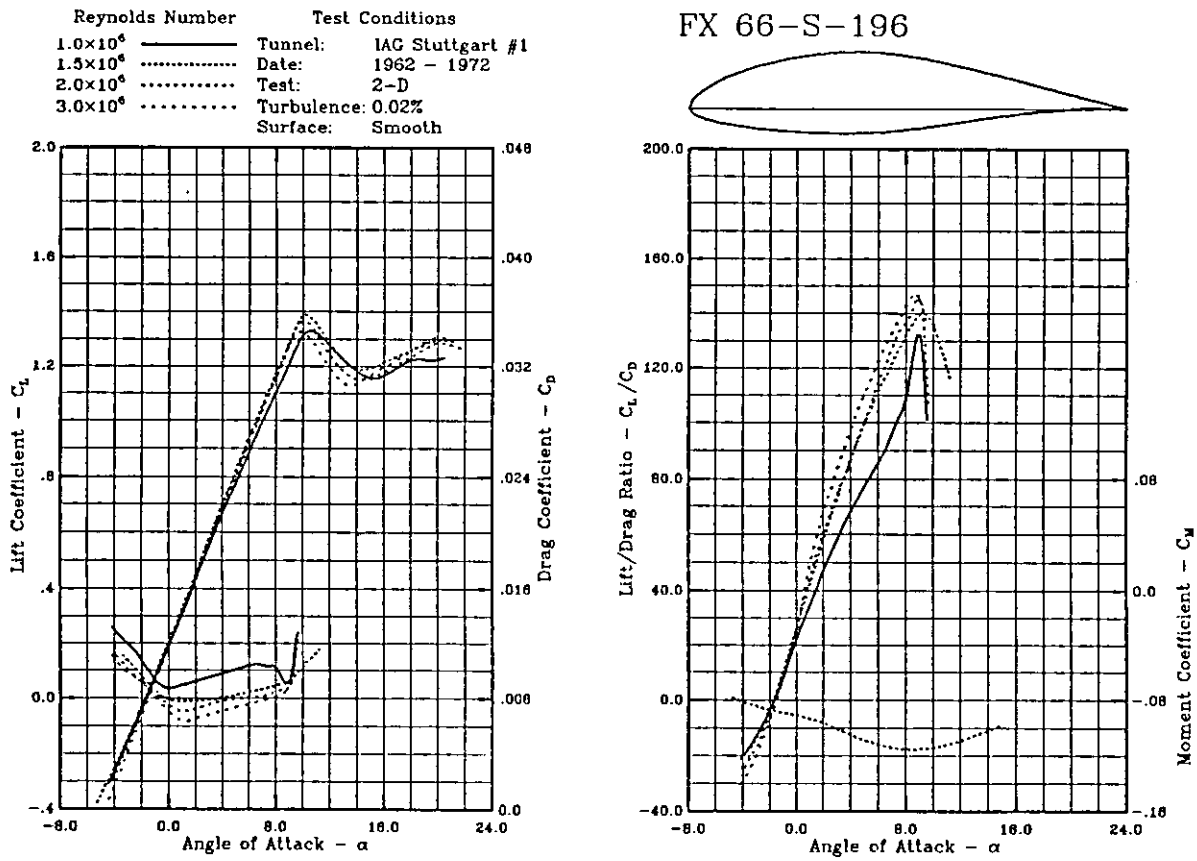

Fig. 2.8 FX 66 Profile Data From Ref. [15].

The inboard region of the blade must be thicker and having more material to withstand the higher stresses and also have a smoother geometry transition to the circular connecting flange at the root. NACA 63-621 shown in Figure(2.9) is selected for the inboard region which has these characteristics and is very similar to the FX 66-S-196 profile, in addition, the profile similarities will simplify the transition from inner to outer board regions.

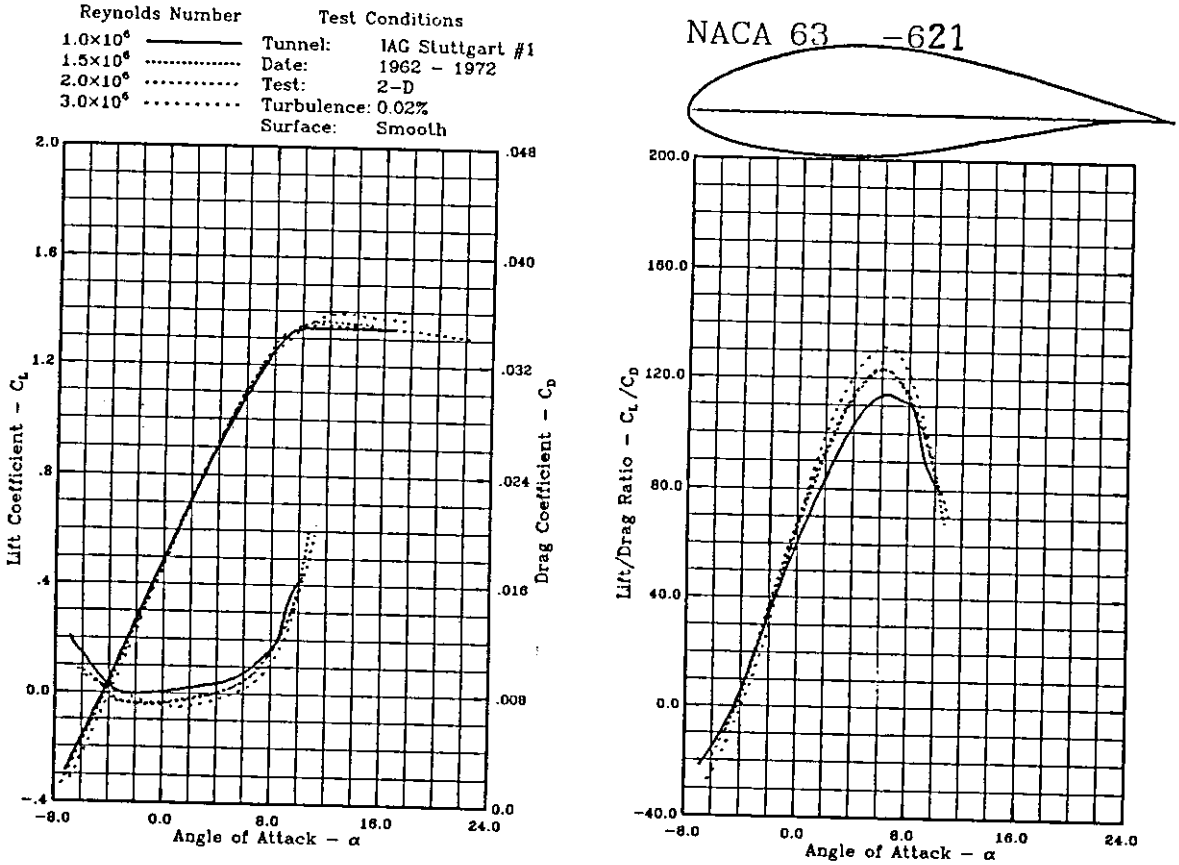

Fig. 2.9: NACA 63 - 621 Profile Data From Ref. [15].

2.5 Determination of Blade Data

The design and construction of a sophesticated wind turbine blades rquires enormous amounts of data. Most important are those describing the geometry and structural characteristics such as length, thickness distribution, chord length distribution, twist, root connection, etc.. .

2.5.1 Rated Power

The rated power can be calculated from the equation:

$$P_{rated} = 1/2\ \rho_{air}\ V^3_{rated}\ A_{rotor}\ C_{p\ rated} \quad \text{.....(2.39)}$$

The first step is to identify the output capacity of the proposed wind turbine. This is an open decision that depends on the desiers of the investor who wants to build the turbine, where it could range from a few hunred Watts to the order of Megawatts. In our case, the rated power of the turbine will be taken at 20 kW. The rated power is only defined for pitch-controlled machines at one value of wind speed and power coefficient. These two values can be chosen by experience and will directly influence the size of the wind turbine rotor, (i.e. the diameter). there are some theoretical bases for chosing the rated wind speed for a given wind turbine [16], however, experience has shown that most machines have rated power around 10m/s and for small fast running machines lower values can be realized. Hence, for this design, a 9.5m/s rated wind speed will be selected.

The maximum power coefficient attained for an ideal wind turbine is 16/27 , or 59% as was previously shown in Figure(2.2). Also from manufacturers data and test results [17], most machines of this size operate at C_p around 0.4 which will be chosen for this design.

with the previous parameters selection and a selected air density equal to 1.25 kg/m^3, the only remaining unknown is the rotor's area :

$A_{rotor} = 20{,}000 / 0.5 * 1.25 * (9.5)^3 * 0.4 = 93.3\ m^2$

and the diameter of the rotor will be:

$Dia = \sqrt{4A/\pi} = 10.9\ m$

2.5.2 Rotor Dimensions

The wind turbine rotor usually consists of two main components; Hub, and Blades as shown in Figure(2.10). The hub can be rigid in the case of fixed pitch ,or can have

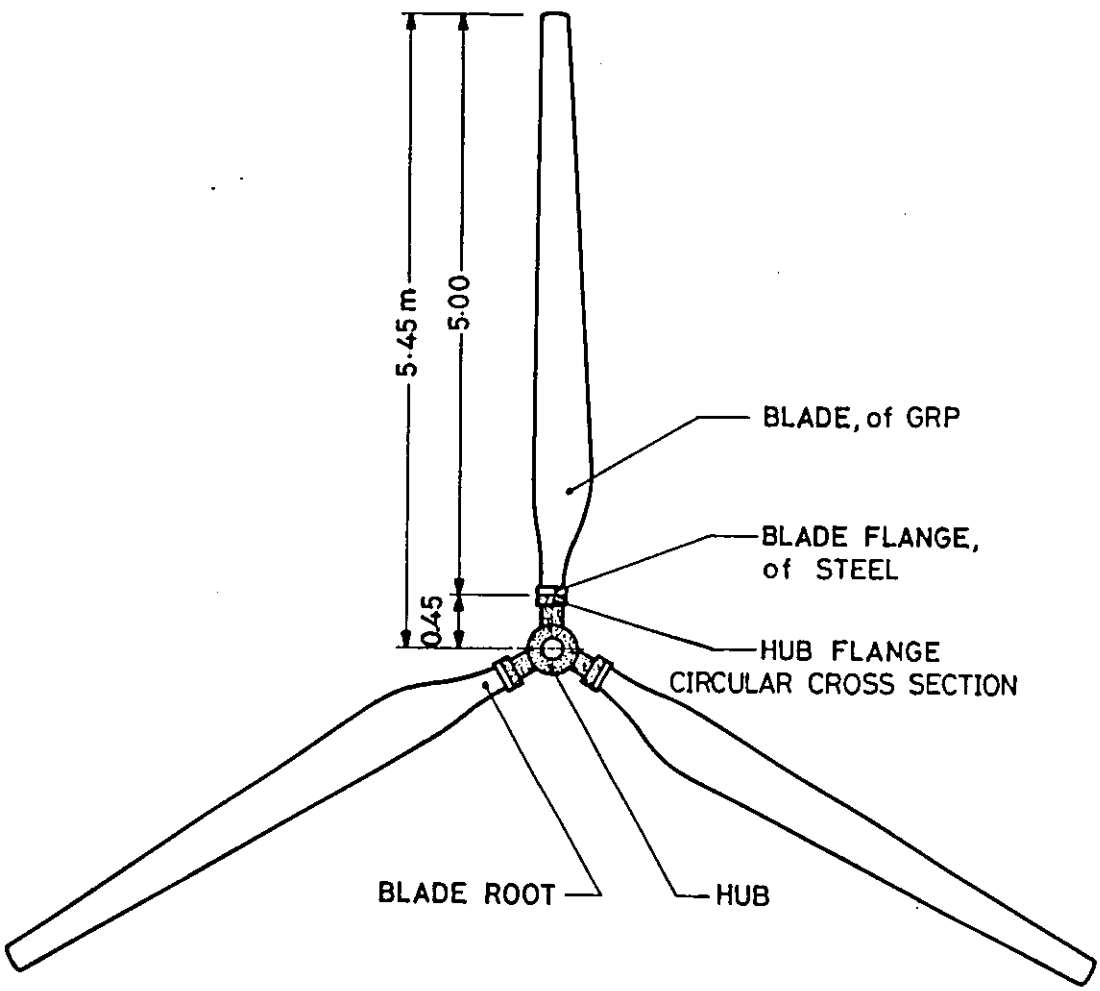

Fig. 2.10: Three Blade Rotor Assembly Showing the Hub and Blades.

rotating flanges for variable pitch machines as in our case. The hub and flange including axle assembly is assigned a radius of 0.45m leaving the rotor blade to be 5.0m long from flange to tip as shown in Figure(2.10).

2.5.3 Blade Root

The blade root is the heaviest and thickest part of the blade because it carries the blade structure and it is the junction point between the blade body and the hub as shown in figure(2.10). The root has to take maximum moments and torques transmitted by aerodynamic forces through the blade to the rotor shaft and therefore stresses and strains will be concentrated in the root area. Another complexity is added from the different types of materials used at the root because the GRP blade must be fitted with a steel flange in order to be bolted to the hub flange. The geometry of the root is the most complex and does not follow any known rules of construction because an airfoil profile section must be continuously and smoothly coallesed to a circular section at the flange; Fortunately, the stress calculations are made for the critical section of the blade root which is circular.

LOADING CONDITIONS:

There are no official design rules for wind turbine blades based on specified loading [12]. The evaluation of the ultimate strength and fatigue characteristics of a rotor blade is based on a static proof test [18].

The static proof load is derived from the assumption of an extreme thrust load of 300 N/m^2 swept area. This load is equally shared among the blades and distributed in a triangular pattern with zero at the rotor center and maximum at the tip. This means that each blade of our three bladed rotor with a swept area of 93.3 m^2 should withstand an extreme load of 9.33 kN. (300 N/m^2*93.3m^2/3blades=9.33kN/blade) The blade should withstand this load without sustaining any damage. On fatigue, the certification criteria [12] states that at a load factor of 0.5 (150 N/m^2* swept area / number of blades), the measured strain for GRP must be less than 0.2% (2000 microstrains) in the side of the blade under compression and less than 0.3% (3000 microstrains) in the side of the blade in tension. Therefore, we have two load cases:

Load Case 1 : 300 N/m^2

Load 1 = 300 N/m^2 * 93.3 m^2/ 3 Blades = 9.33 kN/Blade

Load Case 2 : 150 N/m^2

Load 2 = 0.5 * Load 1 = 4.665 kN/Blade

It is understood that the cross section of the root is circular and must be hollow from the inside just like the blade itself, therefore the root has an outer diameter d_o and an inside diameter d_i.

Using Load Case1 with the distribution mentioned above we have the situation dipicted by Figure(2.11).From the rotor dimensions and load distribution, the moment

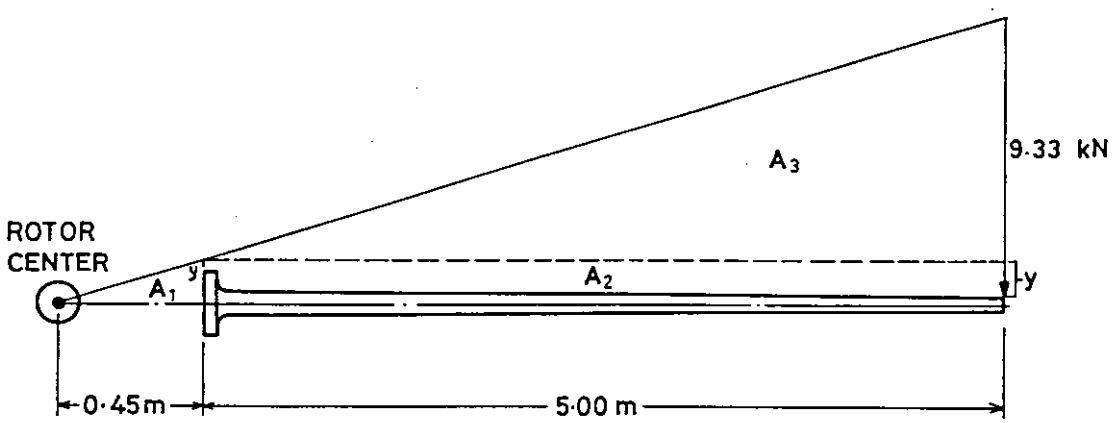

Fig. 2.11: Load Case 1 and Associated Moments.

acting on the blade root is the sum of the areas marked A_2 and A_3, where the concentrated load can have variable values according to the linear curve shown when moved from point to another along the blade length. Using similar triangles, yields:

9.33/5.45 = y/0.45 ========> y = 0.77 kN

Then

A_1 = 0.77 kN * 0.45/2 = 0.173

A2 = 0.77 kN * 5.0 m = 3.85

A3 = 9.33 - (3.85+0.173) = 5.307 , hence,

M_{root} = (3.85*2.5)+(5.307*2/3*5.0) = 27.3 kN.m

Now, from Hooke's law, the stress within the root section is :

$\sigma_{root} = \varepsilon_{root} E_{root}$ .....(2-40)

where E = 30 GPa is the Modulus of elasticity for GRP, and with a strain limit of 0.3% in tension and allowing only half of this amount (0.15%) which is equivelant to a safety factor of 2 ,we get:

$\sigma_{root} = (0.15\%/100) * 30x10^9 \text{ N/m}^2 = 4.5x10^7 \text{ N/m}^2$.

Also, from the flexure formula, we have:

$\sigma_{root} = M_{root} * r_{root}/I_{root}$ .....(2-41)

where, $I_{root} = \pi/64 * (d_o^4 - d_i^4)$

is the cross sectional moment of inertia,

and d_o = root outer diameter

d_i = root inner diameter

r_{root} = the distance from the cross section center to the outer most fiber, which is $d_o/2$.

Therefore, Equation (2-41) becomes:

$\sigma_{root} = (32 * M_{root} * d_o) / \pi (d_o^4 - d_i^4)$ .....(2-42)

or

$4.5x10^7 = 2.73x10^5 d_o / (d_o^4 - d_i^4)$ .....(2-43)

Hence, we need to iterate a few times to get the required root cross section area. Off course, a blades that is 5 meters long cannot in any way have a one meter-thick root neither a 5 centimeter thin. A practical starting value would be 10% of the blade length, however, it should not exceed the hub diameter, therefore, we start with d_o = 0.45 m and find d_i using a small computer program. A graphical solution to Equation(2-43) is given in Figure(2.12) which also shows the difference between d_o

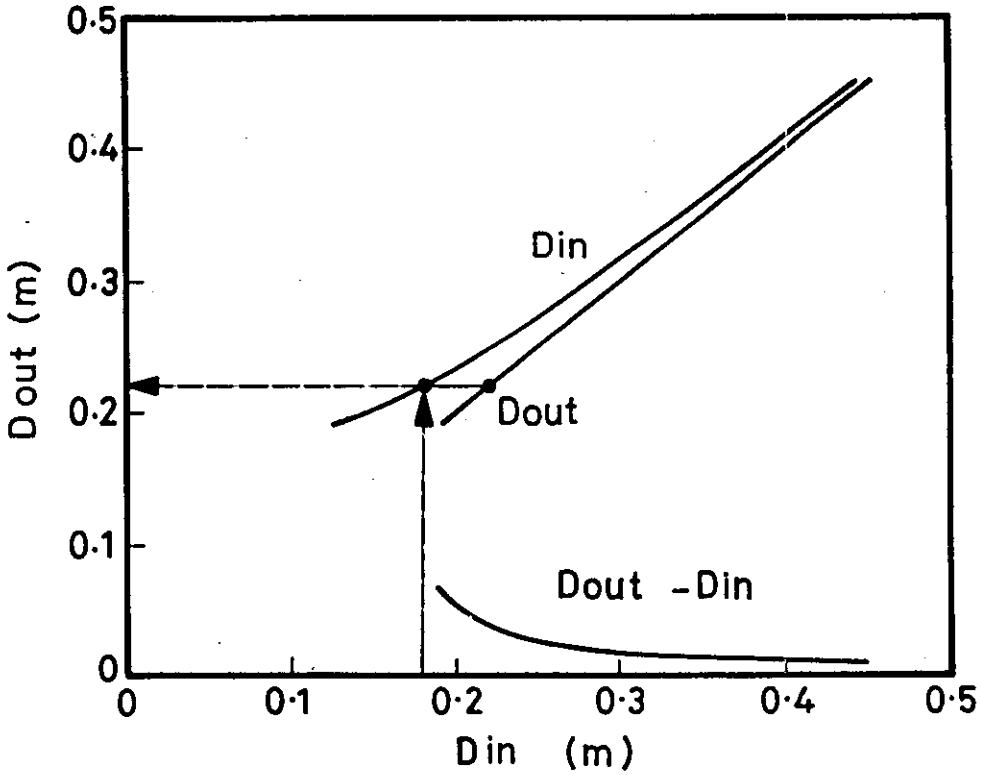

Fig. 2.12: Determination of Outside and Inside Root Diameters.

and di (i.e. the thickness of the blade material at the root). Below $d_o = 0.2$m, the Equation starts to diverge, and therefore, a minimum outside diameter of 0.21m and a corresponding inside diameter of 0.17m will be selected. this means that the thickness of the GRP material at the root will be 20mm.

The root will be fitted with a steel flange to connect the blade to the hub. In order to relief stress concentration from the GRP material, the flange will be designed as a jacket-like strcture from the inside and outside of the blade material as shown in Figure(2.13). There are many different alternative solutions to the flange design but this is outside the scope of this work. The important criteria is avoiding sudden changes in geometry and keeping the Glass Fibers continuous from root to tip.

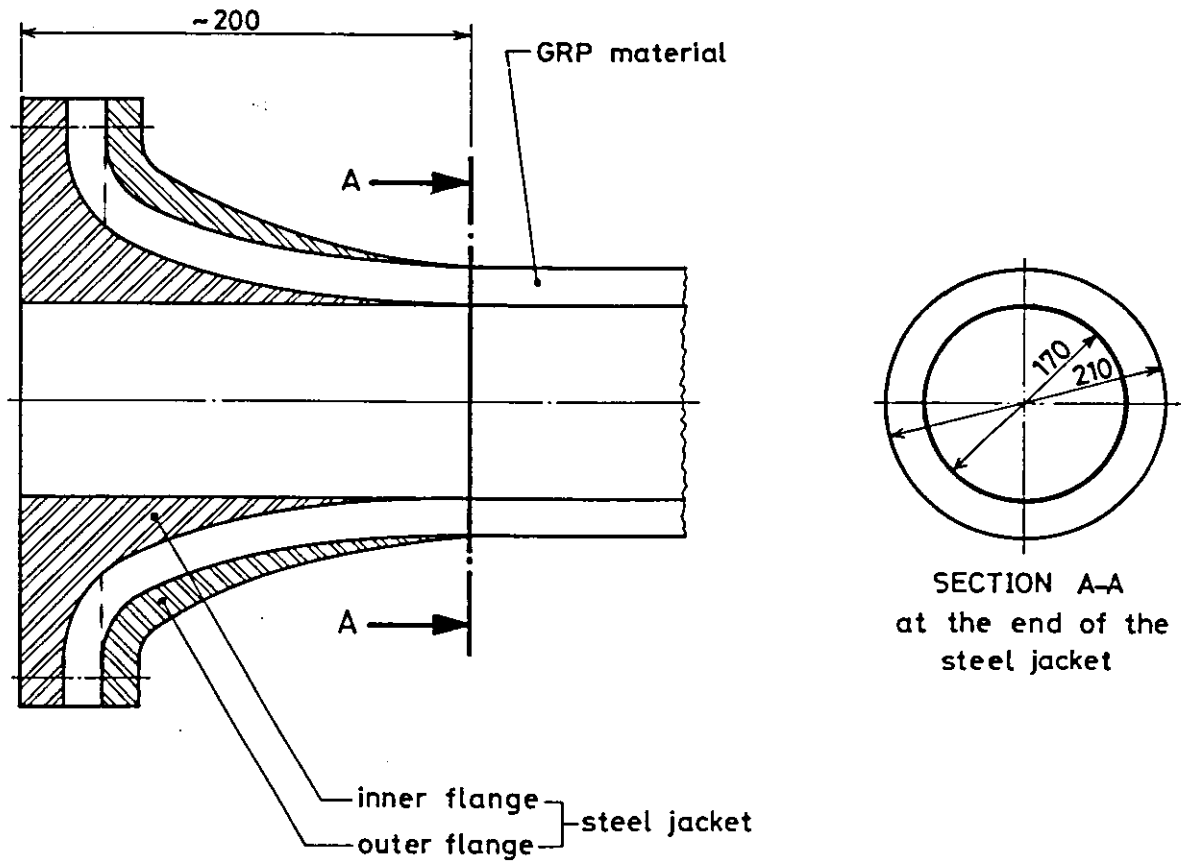

Fig. 2.13 Blade Root Design.

2.5.4 Blade Taper (Flapwise)

Flapwise view of the proposed blade in Figure(2.14) shows the root region and the working region. The working region is the portion of the blade which has the

actual airfoil cross section, and the root region is the portion which compensates geometry between the airfoil profile and the completely circular section at the connection flange, and therefore has no contribution to power generation. The taper of the working region also chosen linear to simplify manufacturing.

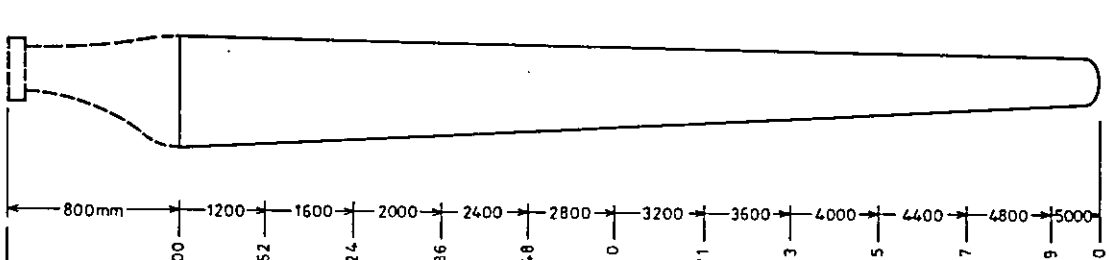

Fig. 2.14: Chord Length Distribution Along the Blade in Millimeters.

For a streamlined body with the dimensions already calculated and defined for the length, root, and tip, the best proportions for the blade according to Figure(2.15) would be when the chord at the begining of the working region is 0.6m and at the tip is 0.2m. This blade shape would have 1.5% efficiency losses from the theoretical optimum as shown by the same figure [19].

The two selected profiles (Figures 2.8 and 2.9) will have to mix with one another somewhere along the blade length. The mixing must be smooth and therefore will be in terms of the two profiles which requires either scaling up or scaling down. The governing parameter for scaling will be the chord of the airfoil section. The chord length distribution will be as shown in Figure(2.14).

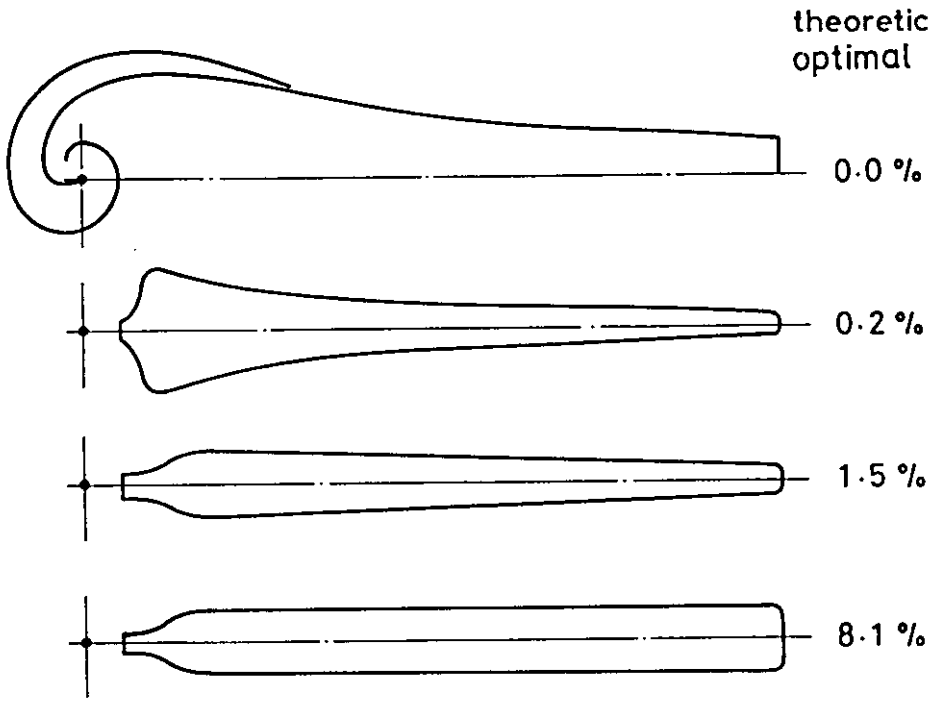

Fig. 2.15: Efficiency Losses Related to Ideal Blade Shape Rotor, Ref.[19].

2.5.5 Blade Thickness (Edgwise)

The blade geometry has two different views; Edgewise, and Flapwise as can be seen in Figure(2.16). The edgwise view defines the blade thickness distribution, and the flapwise view defines the chord length distribution of the selected airfoil.

The thickest portion of the blade must be the root, and viewing the blade from the edgwise position, one concludes that the blade must be tapered down from root to tip for rigidity purposes. The simplest taper (in the working region of the blade) is linear which makes material distribution and manufacturing processes much simpler.

We know that the material thickness at the root is 20mm at each side, and this must be tapered down to the blade tip, but physically, the tip must have a finite thickness at

the point of 5m length in order to have a lower and upper parts of a shell assembly, also to facilitate manipulation of material at the tip. Therefore, the thickness of the tip material will be set at 12mm at each side and allowing 1 to 2mm for resin between them which gives a total thickness at the tip of 25mm.

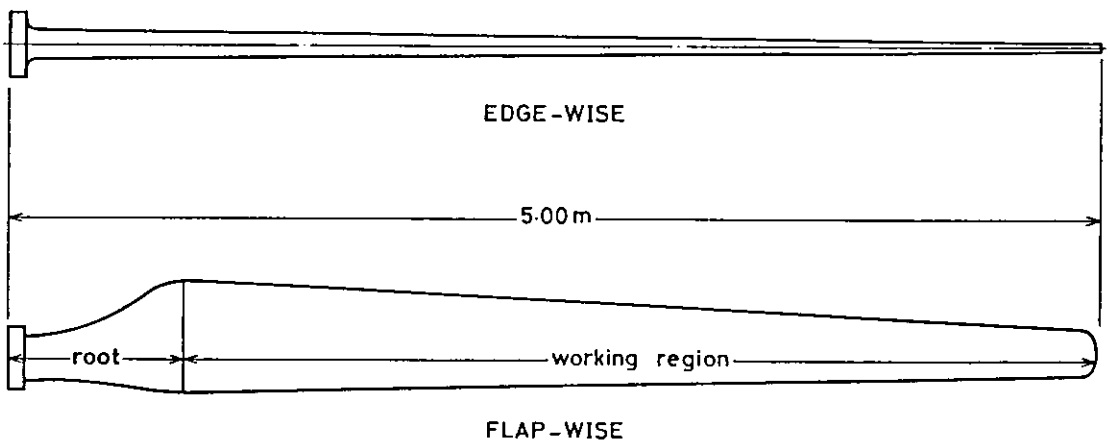

Fig. 2.16: Viewing Rotor Blade Geometry.

The thickness distribution of the blade is calculated in terms of the chord, in other words , the total thickness of the blade at any station will be a percentage of the chord length at that station. The two extreme thicknesses of the blade (210 and 25mm) were established previously, and the thickness distribution must fall between these two values and must also be smooth and steady. Figure(2.17) shows the thickness envelop of this rotor blade design.

Any thickness distribution within this envelop can be selected however under the constraint that thickness must keep steadily decreasing as we move from root to tip along the blade. A linear distribution will be chosen which represents an interpolation between the extreme points, but in order to avoid sudded changes, the distribution curve will be extrapolated as shown in Figure(2.18).

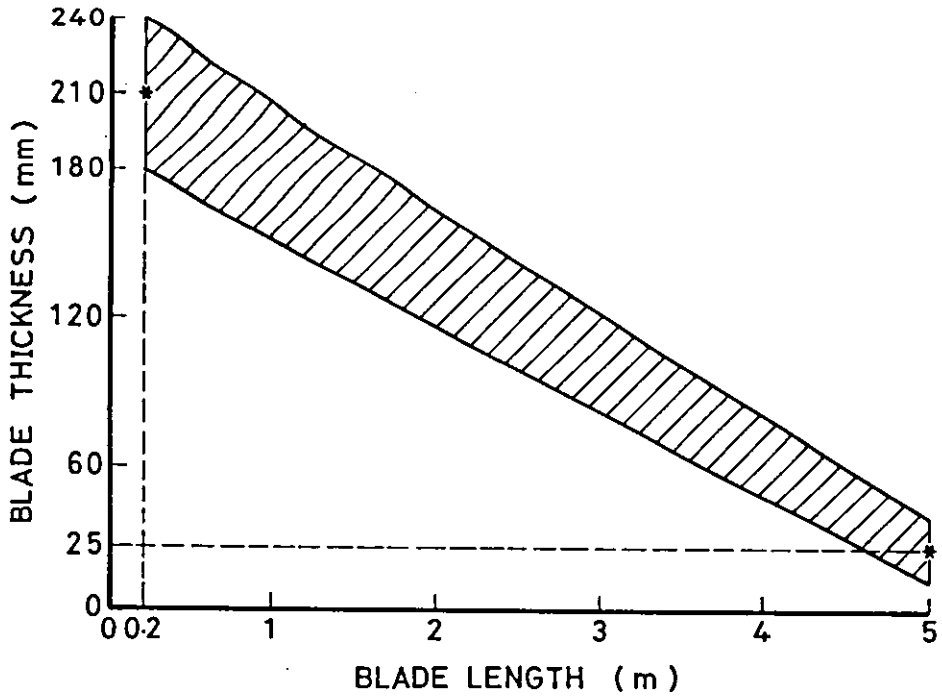

Fig. 2.17: Blade Thickness Envelop.

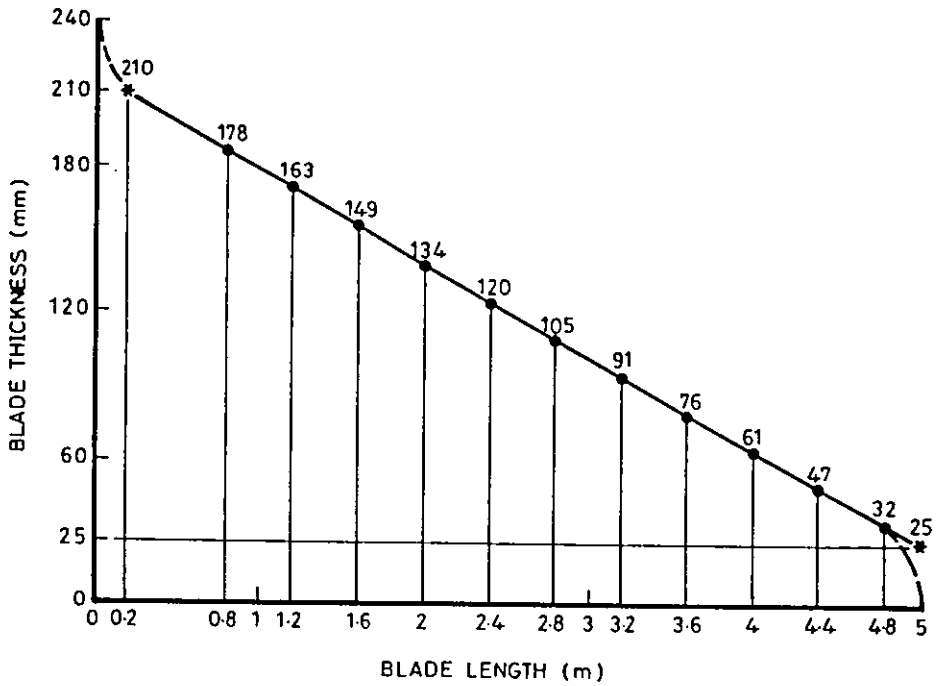

Fig. 2.18 Blade Thickness Distribution.

The higher point is at the edge of the steel flange where this flange should have a curvature (outward) at the end to avoid stress concentration risers. The lower point however cannot fall on the blade because the tip will be chamfered to remove sharp edges for better aerodynamic performance.

2.5.6 Profile Matching

From the airfoil system designation, the two selected profiles (NACA 63-621) and (FX 66-S-196) have maximum thicknesses of 21 and 19.6% of chord respectively. In order to match an airfoil profile to any given thickness, the profile thickness is simply multiplied by a certain percentage that makes it match that thickness. For example, the thickness of the blade at station 0.8m is 178mm which is 29.7% of the chord. Where the chord is 600mm. We have chosen to use (NACA 63-621) in this region, but its thickness is only 21% (i.e 21% of 600mm = 126mm) where it should be 178mm; Therefore, the 21% must be increased by a factor of 1.41 in order to match the thickness at this station.

In this design, the point of mixing the two profiles was chosen at the begining of the last third of the blade which should result in a thick blade. At this point, the FX profile will be inserted but with a small percentage which guarantees a smooth transition from NACA . At the next region however, these percentages will be reversed in favor of FX and depending on the size of the blade, this transition could be carried on for several stations. The following station then will be purely FX with either a scale-up or scale-down factor. Table(2.1) lists the blade parameters with the profile matching sequence.

Table 2.1: Blade Parameters and Profile Matching.

Station (m)	Chord (mm)	Thickness (mm)	Thickness (%)	Profiles
0.8	600	178	29.7	1.41(NACA 63-621)
1.2	562	163	29.0	1.38(NACA 63-621)
1.6	524	149	28.4	1.35(NACA 63-621)
2.0	486	134	27.6	1.31(NACA 63-621)
2.4	448	120	26.8	1.28(NACA 63-621)
2.8	410	105	25.6	1.22(NACA 63-621)
3.2	371	91	24.5	.85(NACA 63-621)+.34(FX 196)
3.6	333	76	22.8	.25(NACA 63-621)+.90(FX 196)
4.0	295	61	20.7	1.06(FX 196)
4.4	257	47	18.3	0.93(FX 196)
4.8	219	32	14.6	0.74(FX 196)
5.0	200	25	12.5	0.64(FX 196)

2.5.7 Blade Twist

The twist of a wind turbine blade is defined in terms of the chord line. It is a synonym for the pitch angle, however the twist defines the pitch settings at each station along the blade according to the local flow conditions. Looking back at the velocity triangle in Figure(2.5), and also as referance [20] expalains, the pitch angle (β) is large near the root (where speeds are low), and small at the tip (where spees are high). This situation suggests a match between the twist and rotational speed, since

the relative wind speed is the vectorial sum of the rotational speed and the free stream wind speed.

Here is a decision point, one has either to fix the rotational speed of the rotor and search for the optimum twist, or fix the twist and find the best rotational speed for the machine. The first choice is better because it is easier for designing the gear and generator. This blade was chosen to rotate at 75 rpm and as a first estimate of the twist we use the equation for twist of zero lift line:

$$\beta = (R/r\ \alpha_t - \dot{\alpha}_t) - k\ (1 - r/R) \quad \text{.....(2.44)}$$

where α_t is the angle of attack at the tip and k is a constant such as ($k > 0$). The zero lift line is the setting angle of the chord line of the profile when the lift is zero. Figur(2.8) and (2.9) show that the zero lift line for the FX profile is at $\alpha_0 = -2.0$ degrees, and that for the NACA profile is at $\alpha_0 = -4.2$ degrees.

Referring to Figure(2.5), the angle of attack at the tip (α_t) can be calculated from the velocity triangle. Knowing that the rotational speed is 75 rpm, this gives a tip speed of 75 rev./min. * min/60sec. * 2π/rev. * 5m = 39.27 m/s . Also taking a mean free stream wind speed of 7m/s which is usually taken as a design wind speed [13], then, from figure(2.5) we get the following:

$\Phi = \tan^{-1}(7/39.27) = 10.1$ degrees.

The pitch angle (β) at the tip is between 0 and 2 degrees, therefore , taking the larger values yield:

$\alpha_t = \Phi - \beta = 8$ degrees.

Using the values of $\alpha_0 = -2$ degrees, α_t becomes 6 degrees, and with equqtion(2.44), a wide band of zero lift twist can be produced for a range of k values as shown in Figure(2.19).

From the design point of view, only the twist distribution that produces the required power level at 75 rpm will be selected. This is a question of how much the rotor should be loaded, where a generator size can be chosen and then one can see how much the rotor is really loaded.

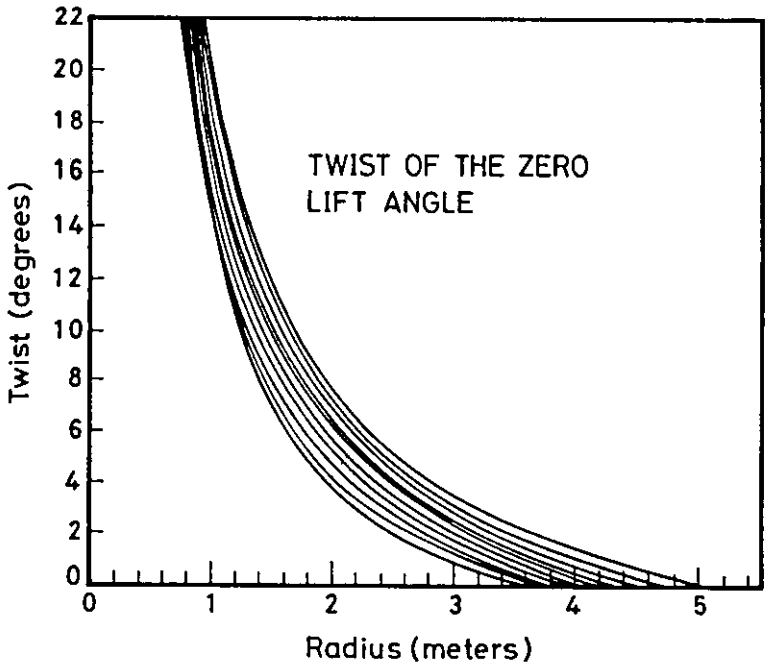

Fig. 2.19: Graph of the Zero Lift Line.

The procedure to calculate wind turbine output using airfoil data was first established by (Wilson & Lissaman,1974) [13], and it reads as follows:

Given the rotor radius (r), number of blaeds (B), chord length (c), lift ($C_l(\alpha)$), drag ($C_d(\alpha)$) pitch angle (β), free stream wind speed (V), and the rotational speed (Ω);

A. Guess a and a′ (a = a′ = 0 is acceptable to start).

B. Calculate Φ from $\tan \Phi = 1\text{-}a / 1\text{-}a' * V/r\Omega$.

C. Calculate α from $\alpha = \Phi - \beta$.

D. Calculate C_l and C_d from graph or table.

E. Calculate C_x and C_y from equations (2-24),(2-25).

F. Calculate a from $a/1\text{-}a = Bc\, C_y / 8\pi r \sin^2 \Phi$.

G. Calculate a′ from $a'/1+a' = Bc\, C_x / 4\pi r \sin^2 \Phi$.

H. Go back to step B and repeat.

Once the above iteration converges, the sectional flow properties will be known and the local contributions to torque and axial forces may be integrated to determine

the overall torque and axial force of the roror. It should be mentioned that airfoil section variations such as twist and blade taper may be accomodated quite easily. A FORTRAN computer code named PROP was written for the above procedure in 1974. This program calculates the theoretical performance of a propeller type wind turbine. It utilized a Simpson's rule method (three-pass technique) for numerical integration. Later, in 1982, this code was modified by Rockwell International under the U.S. Department of Energy Rocky Flats wind System Program (SEACC). The new version was called System Engineering and Analysis (SEA). The new code added several enhancements to the old one by allowing parameters and configuration changes and calculation of annual energy output.

One of the most well developed computer programs written for this purpose is AERODYN™ by Tripod Consult Aps of Denmark. In addition to all the capabilities of the above mentiond software, this aerodynamic program can also calculate a non-axis-symetric airflow. In the folowing, here is a brief description of the different situations handeled by the program :

1- Coning (deg.) = Blade-axis deviation from the rotor plane (0 to 6 deg.)

2- Tilt (deg.) = Inclination of rotor axis from the horizontal (0 to10deg)

3- Yaw (deg.) = Difference between wind directin and rotor axis

4- Hub Height (m) = Height of the rotor center

5- Wind Shear (-) = Wind shear exponent (0.1 to 0.5)

The assumption for calculations are small angles in 1, 2, and 3.

Coning and Tilt are specific for the construction, whereas the wind shear is specific for site where the wind turbine will be located. The value of the Yaw depends on the turbine yaw-strategy, the offset of the wind vane, and changes in wind direction. The program calculates the aerodynamic loads in 18 positions in one revelution, and these aerodynamic loads are added onto the total load on the hub.

Start position for the blades: (with 3 blades)

1) Vertical upward : rotating clockwise.

2) To the right : position = 120 deg. from the top position.

3) To the left : position = 240 deg. from the top position.

Hub loads:

The resulting loads on the blade root (forces and moments) are added together on the hub in a non-rotating coordinate system. The wind turbine is seen from a position in front of the turbine, and the wind is in the back.

FX (N) : Horizontal forces in the rotor plane, positive to the right.

FY (N) : Thrust forces perpendicular on the rotor plane,positive in the wind direction.

FZ (N) : Vertical force in the rotor plane.

MX (N.m) : Tilt moment (Bending moment), around a horizontal axis, positive to the right.

MY (N.m) : Driving moment on the main shaft.

MZ (N.m) : Yaw moment (Bending moment), around a verical axis , positive upwards.

The various twist distributions will be judged for their power output at three different wind speeds namely (4,10, and 16m/s). Table(2.2) shows the input data to AERODYN™ for a twist distribution of 18 degrees. The rotor power output is calculated at 75 rpm and zero pitch angle at the tip as shown in the table and the results of the calculations are given in Table(2.3) for different twist distibutions at the indicated wind speeds.

Table 2.2: Input Data to the AERODYN™ program.

```
********************************* INPUT DATA *********************************

DATE: 06-20-93                                              PC-PROGRAM: ADYN_S
TIME: 14:20:00                                        (C) TRIPOD CONSULT ApS

ROTOR NAME: Glassfiber Re-enforced Plastic Blades
            NACA 63-621 -------> FX-S 196

PROFILE    : FX66S

BLADE DATA:       RADIUS        CORD        TWIST      THICKNESS
                  (M)           (M)         (DEG)        (%)
                   .800         .600        18.00        29.70
                  1.200         .562        14.40        29.00
                  1.600         .524        11.10        28.40
                  2.000         .486         8.20        27.60
                  2.400         .446         6.10        26.80
                  2.800         .410         4.70        25.60
                  3.200         .371         3.10        24.50
                  3.600         .333         2.50        22.80
                  4.000         .295         1.40        20.70
                  4.400         .257          .70        18.30
                  4.800         .219          .10        14.60
                  5.000         .200          .00        12.50

   INFLOW CONDITIONS                        :    AXI-SYMMETRIC
   NUMBER OF BLADES                         :       3
   DIAMETER                                 :     10.90 M
   ROTOR SPEED     (RPM) (FROM,TO,STEP):     75.00     75.00      .00
   PITCH           (DEG) (FROM,TO,STEP):       .00       .00      .00
   WIND SPEED      (M/S) (FROM,TO,STEP):      4.00     16.00     6.00
   DENSITY OF AIR                           :     1.23 KG/M**3

   CALC.POINT:    RADIUS        CORD        TWIST      THICKNESS
                  (M)           (M)         (DEG)        (%)
                  1.250         .600        18.00        29.70
                  1.947         .534        11.95        28.55
                  2.609         .470         7.36        27.28
                  3.225         .412         4.79        25.67
                  3.783         .358         2.90        23.93
                  4.273         .312         1.89        21.63
                  4.686         .273          .99        19.28
                  5.016         .241          .45        16.76
                  5.256         .218          .10        14.54
                  5.401         .205          .02        13.01

******************************************************************************
```

Table 2.3: P(4 m/s), P(10 m/s), and P(16 m/s) for the 4-twist distributions.

Twist(deg.)	rpm	Pitch(deg.)	P(4) (kW)	P(10) (kW)	P(16) (kW)
22	75	0.0	1.06	20.13	23.38
20	75	0.0	1.00	19.45	21.95
18	75	0.0	1.03	19.50	22.11
16	75	0.0	0.98	19.03	21.22

The power level is very close for the four twist distributions and for fast running blades the smallest one (16-degree distribution) will be chosen which fits a generator output of 15 kW as follows:

The rotor output is 19.03 kW, and with gearbox efficiency of 0.93 and generator efficiency of 0.85, the overall power output will be;

P = 19.03 * 0.93 * 0.85 = 15.05 kW of electric power which will be the rated power of a wind turbine equiped with the above blades.

This concludes the detemination of the blade data as described in Table(2.4) and the geometry of the of the blade is completely defined which will allow the determination of the blade loads and other aerodynamic characteristics.

Table 2.4: Complete Blade Data

Station (m)	Chord (mm)	Thickness (mm)	Thickness (%)	Twist (deg.)	Profile NACA 63-621 = N21 FXS 66-196 =F196
0.8	600	178	29.7	16.0	1.40(N21)
1.2	562	163	29.0	12.8	1.38(N21)
1.6	524	149	28.4	10.1	1.35(N21)
2.0	486	134	27.6	7.8	1.31(N21)
2.4	448	120	26.8	5.8	1.28(N21)
2.8	410	105	25.6	4.2	1.22(N21)
3.2	371	91	24.5	2.8	.85(N21)+.34(F196)
3.6	333	76	22.8	1.8	.25(N21)+.90(F196)
4.0	295	61	20.7	0.9	1.06(F196)
4.4	257	47	18.3	0.4	.93(F196)
4.8	219	32	14.6	0.2	.74(F196)
5.0	200	25	12.5	0.0	.64(F196)

2.6 Aerodynamic Loads

The blade geometry acquired in the previous section forms the main data necessary to formulate a model in order to calculate the aerodynamic loads and other data such as the operating parameters. A rotor code called LOADS was developed at Oregon State University in1989 to analyze blade loads for rigid rotors of simple geometry including flapwise flexing and unsteady aerodynamics [4]. The rotor is not allowed to yaw and the rotation is constant with no pitch variations allowed.

For yaw considerations, there is a special code called YawDyn [21]. This program also considers blade flapwise loads and motion and their effects on yaw loads, or, in the case of a free-yaw system the yaw motion. Wind shear, tower shadow and a time-varying wind vector as well as rotor geometry and airfoil characteristics are input to the model. A quasi-steady state strip theory is employed in the aerodynamic analysis and static stall is considered by using airfoil tables. The model makes no assumptions of small yaw angles, though it does assume small flap defflections.

There are many other poweful computer programs for blade loads calculations such as MOSTAB and SEACC, but the most reliable as was mentioned earliear is AERODYN™ which will be used here to predict the blade loads at all positions and yaw angles, and wind speeds. The data input to the program will be the blade geometry as shown in Table(2.4) and will be run for a range of wind speeds and pitch angles, in addition to twelve different yaw positions. Table(2.5) gives the maximum values of the six major components (forces and moments).

Where:

FX (N/m) : Force per length of the blade , edgwise.

FY (N/m) : Force per length of the blade , flapwise.

FXs (N) : Shear force ,edgewise.

FYs (N) : Shear force , flapwise.

MX (N.m) : Bending moment , edgwise.

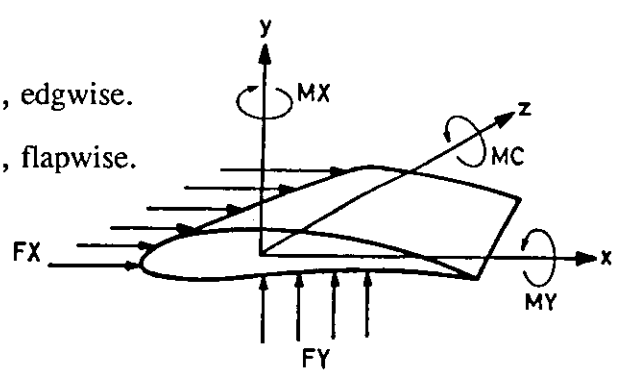

Fig. 2.20 : Aerodynamic Loads and Moments.

MY (N.m): Bending moment , flapwise.

MC (N.m): Bending moment around local chord.

Table 2.5: Blade Loads and Moments Along the Blade During Normal Operation at A Maximum Wind Speed of 25m/s and Zero Pitch Angle.

Radial	Forces and Moments						
Position (m)	FX (N/m)	FY (N/m)	FXs (N)	FYs (N)	MX (N.m)	MY (N.m)	MC (N.m)
0.00	0	0	335	1561	1055	5286	0
1.25	140	320	355	1561	612	3334	3374
1.95	115	346	266	1329	397	2326	2359
2.61	97	373	196	1091	245	1523	1542
3.23	83	394	140	855	142	923	931
3.78	71	401	98	633	76	508	511
4.27	63	400	65	473	36	246	246
4.69	57	391	40	273	15	99	99
5.02	53	374	22	147	4	30	30
5.26	52	359	9	60	1	5	5
5.40	54	344	1	8	0	0	0
5.45	0	0	0	0	0	0	0

The shear force (flapwise) and the bending moment (flapwise) are the dominant components and therefore will be studied at different settings of pitch angles (from $\beta = 0$ to $\beta = 40$ degrees). Table (2.6) shows the input data for these conditions to the AERODYN™ program.

Table 2.6: Input Data For Blade Loads Calculations at Various Pitch Angles.

```
********************************** INPUT DATA **********************************

DATE: 06-30-93                                                  PC-PROGRAM: ADYN_5
TIME: 12:25:13                                                (C) TRIPOD CONSULT ApS

ROTOR NAME: Glassfiber Re-inforced Plastic Blades
            NACA 63-621 -------> FX-S 196

PROFILE    : FX66S

BLADE DATA:      RADIUS        CORD        TWIST      THICKNESS
                 (M)           (M)         (DEG)        (%)
                  .800         .600        16.00        23.70
                 1.200         .562        12.80        29.00
                 1.600         .524        10.10        28.40
                 2.000         .486         7.80        27.60
                 2.400         .448         5.80        26.80
                 2.800         .410         4.20        25.60
                 3.200         .371         2.80        24.50
                 3.600         .333         1.80        22.80
                 4.000         .295          .90        20.70
                 4.400         .257          .40        18.30
                 4.800         .219          .20        14.60
                 5.000         .200          .00        12.50

   INFLOW CONDITIONS                        :    AXI-SYMMETRIC
   NUMBER OF BLADES                         :       3
   DIAMETER                                 :     10.90 M
   ROTOR SPEED     (RPM) (FROM,TO,STEP):      75.00     75.00       .00
   PITCH           (DEG) (FROM,TO,STEP):        .00     40.00      4.00
   WIND SPEED      (M/S) (FROM,TO,STEP):       3.00     25.00      1.00
   DENSITY OF AIR                           :     1.23 KG/M**3

   CALC.POINT:   RADIUS        CORD        TWIST      THICKNESS
                 (M)           (M)          (DEG)       (%)
                 1.250         .600        16.00        29.70
                 1.947         .534        10.79        28.55
                 2.609         .471         7.00        27.28
                 3.225         .412         4.30        25.67
                 3.783         .358         2.47        23.93
                 4.273         .312         1.30        21.63
                 4.686         .273          .60        19.28
                 5.016         .241          .32        16.76
                 5.256         .218          .19        14.54
                 5.401         .205          .05        13.01

*******************************************************************************
```

As shown in Table(2.6), the maximum operating wind speed is 25m/s and the pitch angle range is from zero to 40 degrees in increments of 4 degrees. The rotational speed is fixed at 75 rpm. The maximum values of shear and bending moments realized at 25m/s for these conditions are given in Tables(2.7) and (2.8).

Table 2.7: Maximum Shear Forces For Different Pitch Angles

Radial Position (m)	Pitch Angle Settings (β^o) 0	4	8	12	16	20	24	28	32	36	40
0.00	1561	1497	1440	1392	1347	1314	1255	1115	893	619	0
1.25	1561	1497	1440	1392	1347	1314	1255	1115	893	619	0
1.95	1329	1276	1231	1197	1168	1148	1099	971	760	485	170
2.61	1091	1048	1016	996	978	966	926	809	596	338	153
3.23	855	823	803	793	781	755	746	626	423	209	111
3.78	633	612	601	597	586	589	561	437	273	110	57
4.27	437	423	418	415	407	417	381	276	159	45	0
4.69	273	266	262	259	256	266	226	155	81	11	-9
5.02	147	143	142	138	141	142	113	74	35	-1	-17
5.26	60	58	58	56	60	55	42	27	12	-2	-21
5.40	8	8	8	8	9	7	6	3	1	0	-21
5.45	0	0	0	0	0	0	0	0	0	0	0

It can be seen from the two tables that the maximum values occur near the blade root which indicates the necessaty to emphasize the special attention required for this region. Much higher loads would occur if the wind is blowing at skew angle relative to the blade which is called yaw effect. Another computer run was made to calculate the loads resulting from a 30-degree yaw angle which can be considered the maximum skew encountered during continuous operation. For strength and stress analysis

purposes, only the force per length disribution (flapwise) will be calculated which represents the maximum load in the most critical direction. Furthermore, and according to the German DIN, blade loads shall be calculated at an extreme gust of 42m/s as shown in Table(2.9).

Table 2.8: Maximum Bending Moment For Different Pitch Angles.

Radial Position (m)	Pitch Angle Settings (β^o)										
	0	4	8	12	16	20	24	28	32	36	40
0.00	5286	5079	4914	4791	4673	4604	4378	3767	2832	1737	807
1.25	3334	3207	3114	3051	2989	2962	2809	2374	1716	964	372
1.95	2326	2240	2182	2148	2111	2102	1987	1645	1138	577	168
2.61	1523	1469	1438	1420	1400	1401	1315	1054	687	304	48
3.23	923	893	877	869	857	864	799	611	373	136	-4
3.78	508	492	485	481	475	484	433	314	179	48	-15
4.27	246	239	236	232	232	237	202	140	74	11	-11
4.69	99	96	95	93	95	95	77	51	25	1	-5
5.02	30	29	29	28	29	28	22	14	6	-1	-2
5.26	5	5	5	5	5	5	3	2	1	0	0
5.40	0	0	0	0	0	0	0	0	0	0	0
5.45	0	0	0	0	0	0	0	0	0	0	0

This load distribution is plotted in Figure(2.21) to show the loading configuration during maximum operating conditions. The area under the curves was also graphically integrated to identify the total load. The curves obtained here can be compared with the one presented in Figure(2.11). It is noticed that the total load under the 42m/s curve represents load case 2 in section 2.5.3.

Table 2.9: Blade Loads FX(N/m) and FY(N/m) Distributions For 25 and 42m/s Wind Speeds Respectively and 30 Degree Yaw and Zero Pitch Angles.

	Radial Position (m)											
	0.0	1.25	1.95	2.61	3.23	3.78	4.27	4.69	5.02	5.26	5.40	5.45
FY (25m/s)	0	395	468	531	578	603	611	598	557	531	513	0
FX (25m/s)	0	200	182	166	152	139	130	121	107	103	109	0
FY (42m/s)	0	908	996	1047	1062	1043	1003	948	886	833	791	0
FX (42m/s)	0	414	336	276	227	189	162	142	129	123	124	0

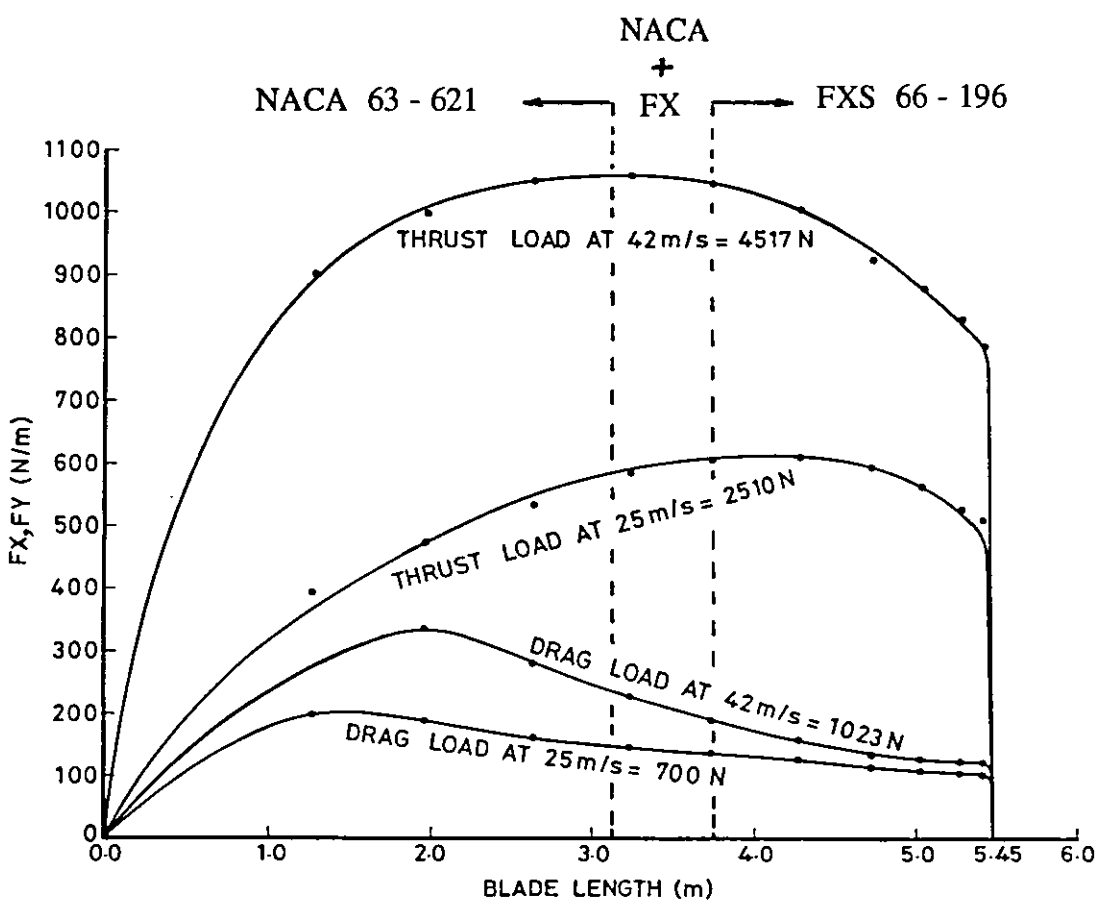

Fig. 2.21: Load Distibution Configuration (N/m) For 25 and 42m/s Wind Speeds.

Chapter 3

STRENGTH & STRESS ANALYSIS

3.1 General

The blade geometry obtained in the previous chapter is one of the most complex shapes encountered in engineering problems. The combination of different airfoil sections at different geometric positions with twist and variable thickness and chords, added to the large physical size of the model, make it extremely difficult to analyze using conventional techniques. Therefore, Finite Element Methods (FEM) will be the ultimate choice of solution, however, some compromises must be made when close accuracy is required from large physical models.

3.2 Geometric Solid Modelling

In order to utilize FEM, a solid model for the blade must be created first to define the surface boundaries and volume contained within it. The contained volume will determine the shape and number of elements that could be used in the analysis.

One of the most powerful solid modelers is the ARIES™ Mechanical Computer Aided Engineering Design (MCAED) software used by the Renewable Energy Research Center (RERC) at the Royal Scientific Society. This package is developed by Aries Technology in Lowell, Massachusetts, USA, especially for mechanical engineering design and analysis of mechanical elements and therefore will be used here to analyze the strength chracteristics of our 5-meter blade in this study.

The solid model is created in ARIES™ in three steps:

Step 1: Depending on the designer's judgment and knowledge of the design at hand, only four section curves (drawn according to the geometry obtained in chapter 2) at four different locations along the blade will be needed as shown in Figure(3.1).

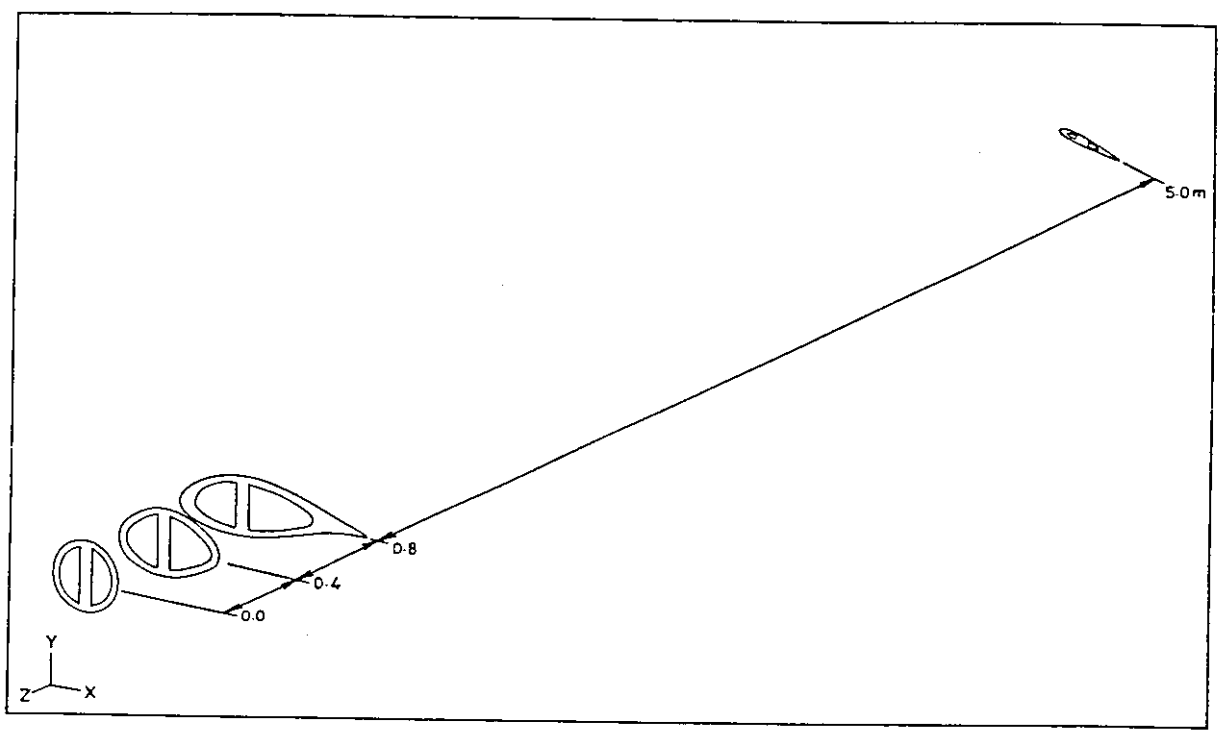

Fig. 3.1: Minimum Number of Section Curves For the Blade.

Step 2: A solid skin is then created for the two inner cavities by linking the four internal curves with straight lines (called pathe curves). These path curves or links must be pricisely positioned at the selected section curves and must not cross one another and also be continuous. The optimum number of links will be selected by the computer if a large number of links was supplied by the user. Once the selection procedure is finished, the computer is ordered to create a solid skin that covers the curves exactly in a three-dimensional space. The same procedure is repeated to create the solid skin for the outer curves as shown in Figures(3.2) and (3.3).

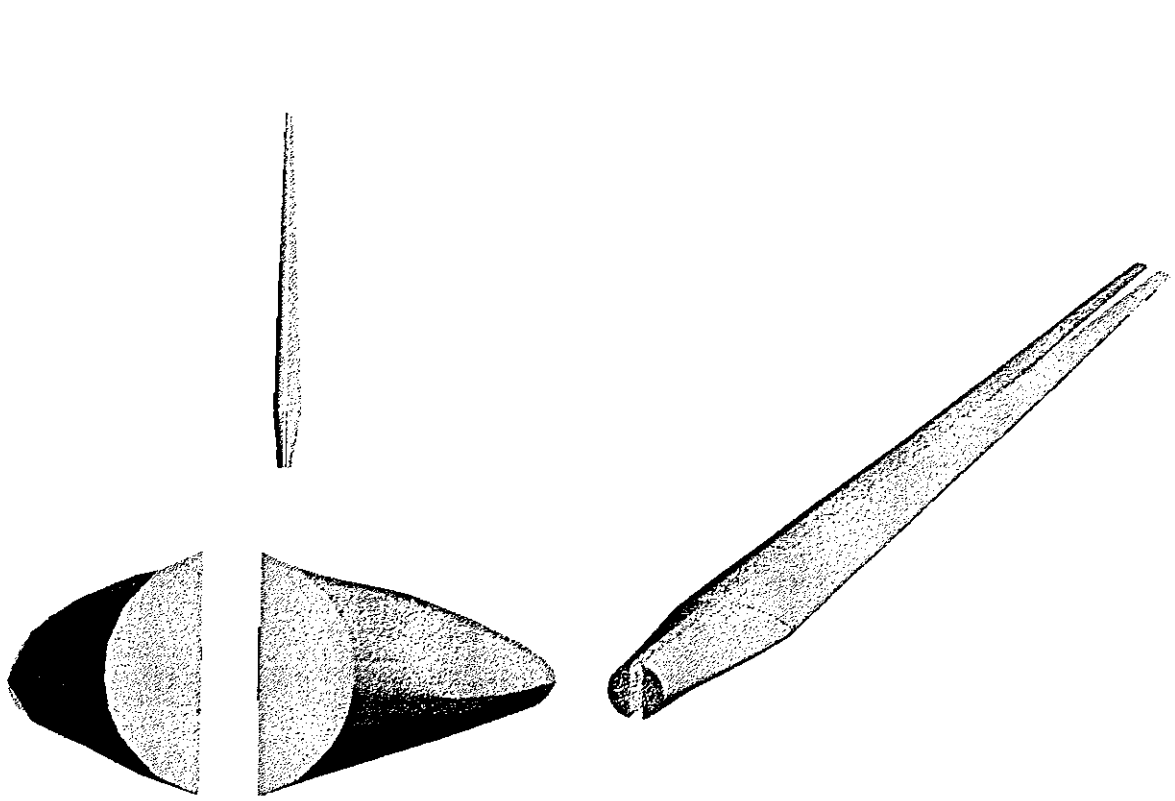

Fig. 3.2: Solid Skin For the Two Inner Cavities of the Blade.

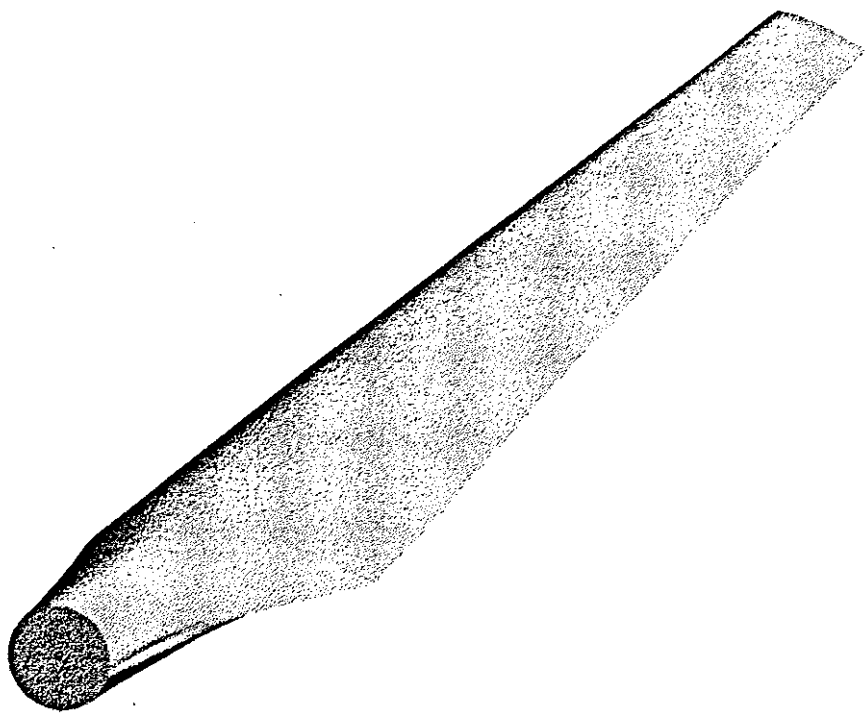

Fig. 3.3: Solid Skin For the Outer Blade Surface.

Step 3: In order to create a true solid model that resembles the blade, the two inner parts will be subtracted from the outer skin which should yield the exact solid geometry of our blade as can be seen in Figure(3.4).

3.3 Section and Mass Properties

The above geometry is assigned a Glassfiber Reinforced Plastic material with the following mechanical properties given in Table(3.1):

Table 3.1: GRP Mechanical Properties

Density	= 1.4 x 10^{-6} kg/mm^3
Tensile Yield Strength	= 63 N/mm^2
Ultimate Tensile Strength	= 129 N/mm^2
Modulus of Elasticity	= 6000 N/mm^2
Compressive Strength	= 170 N/mm^2
Shear Modulus	= 2542.4 N/mm^2
Possion's Ratio	= 0.18
Glass Content	= 50 %

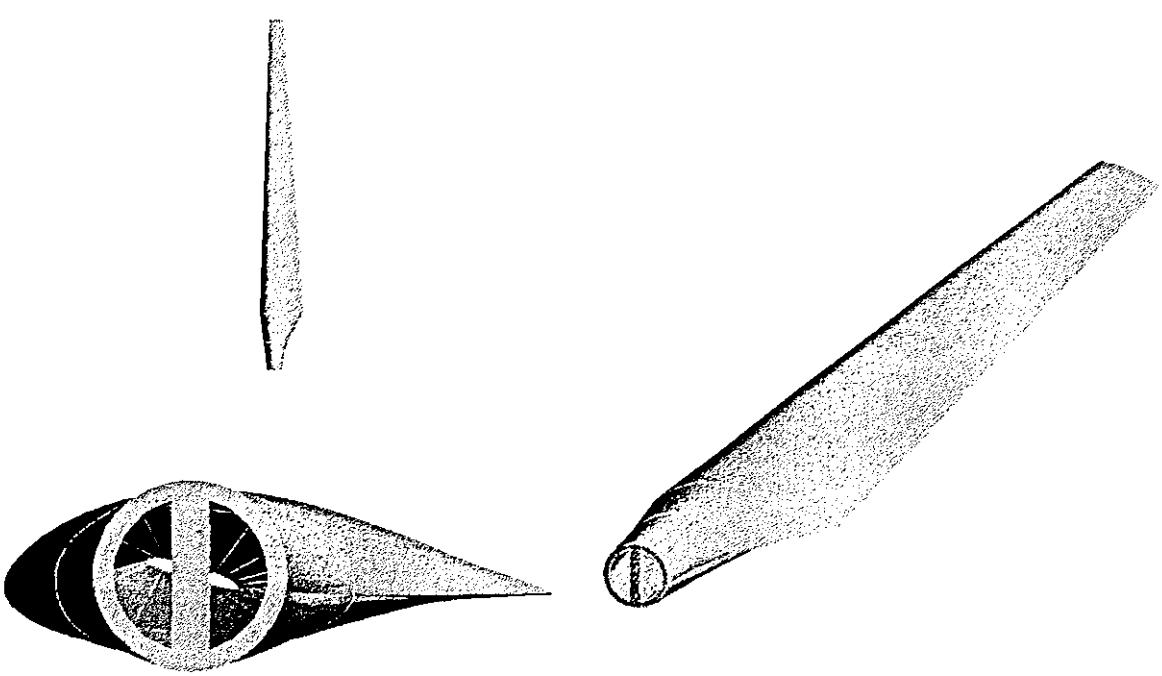

Fig. 3.4: Complete Solid Geometric Model of the Blade

The second moment of area (I_x , I_y) are calculated for the four critical sections shown in Figure(3.1) and given in Figure(3.5), which shows the sectional area

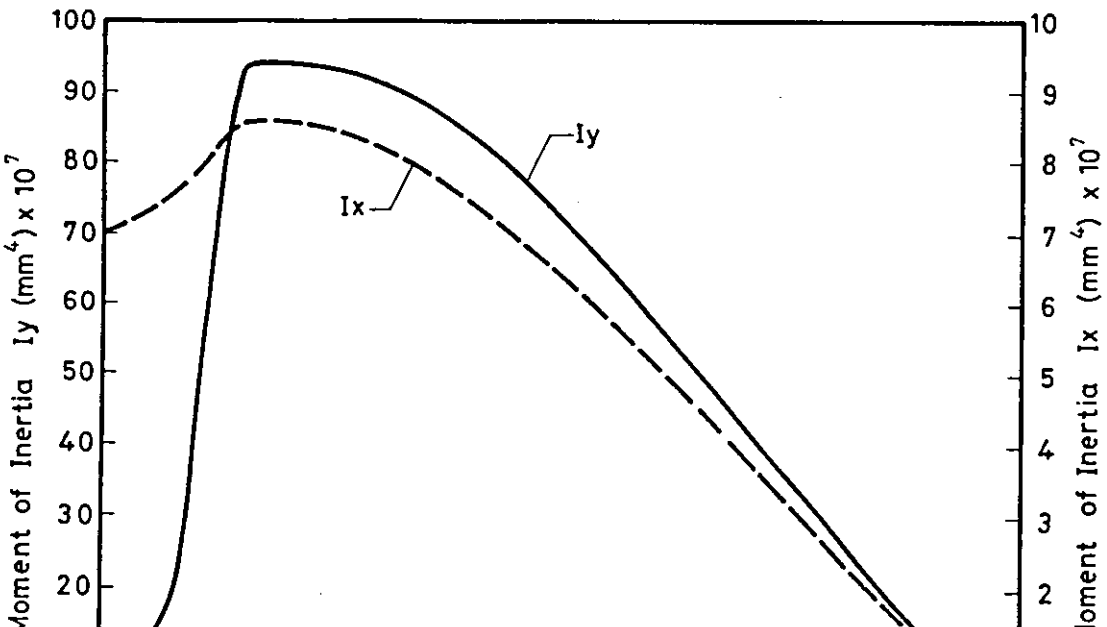

Fig. 3.5 : Second Moment of Inertia I_x, I_y Distribution Along The Blade

moment of inertia distribution from root to tip. The blade mass properties are also calculated and given in Table(3.2).

Table 3.2: Blade Mass Properties

Weight = 1156.87 N		Mass = 117.97 kg
Volume = 8.4263×10^7 mm^3		Density = 1.4×10^{-6} kg/mm^3
Area = 7.4522×10^6 mm^2		gc = 9.80665 N/kg
Properties With Respect to Origin at .....(mm)		
O_x = 0.0	O_y = 0.0	O_z = 0.0
Mass Moment of Inertia (kg/mm2)		
$I_x = 2.544 \times 10^8$	$I_y = 2.560 \times 10^8$	$I_z = 2.172 \times 10^6$
Center of Gravity (mm)		
C_{gx} = 44.27	C_{gy} = 17.59	C_{gz} = -1668

3.4 Finite Element Modelling

The first phase of the analysis using FEM begins with understanding the structural behaviour of the part, the characteristics of the material used, and the load and restraint conditions. The rotor blade is required to transmit torque to the rotor shaft and in due course will be subjected to the various aerodynamic loads mentioned previously in Tables (2.7) and (2.8), in addition to centrifugal forces.

From the structural point of view, the blade is a cantilever beem, however, it has a complex geometry and the loading configuration and distribution depend on this geometry. The finite element method which will be used in this context is the process of using software prototypes to numerically and graphically simulate the behaviour of the blade. Therefore, the application of the finite element method is called the finite element process.

Finite element modelling consists of three phases, as shown in Figure(3.6) and as described in ARIES™ software manuals [22].

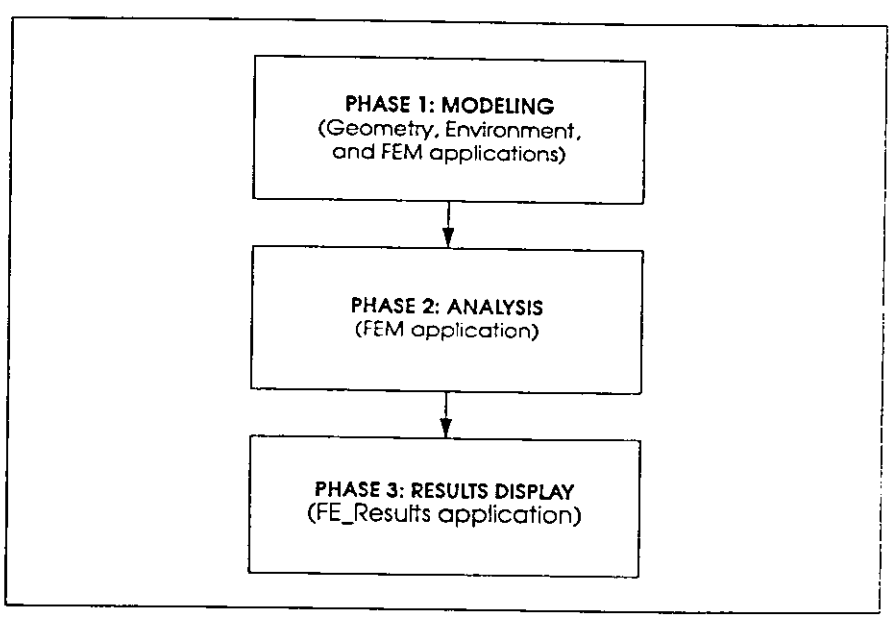

Fig. 3.6: Phases of Finite Element Modelling.

Modelling is the pre-processing phase of the finite element process. In this phase, the geometry is created, the loading and restraining conditions will be defined, and then, a finite element model that divides the part into elements and nodes is built. The nodes and elements can be generated by ARIES™ manually or automatically. However, in both cases, the geometry of the part must have reasonable dimensions. This means that if the part has small edges compared to the bulk of the solid part, the mesh generator will create excessive density of elements at this edge. In the blade model of airfoil sections, this problem cannot be avoided because the trailing edge of the airfoil is much smaller than most of the blade body. Furthermore, when dividing the blade into sevsral regions, the region containing the small edges required enormouse amount of elements. Therefore, a compromise must be made where the attention should be directed and focused on solving for the critical part of the blade (i.e., the root region). This requires rearranging the loads on the blade but still having the original loading situation.

The root region is 0.8m long and fixed at the root flange where no translational or rotational displacements are allowed. The loads on the blade will be shifted to this section as follows:

Taking the maximum loads on the blade at 42m/s from Table(2.9) and Figure(2.21) we get:

Maximum thrust load (flapwise) FY = 4.517 kN which is applied at the aerodynamic center of the blade 2/3ed the blade length from the root. Then, in order to transfer this force to the end of the root section (0.8m) from the root (i.e., 2.5333m closer to the root), we will get this force and a moment M (moment of force about the root), i.e.:

FY = 4.517 kN

M X = 4.517 kN * 2.5333 m = 11.4431 kN.m

Also, the maximum darg load edgewise FX = 1.023 kN, and applying the same principle yields:

FX = 1.023 kN

MY = 2.5916 kN.m

The blade is also subjected to a centrifugal force F_c due to rotational motion. This force is simply:

$$F_c = m\Omega^2 r_{cm} \quad \text{.....(3-1)}$$

where; m = 117.97 kg (the blade mass).

Ω = 100 rpm (rotor overspeed from the design rpm of 75).

r_{cm} = 1.668 m (blade center of mass measured from the root).

Hence;

F_c = 117.97 kg * (100 rev./min *1 min./60 sec. * 2π/rev.)^2 *1.668 m = 21.58 kN

At this point, the geometry, the restraint, and the load conditions are all avilable. The root region geometry will be meshed using a TETRAHEDRON element from the ARIES™ library which is a solid element because the nodes of this element specify its geometry completely so as no additional properties of the material are required, see Figure(3.7). The order of this element is linear with 4 nodes and three degrees of freedom. The completely meshed root region by the ARIES™ automatic mesh generator is shown in Figure(3.8), where the loads and restraints are also imposed.

3 - Degrees of Freedom
at the nodes.
Translation
TX , TY, TZ

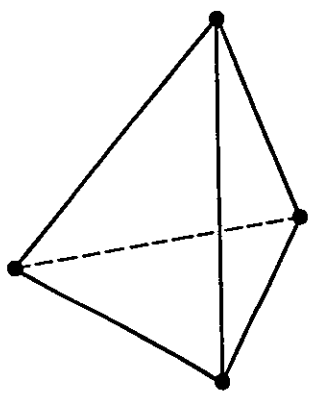

Fig. 3.7 Tetrahedron Element

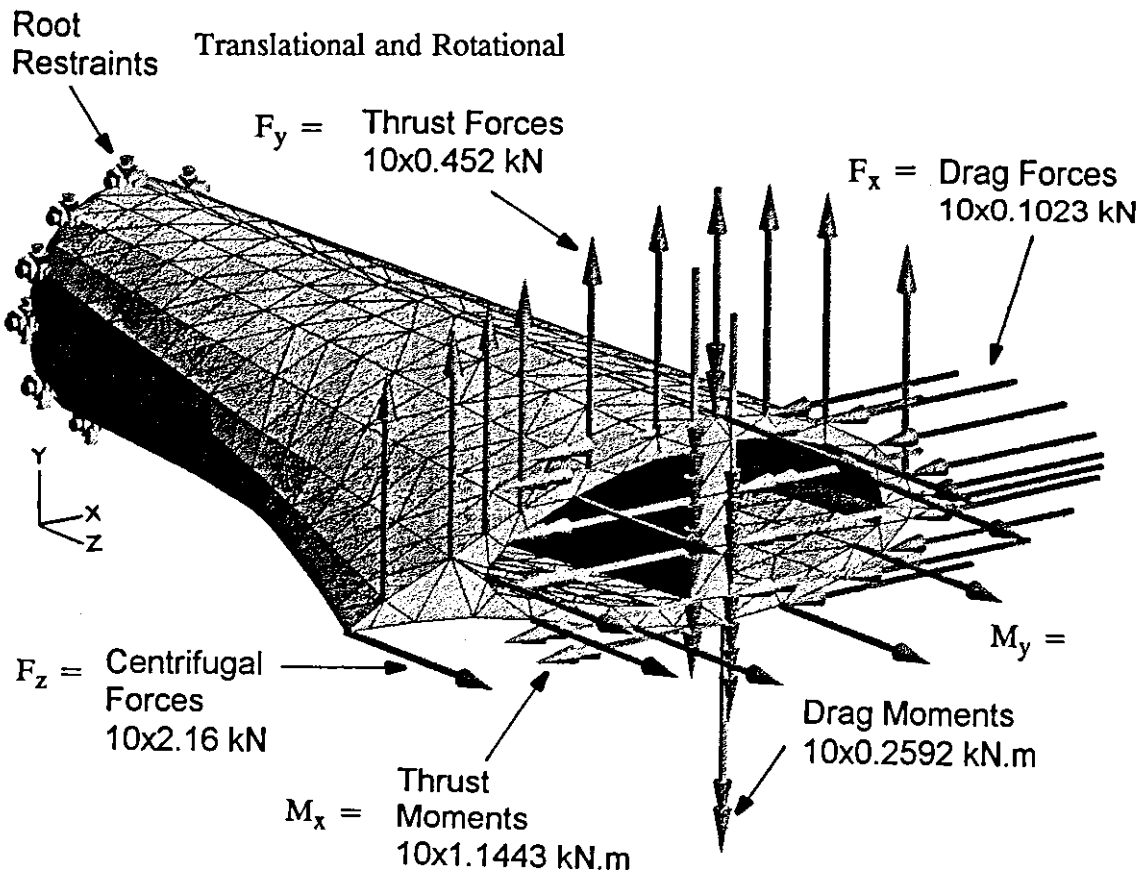

Fig. 3.8: Complete FE Model of the Rotor Blade Root Region by ARIES™.

The modelled region contains 1103 nodes and 3867 elements. The model at this point is considered complete and ready to be submitted to the built-in module of the well known FE package ANSYS™ within ARIES™ in order to be analyzed.

This is the second phase of the FE modelling which is the processing phase. The FE model is submitted internally (within ARIES™ environment) to ANSYS™. ANSYS™ first checks the model and identifies the space coordinates of each node and element and makes sure that the model is coherent and the boundary conditions and loads are also well defined at the indicated nodes.

The following information is given by ARIES™ after ANSYS™ has finished the processing phase successfully:

```
Model name                    = fe 1
Model type                    = Linear Static General 3D
Analysis code                 = ANSYS
Model DOF                     = TX TY TZ RX RY RZ
Number of:
 elements                     = 3867
 nodes                        = 1103
Pending results for model (if any):
Existing results for model (if any):
Model name                    = fe 1
model restraints:
Number of:
 nodal_translational_restraint = 10
 nodal_rotational_restraint = 10

Model name                    = fe 1
Result Case name              = LINEAR_STATIC_7
Code                          = ANSYS
Type                          = Linear Static General 3D
Start time                    = Sat Dec 25 14:01:39 1993
Completion time               = Sat Dec 25 14:10:39 1993
Restraint case name           = rc 2
 geom restraints              = 0
Load case name                = lc 2
 geom loads                   = 0
model loads:
Number of:
 nodal_force                  = 30
 nodal_moment                 = 20
```

The third and final phase is the results display. This is the post processing phase of the finite element modelling process. The most important information required here are the displacements and stresses resulted from the applied loads. Figure(3.9) shows a graphical display of the analysis results where the color contours indicate the range of stress present in the part, the deformed geometry and a displacement curve gives the maximum deflection magnitude in the XY plane. The result of the analysis shows that the maximum principal stress at the root is 9.348 N/mm^2. When this is compared to the yield strength of the GRP which is 63 N/mm^2, it means that we have a factor of safety equals 6.74. This value is also compared to the root stress σ_{root} = 45 N/mm^2 which was found in section 2.5.3 for a factor of safety equals 2.

The difference of the two results is due to the centrifugal and drag forces added to the model in the FEM analysis and the additional cross sectional area at the root section represented by the rectangular spar at the balde center. The strain at the lower-most fiber which suffers maximum tension is 0.15%, and according to the certification criteria of [18], this value is below the allowable 0.3 %.

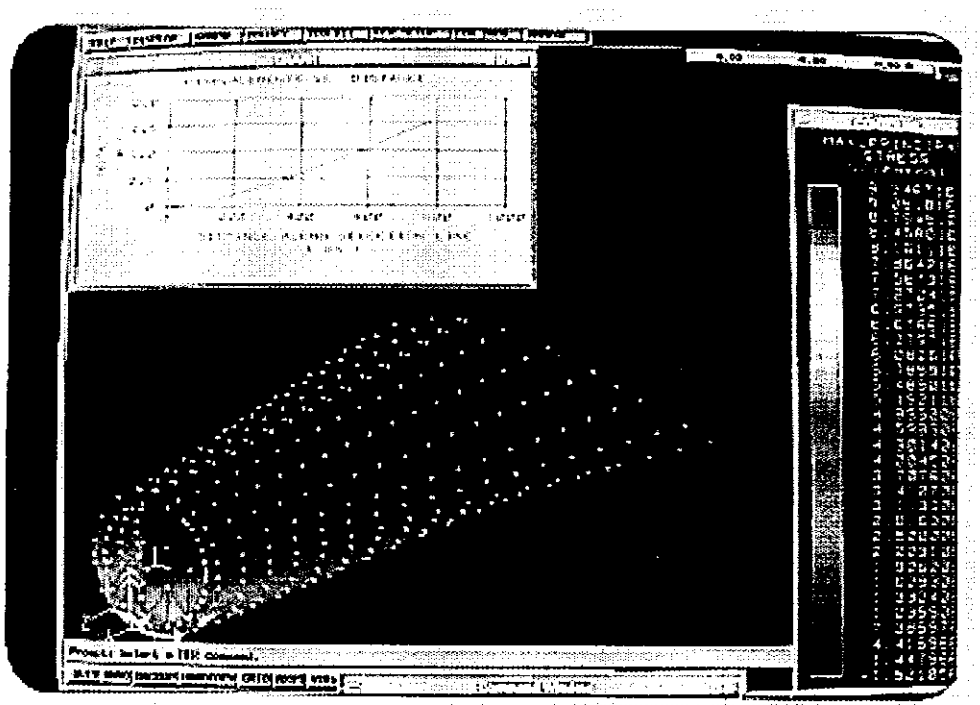

Fig. 3.9: FE-Results Display After Completing the Finite Element Analysis Using ANSYS™ Module Witin ARIES™.

The blade deflection curve for the root section is shown in Figure(3.9), however, a curve fit is made to this portion of the blade in order to predict the overall deflection curve, and a linear extrapolation is used on the available data and a plot is produced as shown in Figure(3.10):

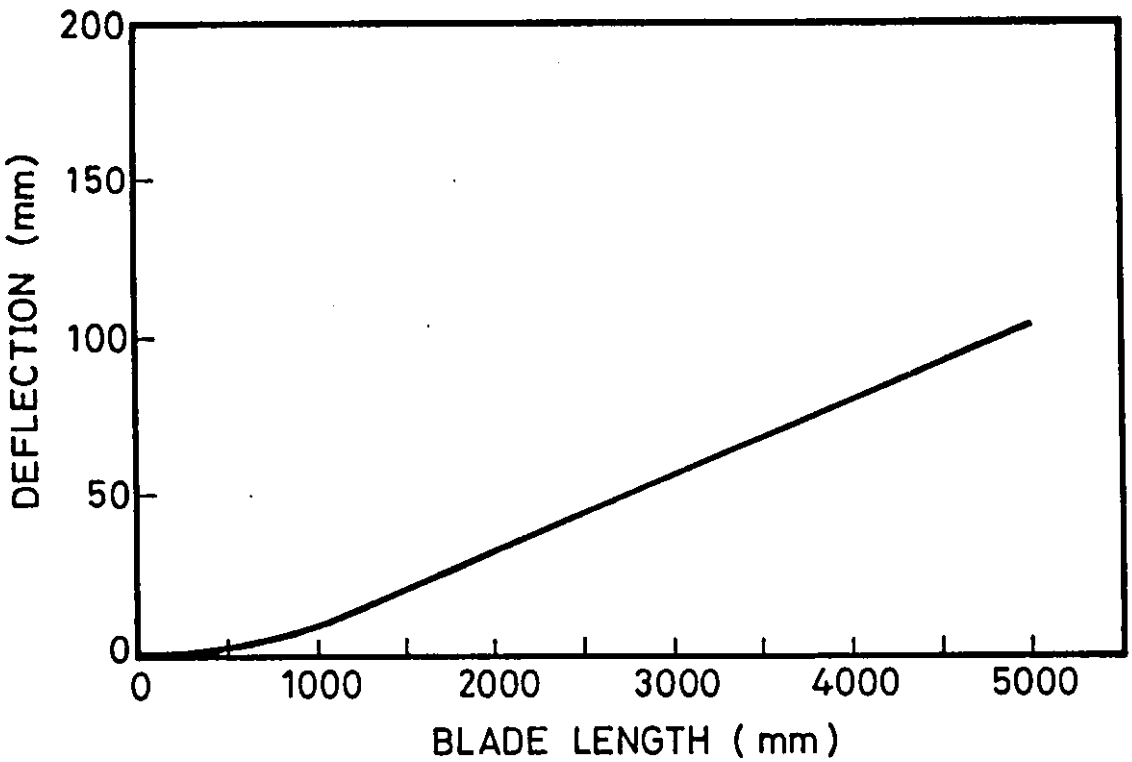

Fig. 3.10: Curve Fit Extrapolation of Blade Deflection During Extreme Operating Conditions at 42 m/s.

The maximum calculated deflection at the tip is 104.3mm under the given loads which concludes the analysis by insuring enough margine for safety of the design especially during extreme operating situations.

3.5 Post Solution Analysis

The above results are assuring, but reassurance is necessary. In order to analyze the FEM solution, a simple straight forward bending strength calculations will indicate its accuracy. This is accomplished through the use of superposition of the flexure formula with combined stresses.

Taking the exact cross section geometry at the root where maximum loads and moments usually occur, we get the situation depicted by Figure(3.11), from which we will have:

$I_x = \pi/64\ (d_o^4 - d_i^4) + bh^3/12$ .....(3-2)

$= 70{,}844{,}030\ mm^4$

$I_y = \pi/64\ (d_o^4 - d_i^4) + hb^3/12$ .....(3-3)

$= 55{,}374{,}030\ mm^4$

and the area $A = 18800\ mm^2$

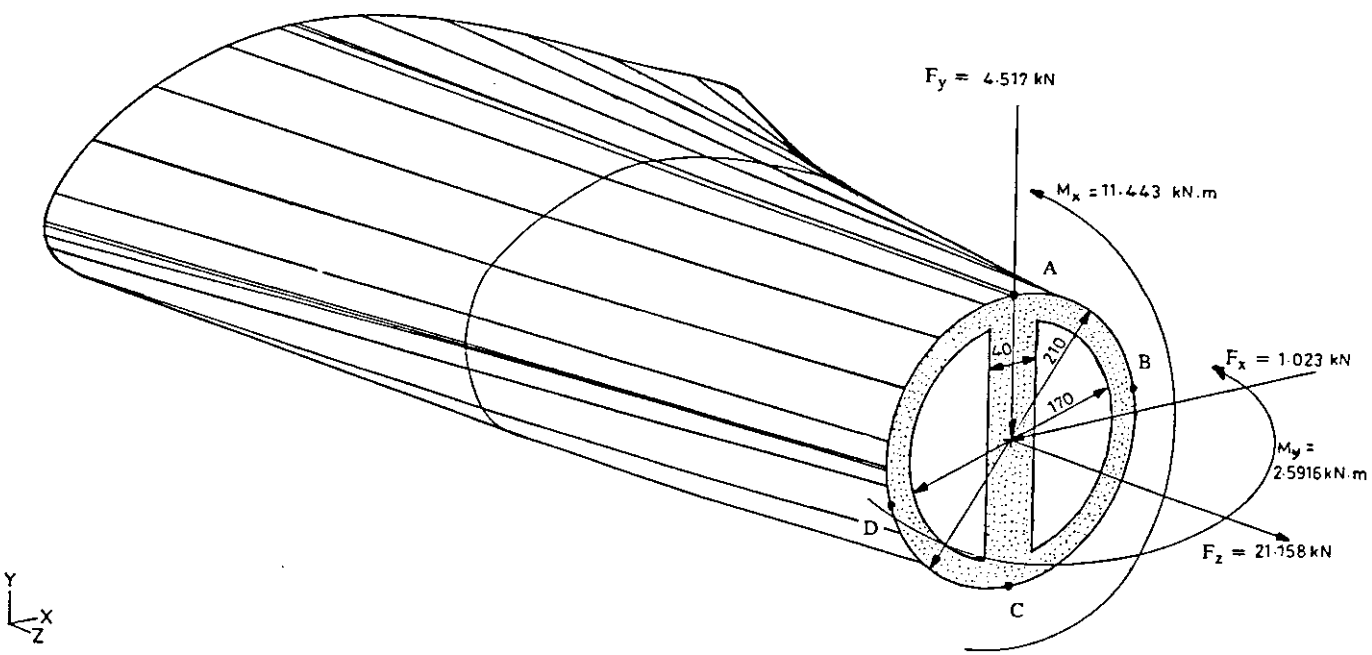

Fig. 3.11: Blade Root Cross Section With Loads and Moments Imposed.

Then, by the superposition technique outlined by Popov [23], we get:

$\sigma_z = + F_z/A + M_y\, x/I_y + M_x\, y/I_x$ .....(3-4)

Where the positive signs correspond to tensile stresses, and negative signs correspond to compressive stresses, and from Figure(3.11) we have :

$\sigma_z = 21158/18800+2591600*105/55374030+11443000*105/70844030$

$\sigma_z = \pm 1.1254 \pm 4.9142 \pm 16.9600$

The sense of the forces and moments shown in Figure(3.11) determines the sign of the stresses. Therefore, if the subscript of the stress signifies its location, the outer-most fiber stresses at points A,B,C, and D are:

$\sigma_A = (1.1254 - 0 - 16.9600) = - 15.835 \text{ N/mm}^2$

$\sigma_B = (1.1254 - 4.9142 + 0) = - 3.789 \text{ N/mm}^2$

$\sigma_C = (1.1254 + 0 + 16.9600) = + 18.085 \text{ N/mm}^2$

$\sigma_D = (1.1254 + 4.9142 + 0) = + 6.040 \text{ N/mm}^2$

These stresses are shown in Figure(3.12). The highest is tensile at point C and the lowest is compressive at point B. The stress vectors represent a complex surface that passes through the cross section of the blade root at some points between A&D, and B&C where stress vanishes. The maximum tensile stress is 18.085 N/mm^2 which is much below the yield strength of the used GRP material of 63 N/mm^2 with a factor of 3.5. The maximum compressive stress is 15.835 N/mm^2 which is also much below the compressive strength of the used material of 170 N/mm^2 with a factor of 10.7.

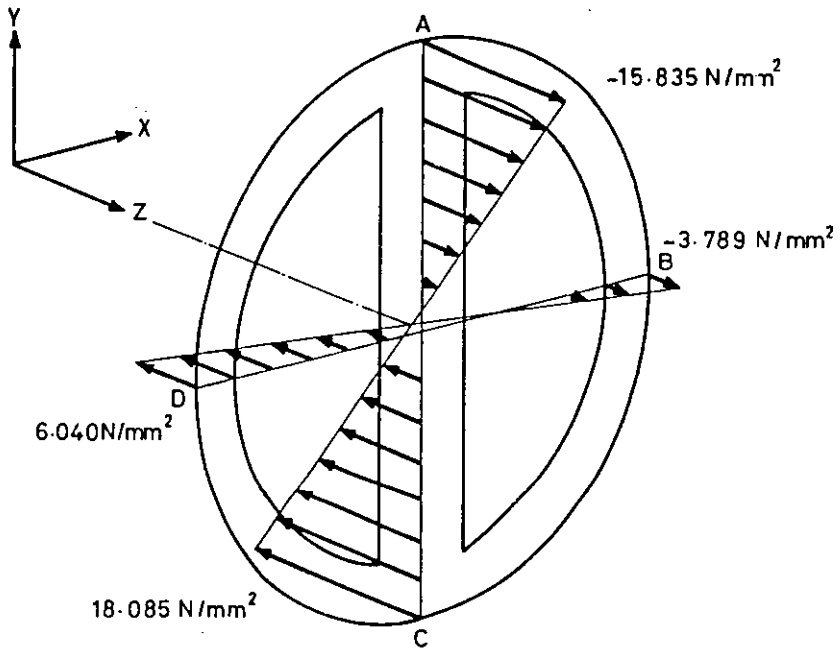

Fig. 3.12: Stress Distribution at the Root Section of the Rotorblade.

The results obtained by the FEM solution gave the maximum principal stress as 9.3487 N/mm^2 which certainly falls within the stress distribution shown above and one explaination why it was different from the results of the forward analysis is that in the latter one, concentrated load representation was used at the root to represent the actual distributed aerodynamic loads.

In light of the above, two conclusions are obtained:

1. The FEM analysis are satisfactory and acceptable.
2. The blade material for the given root design can withstand the applied loads with enough safety margine.

Chapter 4

MANUFACTURING THE GRP BLADES

The method of manufacturing the proposed prototype blade will be described in three stages; namely, manufacturing the model, manufacturing the mold, and manufacturing the prototype blades. Each stage is independent from the other two but in this prototype environment, the first stage is the most critical one from the strength viewpoint. This method is appropriate for blades of this size catagory because the blade will be relatively light weight and can be easily handeled. For large blades however (when weight becomes a problem) other methods are used such as winding on mandrels [3].

4.1 Stage 1: Manufacturing the Model

A full scale exact geometry blade model will be made from wood. This model will allow the designer to investigate and check the dimensional coherence of the blade

especially continuity of the twist and smoothness of surfaces. If any irregularities were found, they could be treated and traced back to the design calculations.

The first step in making the model is to divide the blade length into a number of intervals keeping in mind that the data available is for the outer 4.2 meters of the blade as shown in Figure(2.14). There we have 12 stations and the 0.8m root section will be streamlined and dimensionally -and continuously- fitted from the circular flange at the root to the first airfoil section 0.8 meters away where the actual airfoil starts. For the 12 stations mentioned there, the twelve airfoil sections given in Table(2.4) will be produced from 20mm thick white wood. The perimeter of each sectin will be reduced by 10mm to allow for the installation of 15x15mm cross section wood sticks as shown in Figure(4.1).

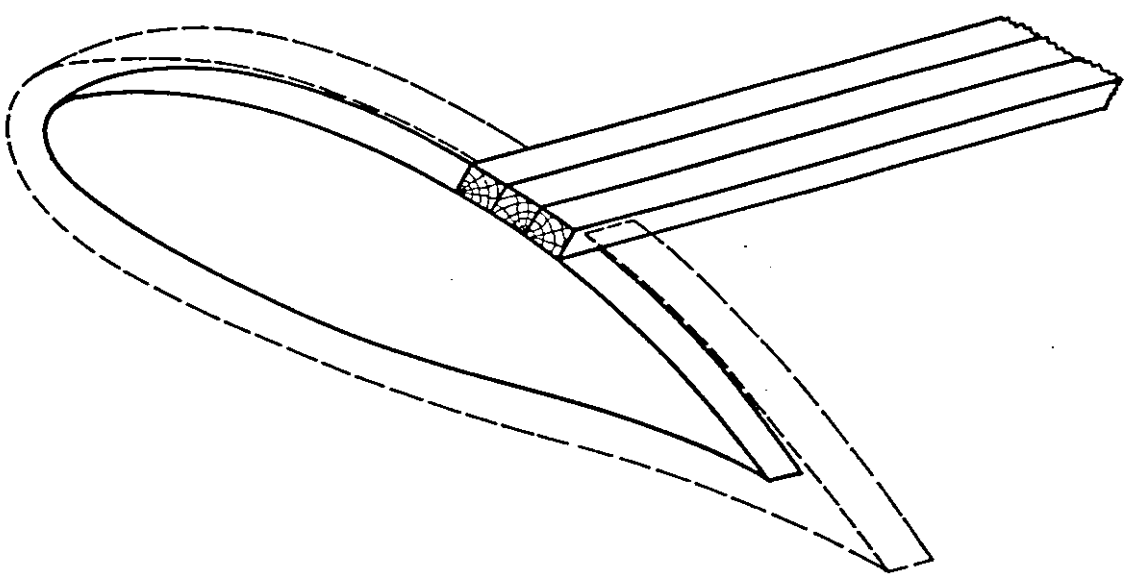

Fig. 4.1: Airfoil Section Cut From Wood and Reduced to Allow For Skin Segments Buildup.

These sticks when stacked next to each other and bonded to the twelve airfoil sections using binding resin for wood and hiden nails, will form the skin of the blade

which can be later shaped and smoothed and finally sanded to a very fine finish. Then, wood sealant is applied in order to protect the wooden model from the atmosphere's moisture. The twist distribution given in Table(2.4) is incorporated in the blade model by fixing the sections at their respective stations as shown in Figure(4.2), keeping in mind that the alligning datum is the aerodynamic center of each section which shall also pass through the center of the root flange.

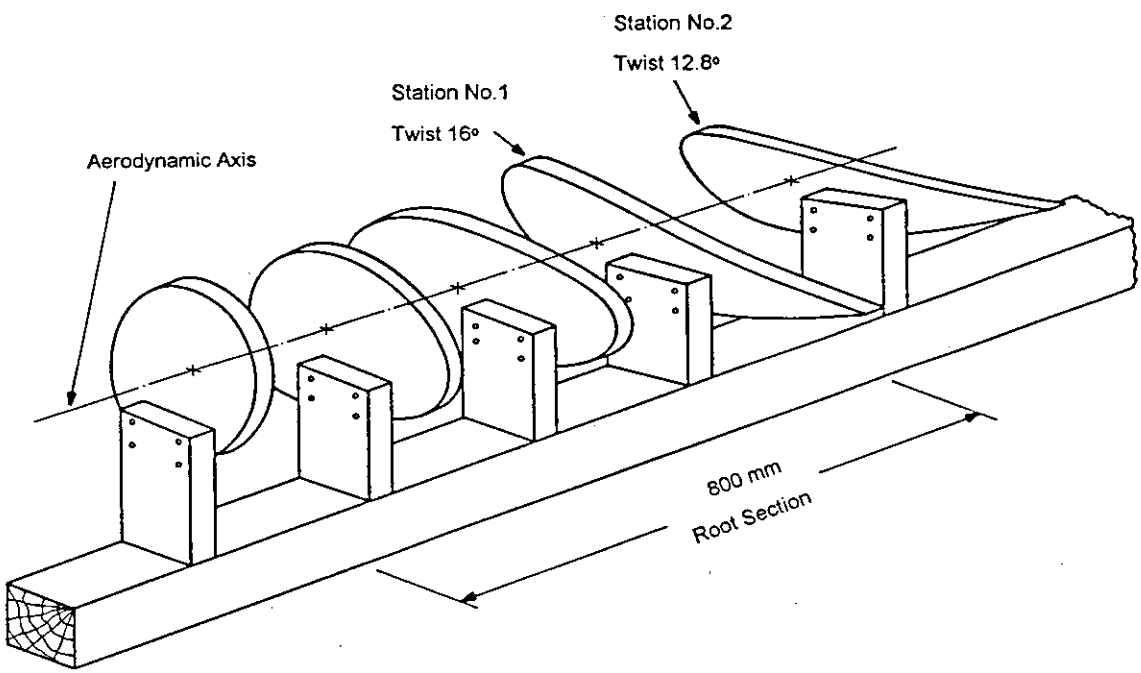

Fig.4.2: Method of Fixing the Airfoil Sections in Their Respective Chord and Twist Distribution Prior to Installing the Skin 15x15mm Segments.

After all segments are installed and all finishing has been done, the completed full scale (5 meter) rotor blade wooden model is shown in Figure(4.3).

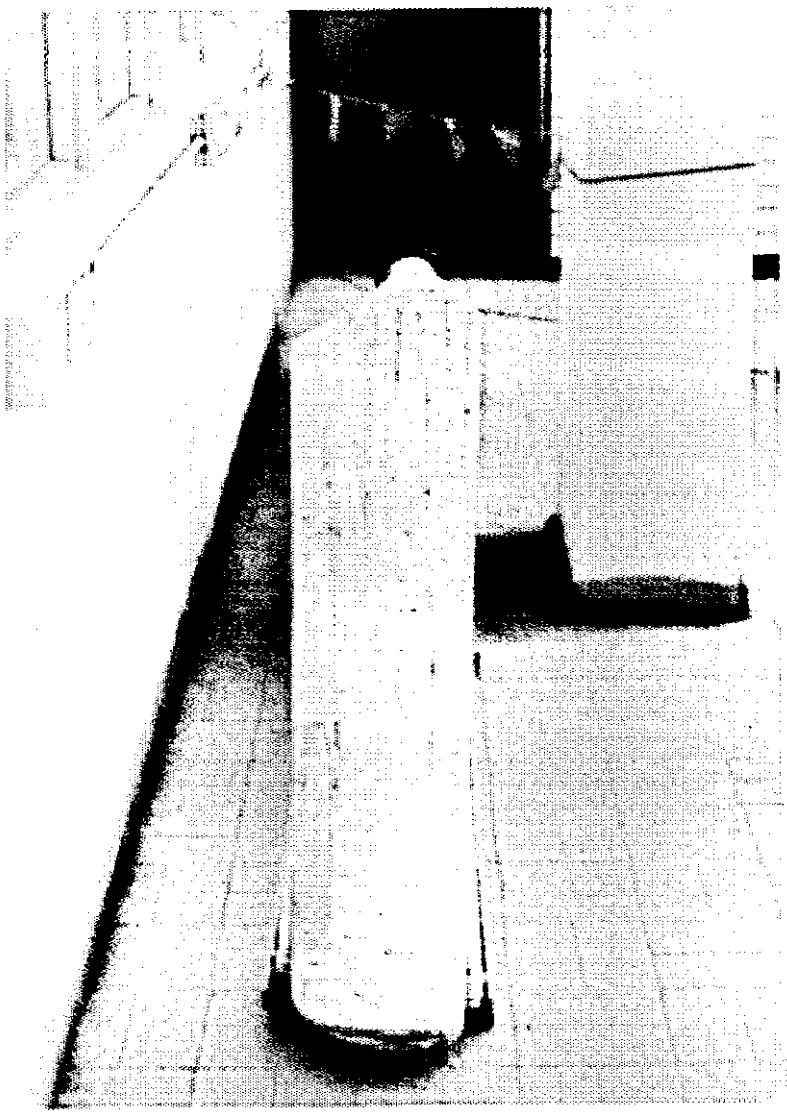

Fig. 4.3: Blade Model 5-meter Long Made From Wood.

4.2 Stage 2: Manufacturing the Mold

The mold will be made from GRP and consists of two parts; upper and lower halves which are then strengthened using lateral rip stiffeners.

The wooden model is prepared first by waxing it with a special separation agent (non-stick) which builds up a thin film between the wooden model and the GRP mold layers. The first layer of the mold cavity is a one millimeter thick gelcoat mixed with a hardening epoxy to form a tough internal mold surface. After the hardening period of the gelcoat, successive layers of glassfiber laminates soaked in polyester resin are layed on the wooden model to take its exact shape as shown in Figure(4.4).

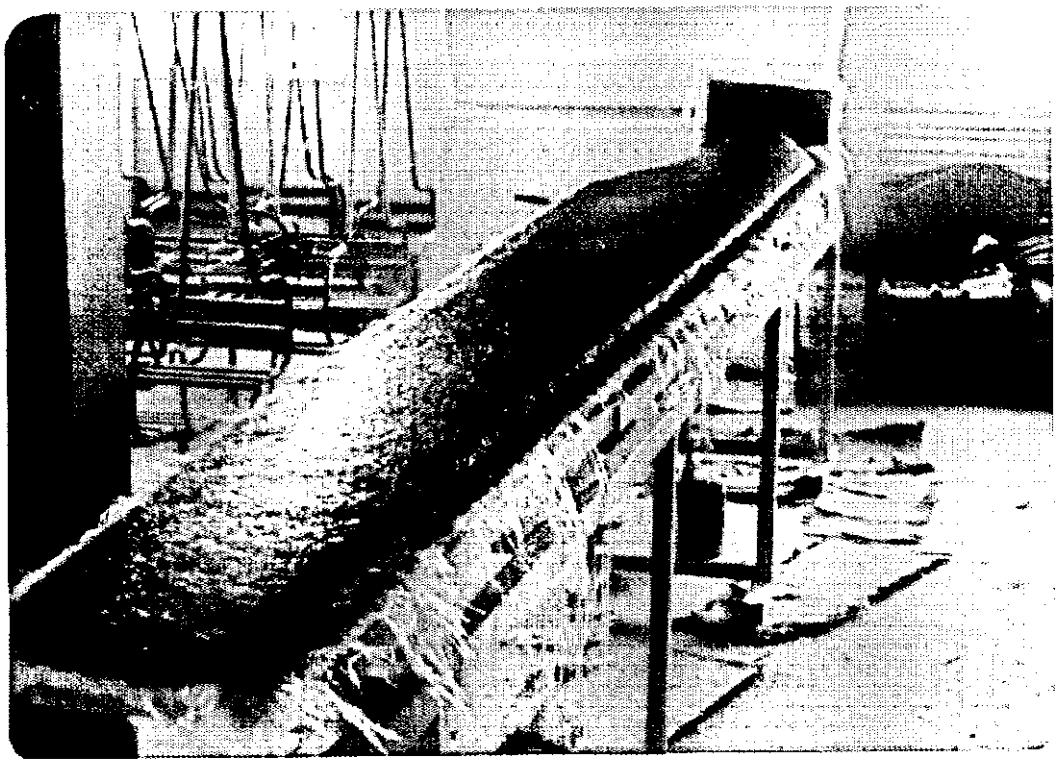

Fig. 4.4: Fiberglass and Polyester Resin Laminates are Being Layed on the Wooden Model to Get its Shape.

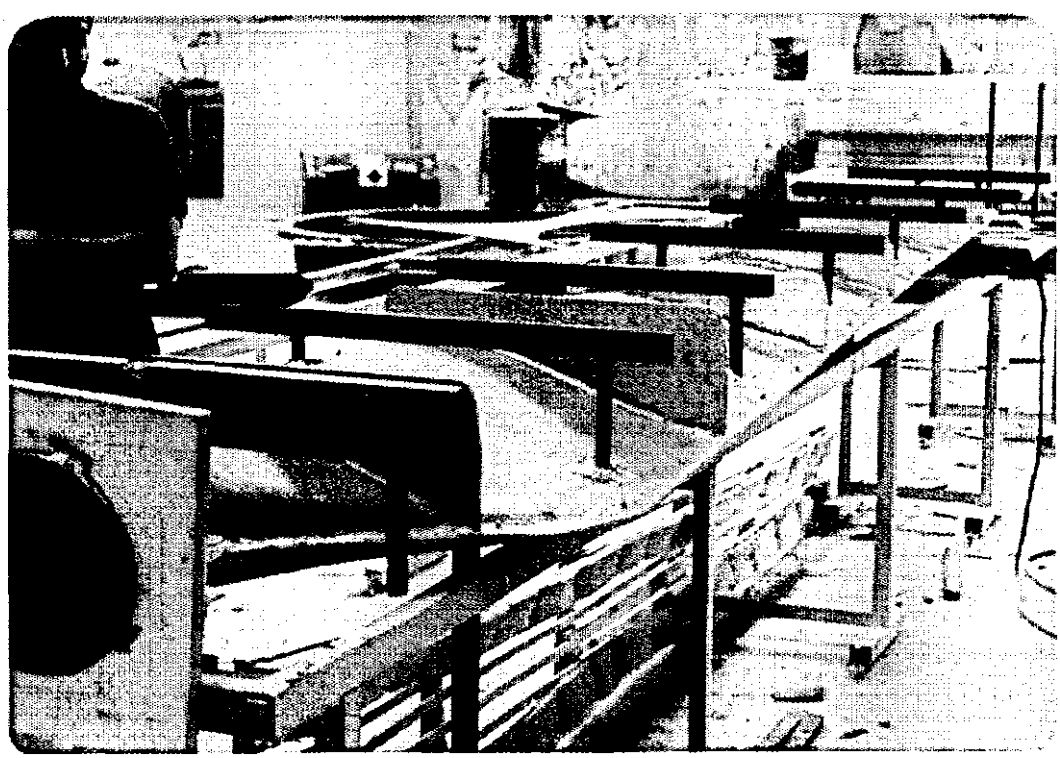

Fig. 4.5 The Two Mold Halves After Finishing Are Being Strengthened by Lateral Rips and Steel Frame.

After the curing period of the first mold half, it is pulled off the model and cleaned up from all extra materials especially around the edges as can be seen from Figure(4.4). The second mold half is also made in a similar fashion and the two halves are then assembled on the wooden model and any extra material will be removed untill complete fitness on the model is achieved for the two halves combined. The two mold halves are then strengthened using lateral rips made from wood and covered with GRP in addition to installing a steel frame to insure extra strength and ease of handeling as shown in Figure(4.5).

It is of great importance to locate the line where the two halves meet to avoid overlapping which because of the blade twist will result in a complicated surface; However, the best guide is the chord line which passes through the leading to the trailing edge of the airfoil section.

4.3 Stage 3: Manufacturing the Prototype Blade

The blade is made of two shell halves and a central axial spar. Each shell is fabricated in its respective mold half (i.e. upper or lower) by applying a one millimeter thick white color gelcoat and an exact number of fiberglass laminates of different fiber orientations inside the mold cavity and saturating each layer with polyester resin. This process is continued untill the required blade shell thickness and thickness distribution along the blade is reached. As was mentioned earlier, the blade shell will be thicker at the root and thins out linearly towards the tip.

The two blade shells will be joined and glued together at the leading and trailling edges and therefore some means must be provided to allow enough area for adhesions as shown in Figure(4.6). The spar is molded and cured in a separate and simple rectangular mold but carefully tapered down to fill exactly the allocated space and length.

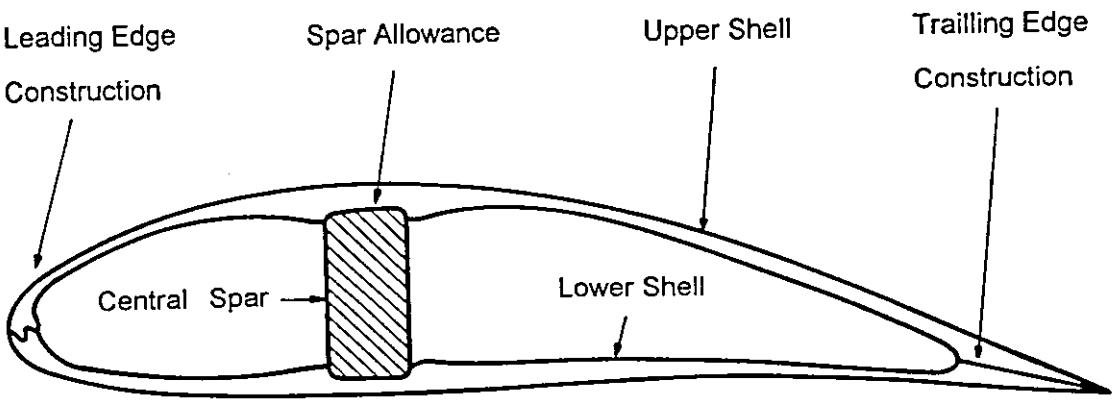

Fig. 4.6: Cross Section of Upper and Lower Shell Construction and Area For Adhesion Allowance.

The spar will be fitted to the lower shell and the upper shell is then glued to it along the designated areas. The blade mold can be used as a pressing device to house the blade parts untill totally cured for a period of 24 hours.

After curing, the blade is taken out of the mold and cleaned from any extra materials at the edges. The root section will be prepared to be fitted with the steel flange assembly. This flange will be an integral part of the blade that facilitates installation on the wind turbine. The design of this flange was proposed earlier in section 2.5.3 and shown in Figure(2.13).

This should prove the importance of having manufacturing in mind when designing mechanical elements in the very early satges of the design process. A three-dimensional view of this steel flange assembly is shown in Figure(4.7) where the

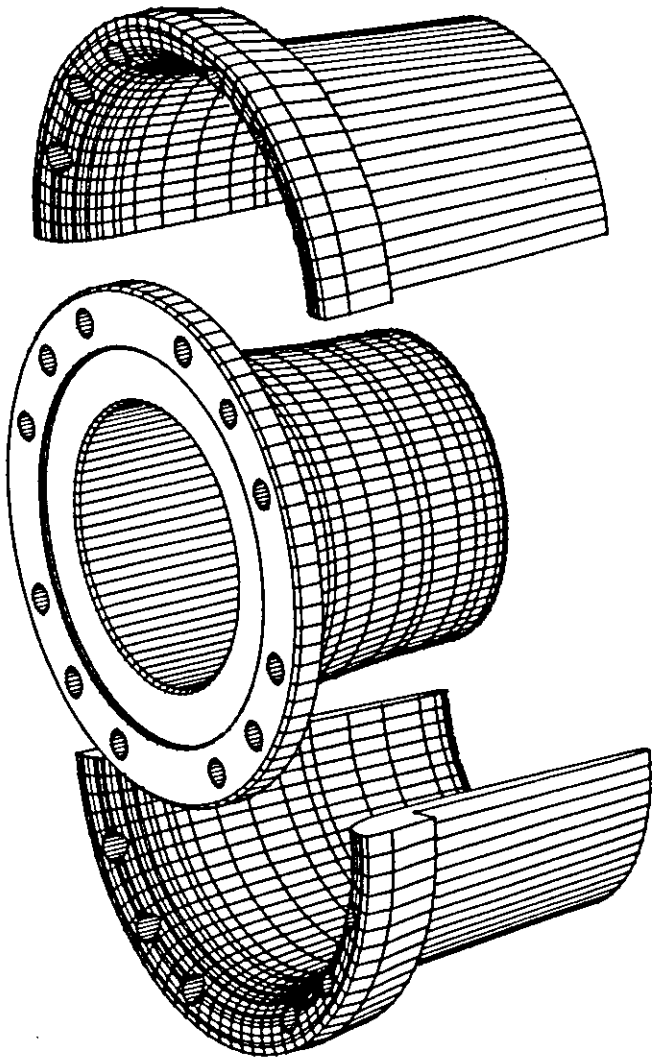

Fig. 4.7: Steel Flange Configuration For the Blade Root.

central flange will be inserted into the blade but allowing the spar to go inside its bore and then is completely glued. The outer two halves of this flange are then fitted on the outside surface of the root and also glued with great care to the fiberglass and pressed and tack-welded together. The weld will be done in a careful manner in order not to burn the GRP material. During the process of fitting the flange assembly to the GRP blade, close attention is also taken to allign the threaded holes which will connect the blade to the turbine hub. Figure(4.8) shows the completed 5 meter GRP blade which weighs 120 kg.

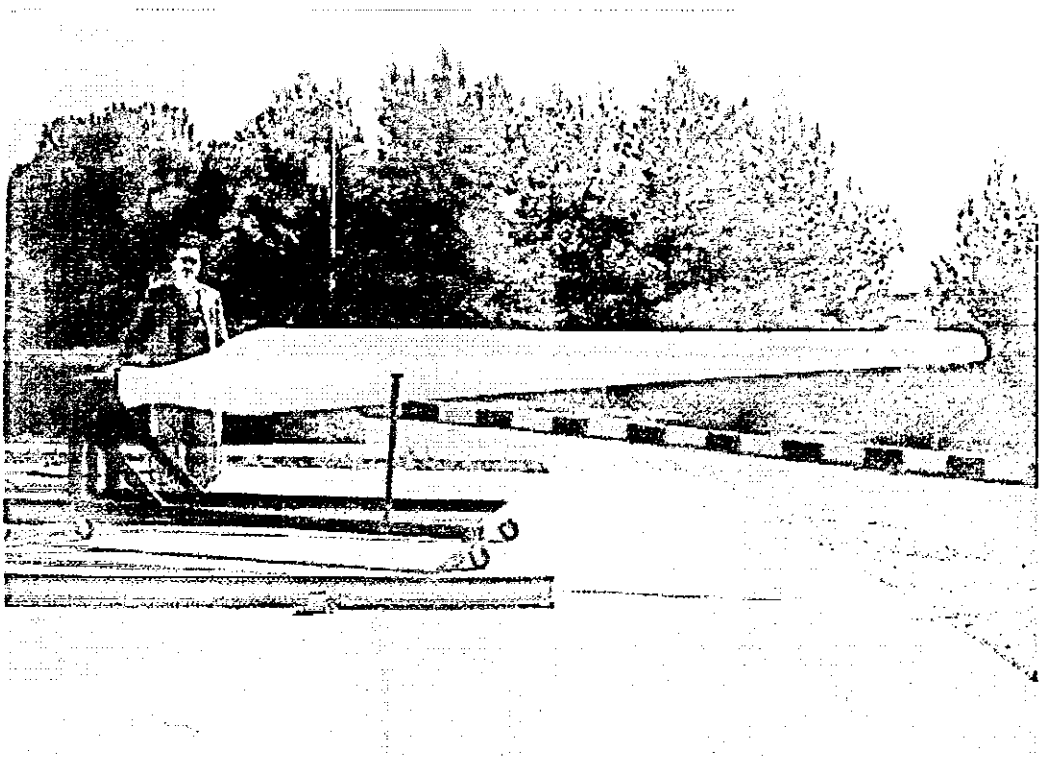

Fig. 4.8: Photograph of the First Prototype GRP Blade.

Four blades were manufactured, one was taken at random to be proof-load tested using the load case mentioned in section 2.5.3. This test is part of the manufacturing process and a condition was set forth to the manufacturing company that the blade must pass this test successfully otherwise all the blades will be rejected.

For the purpose of this test, the blade was bolted in the flapwise position from the root flange to one of the vertical structural columns at the factory building and loded around 2/3 ed. of its length as shown in Figure(4.9). The tip position was recorded first under the blade's own weight and then with the platform shown which will carry the load. The load was then applied in increments of 27 kg untill the 640 kg load was reached making a total of 740 kg with the platform and ropes. The blade took the load without any signs of strain or damage and from that a load-deflection curve for this blade was obtained as shown in Figure(4.10).

Fig. 4.9: Proof-Load testing the Prototype Blade After Manufacturing

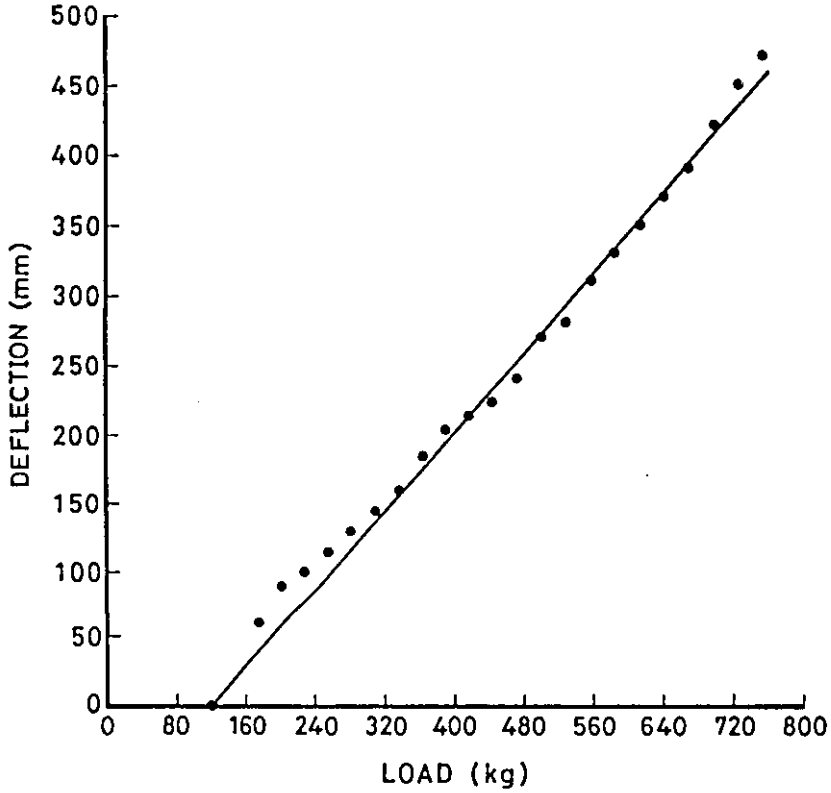

Fig. 4.10: Blade Load-Tip Deflection Curve.

Chapter 5

PERFORMANCE TESTING

5.1 Introduction

The performance of a rotor blade is measured by the amount of power it delivers during rotation compared to the theoretical power available in the wind passing through the same swept area by the blade. Abviously, the main parameters to be measured for this purpose are power and wind speed which will then produce the so-called Power-Wind speed (P-V) curve. This means that the blade must be installed on and be an integral part of a working wind turbine or as it is also called Wind Energy Converter (WEC). Through the ambitious drive of RSS to develop and transfer wind energy technology, this was accomplished by building (in the course of this study) the first 15kW wind turbine prototype in 1992. A photograph of this WEC is shown in Figure(5.1).

A comprehensive list of the (design) technical specifications of RSS WEC is given in Table(5.1). Some of these specifications will be verified by the performance test such as cut-in and rated wind speeds, rated power and power coefficient. Other parameters like voltage, current, and frequency must be measured and analyzed.

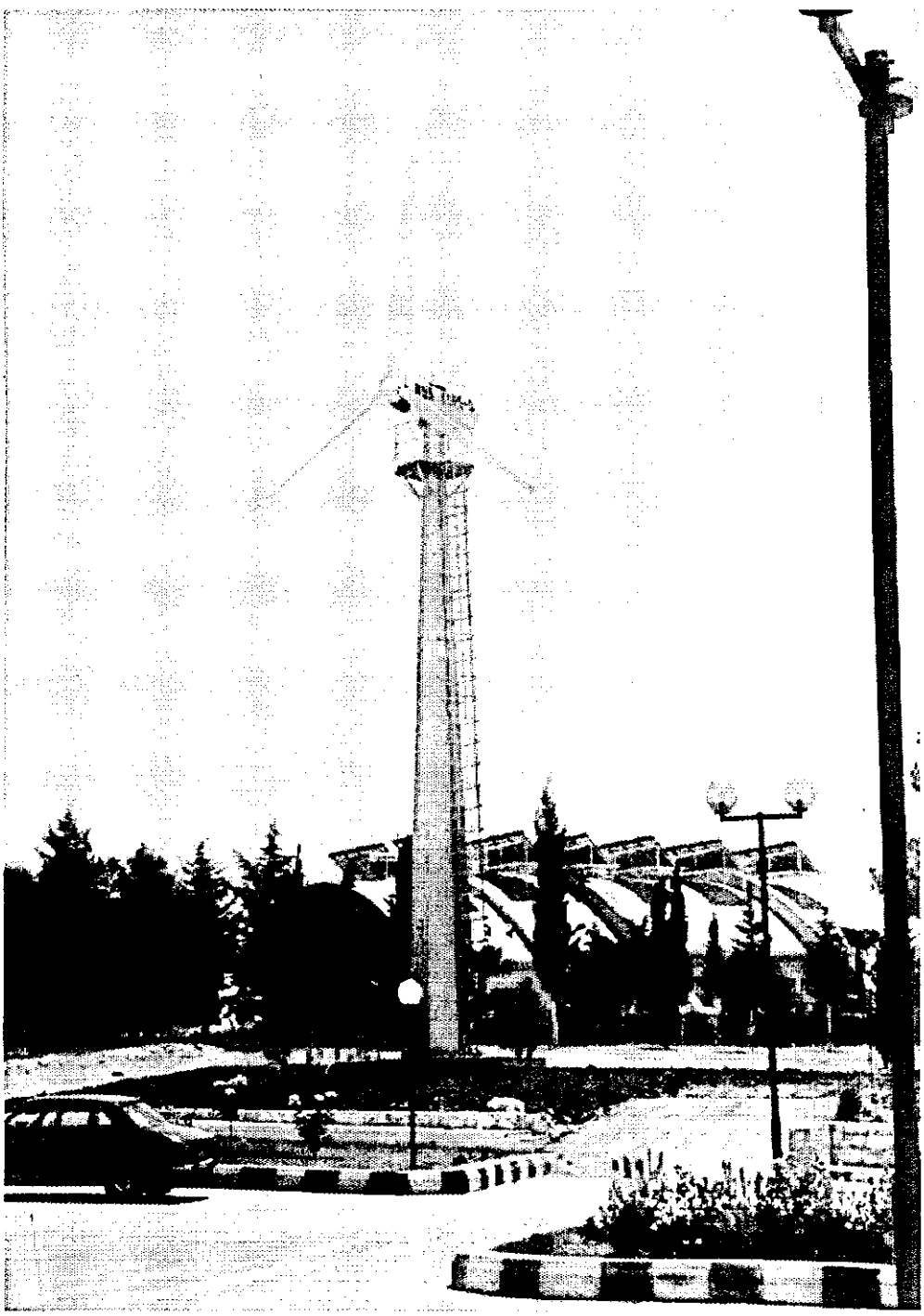

Fig. 5.1: Photograph of the RSS 15 kW Wind Turbine Prototype.

The acquisition of the P-V curve will ultimately lead to the production of a power coefficient (C_p) curve for this WEC which is usually calculated in terms of the dimensionless tip speed ratio (λ) of the blade. The net performance of the wind turbine blade will be obtained after deducting the efficiencies of the various mechanical and electrical components in the WEC.

Table 5.1: Technical Specifications of the RSS WEC.

WIND TURBINE TYPE	: RSS - 1
BLADES	
Blade Length	: 5 m
Material	: GRP
Airfoil	: NACA 63-621 ---> FXS 66-196
Twist	: 16 degrees
Thickness (Root - Tip)	: 25 - 13 %
Chord (Root - Tip)	: 0.6 - 0.2 m
Maximum Power Coefficient	: 0.4
Pitch Control	: Yes
Weight Per Blade	: 120 kg
Design	: RSS
Manufacturer Under RSS Supervision	: Abu-Hamdan Synthatic Products Industries, Amman-Jordan
ROTOR	
Diameter	: 10.9 m
Swept Area	: 93m^2

Table 5.1: Technical Specifications of the RSS WEC (continued)

Number of Blades	: 3
Hub Height	: 15 m
Position	: Upwind
Rated Speed	: 75 rpm
Design Tip Speed Ratio	: 6.1
Over Speed	: 90 rpm
Type of Hub	: Rigid
Method of Control	: Blade Pitch Regulation
Coning Angle	: 0 degrees
Tilt Angle	: 0 degrees
Torque Output	: 2.5 kN.m
Weight of Hub	: 100 kg
Solidity	: 7 %
Yaw Type	: Active Mechanical Side Wheel Drive (ratio 1 : 5000)
Hub and Pitch Control Design and Manufacturer	: RSS
TOWER	
Type	: Octogonal- Conical Free-Standing (2- segments)
Material	: St.37 Steel Sheet Metal
Thickness	: 6 mm
Height	: 14 m

Table 5.1 : Technical Specifications of the RSS WEC (continued)

Weight	: 3800 kg
Design	: RSS
Manufacturer	: Ashour Industrial and Trading Co., Amman-Jordan
GEAR UNIT	
Type	: Three-Stage Helical
Rated Power	: 25 kW
Ratio	: 1 : 20
Weight	: 190 kg
Manufacturer	: Loher, Germany
PITCH CONTROL	
Type	: Electrohydraulic Speed and Power Control for Automatic Operation
Manufacturer	: M.A.N. - SMA, Germany
GENERATOR	
Type	: Asynchronous, 4-Pole Three Phase Induction Motor
Rating	: 15 kW
Voltage	: 380 VAC
Frequency	: 50 Hz
Cos Φ	: 0.86
Weight	: 130 kg
Manufacturer	: Loher, Germany

5.2 Testing Strategy

The test methodology was established in a special study done by RSS [24] in 1985 during which time there was no agreed uppon international standards for testing wind turbines. The most recent reports [25],[26] from the Testing Station For Wind Turbines at RISO, Denmark, support the methods used by RSS and therefore they will be applied here for testing and evaluating the RSS wind turbine and hence the rotor blades.

The main objective of the test will be to obtain a set of performance curves for the WEC which will be indicative of the overall performance of the individual blade. In this test, a reduced 10-minute averaged data sets are used in the constrction and derivation of these curves. The physical parameters measured for this purpose are:

1. Wind Speed (V).
2. Voltage (U).
3. Frequency (f).
4. Power (P).

The independent variable for these measurements is the wind speed; However, time dependent curves can also be produced in order to see the variation in responce and the simultaneous effects among these variables. According to the European wind turbine standard on performance determination [25], the data must be corrected to standard air density of 1.225kg/m^3 and averaged for power values below 70% of the nominal power. Above 70% of the nominal power, no correction is needed.

5.3 Description of the Measuring System

The measuring system used in this test is a data acquisition system utilizing electronic measuring transducers and a (BCS 16) computer furnished with a terminal and a printer. Figure(5.2) shows the measurements taken and the flow of data within the

compiled in the form of a DC-signal with values range from 0 to +10 volts for further processing by the computer, see Tbale(5.2).

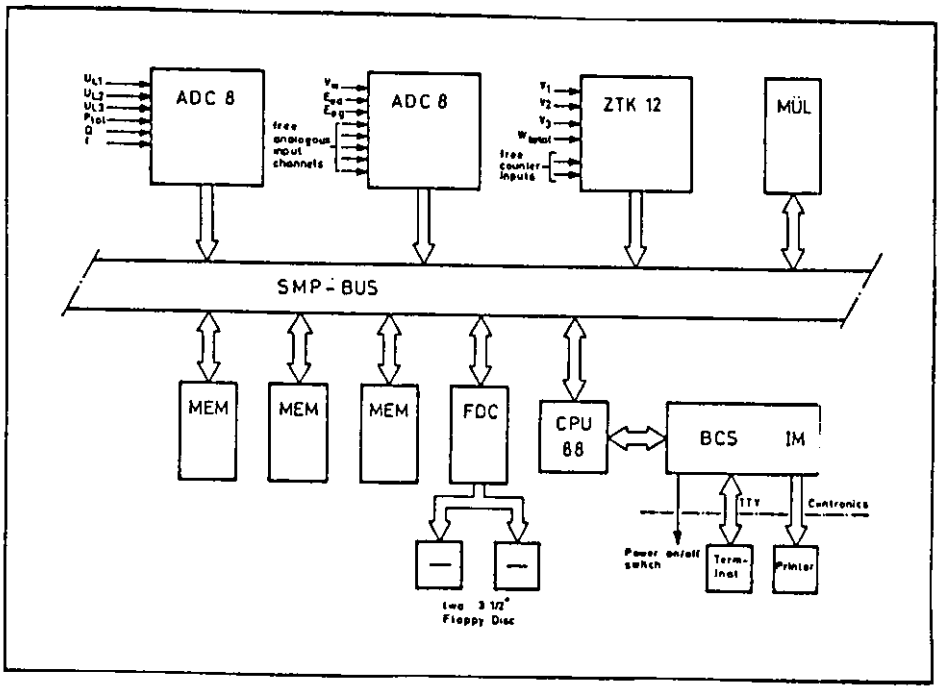

Fig. 5.3: Block Diagram of the Data Acquisition System, adapted from ref.[27].

Table 5.2: Ranges For Measured Values.

Item	Measured Quantity	Measured Vlaue (volt DC)	Transducing Range
1	Wind Velocity	0 - 10	0 - 20 m/s
2	Total Active Power	0 - 10	0 - 40 kW
3	Frequency	0 - 10	0 - 100 Hz
4	Current Phase 1	0 - 10	0 - 60 Amp
5	Current Phase 2	0 - 10	0 - 60 Amp
6	Current Phase 3	0 - 10	0 - 60 Amp
7	Phase Voltage 1	0 - 10	0 - 300 volts
8	Phase Voltage 2	0 - 10	0 - 300 volts
9	Phase Voltage 3	0 - 10	0 - 300 volts

The measuring system scans these listed parameters every second for 600 seconds and then takes the statistical average and records it on a mass storage media as a single 10-minute averaged data point for each measured parameter. This function is continued around the clock and at the end of a 24-hour period, the compiled 144 (10-minute) averaged data points are recorded on a data disc.

5.4 Results of the Measuring Program

The data is treated by eliminating eroneous records which usually result from the behaviour of the control system of the WEC. For example, when power output production decreases from the WEC below the acceptable limits set by the control strategy, the control system shuts the WEC down for a pre-assigned time interval of 15 minutes. During this time the wind speed might increase and it is off course being recorded but with zero power from the turbine. This data point will be eliminated and only wind speed records with power values are kept.

The data is then classified according to wind speed classes up to 20m/s which is usually a satisfactory range for performance purposes. The treated (original) data is presented in the appendix. It consists of 10-minute average values of wind speed, power, line voltage, and line frequency with means and standards of deviation. This long list is useful for detecting the wide but true variations in all parameters which can help in understanding and enhansing the control system. The maximum cumulative error in the measurements is 3% according to the manufacturer catalog [27].

From this original data, and with no averaging within each class, a true (virgin) power curve is constructed as shown in Figure(5.4). The reason that no curve fitting was done is that as mentioned above, one can see the greate deviation in the data which can be traced back to the control system. However, the trend is clear and a single line curve cannot be a true represtative of the WEC's behaviour and ultimately the blade's , especially at low wind speeds.

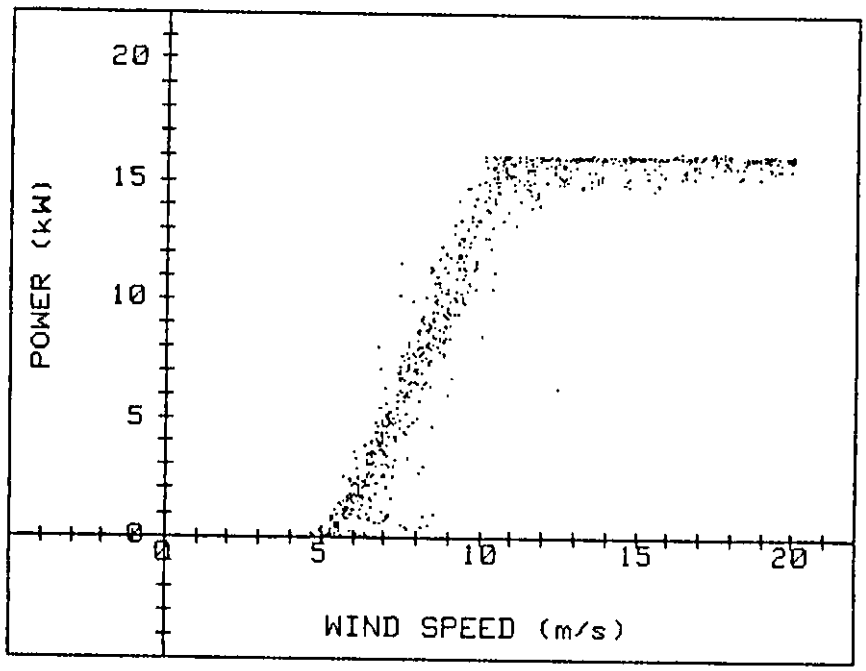

Fig. 5.4: P - V Curve of RSS WEC.

This note came from long experience and observations of many WECs under test where power production can have too many different values for the same wind speed class at the unregulated part of the power curve below rated power. Over rated wind speed (which is the regulated part of the power curve), the power values are seen to be closer within the same wind speed class because the control simply uses the blade pitch angle to lower the lift force in order to keep the power level from exceeding a pre-set value which is usually the rated value of the installed generator. And with the availability of high wind speeds at this part of the curve, power values tend to remain almost constant. The cut-in and rated wind speeds can be seen at 5 and 10m/s respectively. The rated power is seen to have exceeded the installed generator capacity to a little over 16 kW. This is due to the nature of asynchronous motors where they tend to produce 10% more power when used as generators as is the case here which is why these machines are favored by most comercial wind turbine builders.

The line voltage and frequency behaviour as a function of wind speed are also shown in Figures(5.5) and (5.6) respectively. It is clear that below rated wind speed, voltage and frequency can have any value including the nominal values of 220 volts and 50 Hz. However, it should be reiterated that these are 10-minute average values from 600 scans, where some scans could be taken during normal operation, and the rest taken during shutdown because of below cut-in wind speed as was explained earlier. This situation will result in a data point having values below the nominal for above cut-in wind speed class. Nevertheless, nominal voltage and frequency can be seen to start from cut-in which is also a condition for grid connection machines.

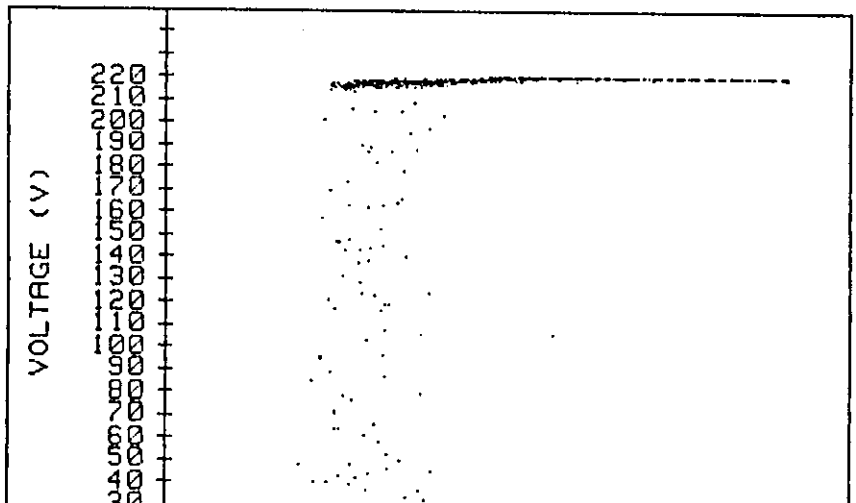

Fig. 5.5: Line Voltage vs Wind Speed For RSS WEC.

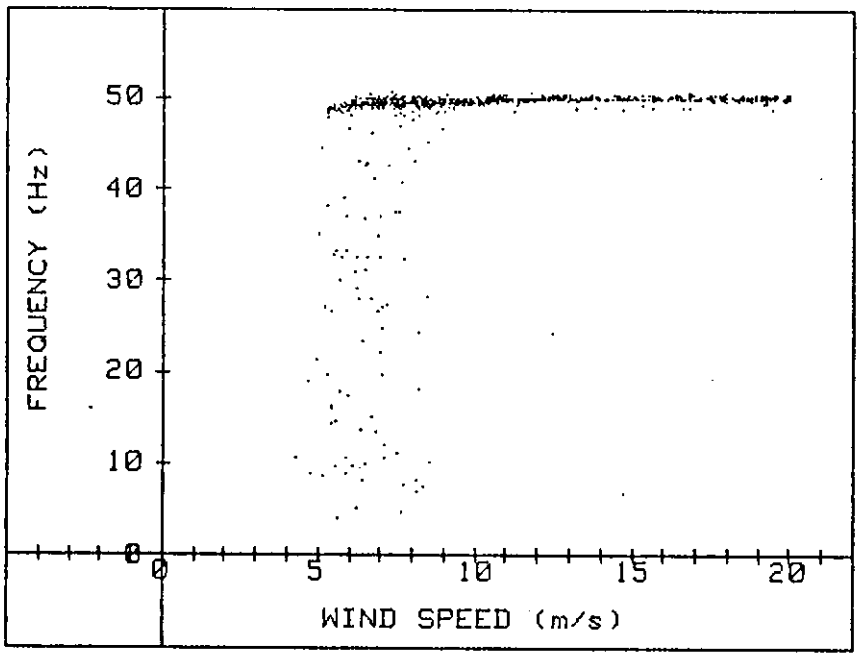

Fig. 5.6 : Line Frequency vs Wind Speed For RSS WEC.

The efficiency of a wind turbine is usually characterized by its power coefficient (C_p). But pitch regulated wind turbines have variable C_p and therefore their efficiency is best represented by a C_p versus tip speed ratio (λ) curve, where λ is a dimentionless parameter given by:

$\lambda = \Omega R/V$ .....(5-1)

Here the rotor radius R and the angular speed Ω are constant but the wind speed V is variable according to the wind speed class which will facilitate the abscissa for the curve. The C_p values are calculated according to Equation(2-9) from the measured values and the results are shown in Figure(5.7).

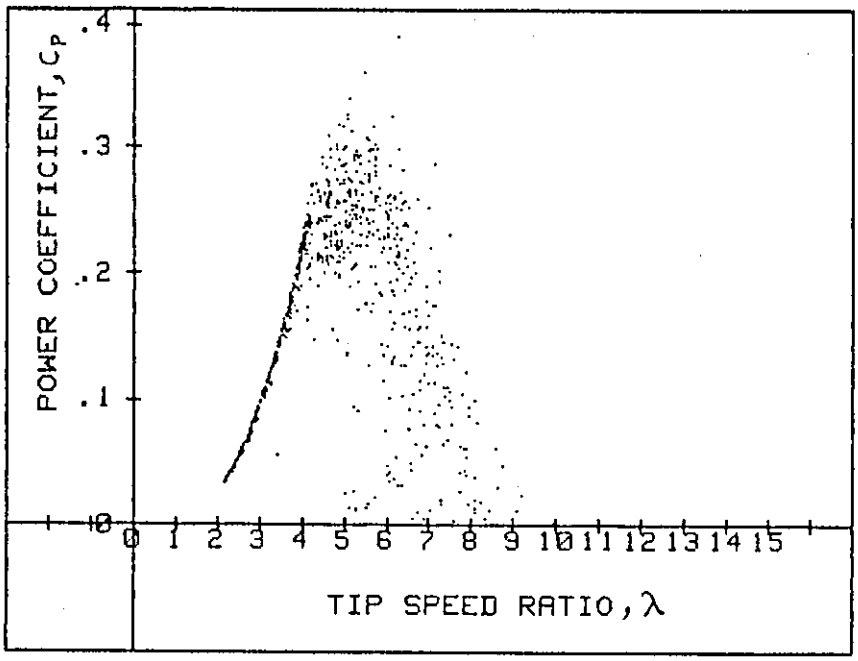

Fig. 5.7: Cp - λ Curve For RSS WEC.

From the above figure, the WEC reached a maximum C_p of 33% at $\lambda = 5$, again, the data points are more coherent at high wind speeds (low tip-speed ratios) and more spread apart at low wind speeds (high tip-speed ratios) but the theotetical shape of the curve is evident. The performance of the rotor alone can be obtained by eliminating the efficiencies of the following components from the WEC:

Drive Train assembly : $\eta_{D.T.} = 0.95$

Generator : $\eta_G = 0.86$

Power Line and Electronics : $\eta_E = 0.98$

Therefore, the isolated rotor performance which is the performance of the blades will be:

$$C_p \text{ (Blade)} = C_p/\eta_{D.T.} * \eta_G * \eta_E \quad \text{.....(5-2)}$$

$$= 0.33/(0.95 * 0.86 * 0.98) = 0.412$$

This value is compared with the Bitz limit of 0.59 and is therefore considered acceptable. The performance data is presented on a time scale as shown by Figure(5.8) which tells the history of power production and the time lag of the control. In this figure, a continuous string of data for 24 hours is plotted without classification where the variation in all parameters are seen to follow the variations of the wind speed where also the effect of the control can be noticed.

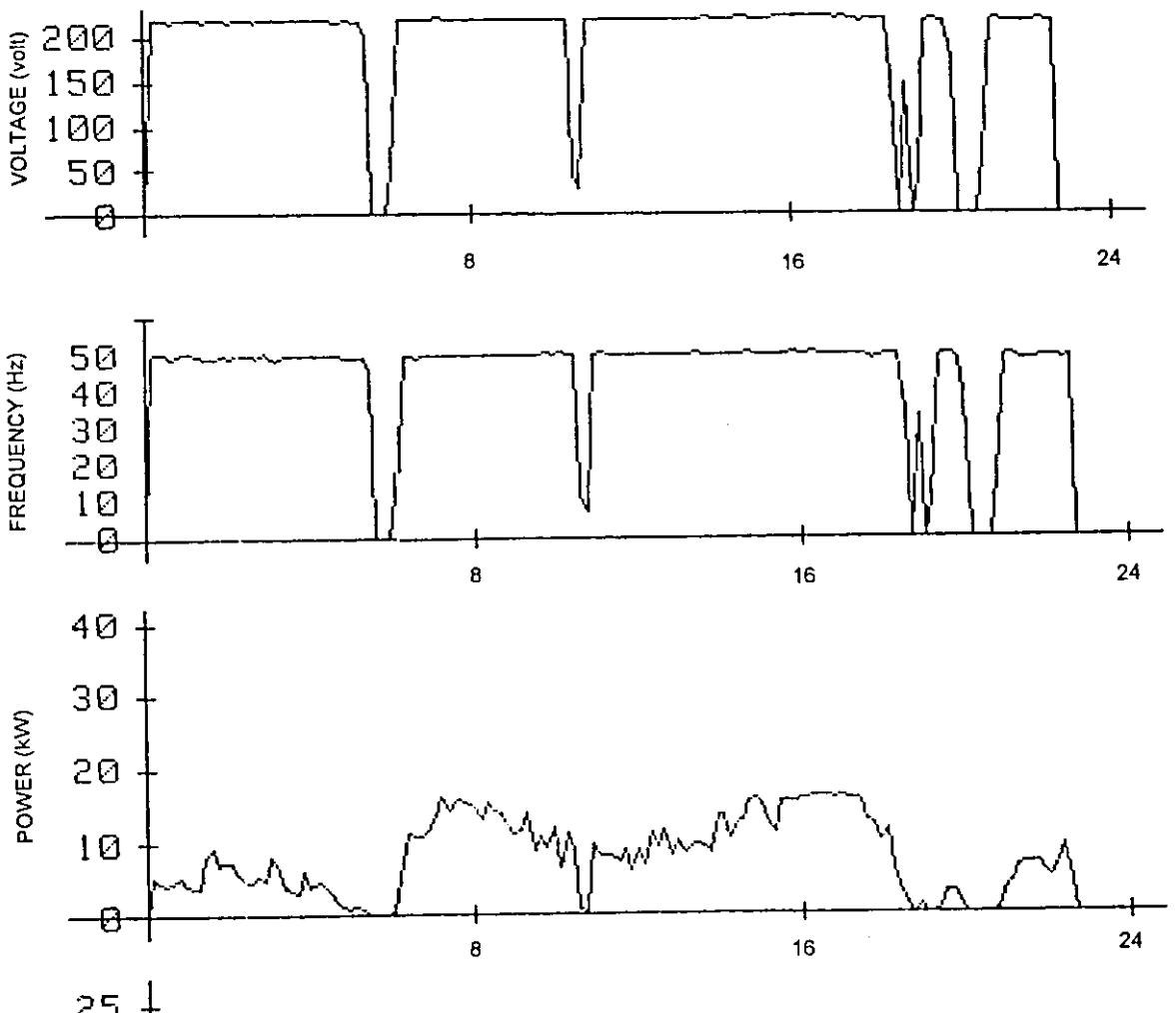

Fig.5.8: Instantaneous Measurements of RSS WEC.

Chapter 6

CONCLUSIONS AND RECOMMENDATIONS

The results of the measurements have produced the necessary data for the evaluation of the rotor blade performance. The single most important peice of information is the power curve. Being installed on a pitch regulated wind turbine, the performance of this design of GRP blades can only be seen in the part of the curve up to rated power (i.e. 15kW at 10m/s). Beyond this point, the performance of the blade is overshadowed by the control system which litterally dumps all excess power (over the rated) thereby showing up as a decrease in efficiency as indicated by the C_p-λ curve.

The power production characteristics of the blade are best seen in the part of the power - wind speed (P-V) curve from cut-in to rated wind speed where the theoretical cubic behaviour is abvious. From this part of the curve where no pitch regulation occurs, the following characteristics can be seen:

1. The rotor blade can produce a wide range of power outputs within the same wind speed class which is largely due to the production history. After cut-in, the rotor

will be "trying" to produce power while following an increasing wind speed . This will always produce power less than expected for that given wind speed class. However, after a while in operation during high winds, the rotor will- if the wind starts to calm down- be producing more power than expected for that wind speed class. This explains the large scatter of data from cut-in to rated values.

2. The scattering of power production is referred to a variety of reasons:

- Rotor inertia, where during start-up before cut-in, the rotor requires higher torque to start turning and production but much less torque is needed to produce the same "unit" power after it had run up to full speed.

- Yaw error, where sometimes the rotor is not facing the wind stream as it should becuase the wind tracking device cannot instantaineously follow the wind direction changes. This situation will alter the wind vector configuration at the blade from the design settings leading to a big drop in power output.

- Wind shear, where the effect of this phenomenon is more clear with large rotors but still has a markable influence on small turbines whether this shear is vertical or horizontal.

The performance of the rotor blade ($C_{pmax} = 0.412$) is considered extraordanary being the first prototype designed and manufactured in Jordan. This leads to conclude that the design procedure is valid and all the assumptions put forth are justified . This also leads to conclude that the manufacturing method is acceptable despite the fact that this was a one-time undertaking by the manufacturing company. The extreme proof-load test had proven the ability of the blade to sustain severe conditions during operation, and moreover no vibrations from imbalance or fabricating errors were detected throughout the testing program of the WEC.

The analysis of the blade model through the use of FEM was only possible on large computers with very advanced softwares. Using ARIES™, it was easy to develop the balde's solid model. The calculated section and mass properties were quite accurate when compared with the actual physical prototype.

The resulting stresses were within the strength limits of the Glassfiber Reinforced Plastic for the designed geometry.

In light of these findings, the following recommendations are due:

1. In order to fully understand the mechanical behaviour of rotor blades, the test should be carried further by conducting a thorough fatigue test program which is usually characterized by being costly and time consumming.

2. Since the blade root exibited durability and resileance during testing and operation, it is recommended that the design of the blade root be more theoretically investigated using the theory of elasticity with inisotropic materials and composites in three dimensions.

3. It is recommended that some local basic research be done on locally manufactured GRP materials (for all applications whether industrial or domestic) to aid future designers and encourage them to use this extraordanary composite in many daily uses.

4. The cost of this 5-meter blade as a prototype is JD 1250 (JD = Jordanian Dinar = $1.42) ,and according to the manufacturer, this cost will be reduced by 30% to 40% for mass production (i.e. 100 blades or more). The cost of the mass produced 7.5-meter Aeroman blade made in Germany by M.A.N. company is DM 10000 (DM = German Mark = $ 0.6) which is equivelant to JD 4200. Although the the German blade is longer , the difference in weigtht is small and similar blades can be made in Jordan using this technique with only a fourth of the cost. Therefore, it is recommended that this blade design and manufacturing procedure be considered for future improvements.

5. The real transfer of this technology resides in developing a local industry concerned with wind energy in all its aspects. Therefore, any future development should be directed toward producing blades of 10 meters in length and above, or WECs of over 100kW capacities in order to be cost effective and more meaningful to investors.

References

[1] Jensen, P.H.,"Development of Wind Farms After Cutting Tax Incentives," Proceedings of the Fourth Arab International Solar Energy Conference, Royal Scientific Society, Amman, Jordan, November 1993.

[2] MEMR (Ministry of Energy and Mineral Resources) and JEA (Jordan Electricity Authority), "Final Report, Wind Energy Project in Jordan," Amman, Jordan, May 1989.

[3] Boeing Engineering and Construction, "MOD-2 Wind Turbine System Concept and Prelimanary Design Report," U.S. Department of Energy/NASA 002.80/2, Seattle, Washington, July 1979.

[4] Hartin, J.R., "Evaluation of Prediction Methodology For Blade Loads on A Horizontal Axis Wind Turbine," Ninth ASME Wind Energy Symposium, SED-Vol.9, New Orleans, Louisiana, January 14-18 1990, pp. 105-110.

[5] Peterson, H., "Technical Assistance to Jordan's NRSE Activities in Industrial Solar Water Heating and Wind Energy Power Applications," SI/JOR/88/801,UNIDO, April 1991.

[6] Park, J., Simplified Wind Power Systems For Experimentation, Brownsville, CA, Helion Inc., 1975.

[7] Jackson, K.L. and Migliore, P.G, "Design of Wind Turbine Blades Employing Advanced Airfoils," West Wind Industries, Inc., Windpower'87 Conference, San Francisco, CA, October 1987.

[8] Lysen, E.H., Introduction to Wind Energy, 2nd Ed., CWD 82-1, Amersfort, The Netherlands, May 1983.

[9] Davidson, R., "Danes to Test Run New American Blades," Windpower monthly , December, 1990.

[10] Tangler, J., Smith, B., Jager, D., and Olson, T., "Atmospheric Performance of the Special-Purpose SERI Thin-Airfoil Family: Final Results," Solar Energy Research Institute, 1817 Cole Blvd., Golden, Co., Presented at ECWEC 90, Madreid, 1990.

[11] Holister, M. A., and Thomas, C., "Fiber Reinforced Material," American Elsevier Publishing Co. Inc., NY, NY, 1966.

[12] Jensen, P.H., Krogsgaard, J., Lundsager, P., Rasmussen, F., "Fatigue Testing of Wind Turbine Blades," EWEA Conferencs and Exibition, Rome, Italy, October 1986.

[13] Wilson, R.E. and Lissaman, P.B.S., "Applied Aerodynamics of Wind Power Machines," National Science Foundation, Under Grant No. GI-41840, Oregon State Univesity, Oregon, May 1974.

[14] Prandtl, L., Appedix to Wind Turbines With Minimum Energy Losses, by A. Betz, Gottinger News, pp 193-217, Gottinger 1919.

[15] Miley, S. J., A Catalog of Low Reynolds Number Airfoil Data For Wind Turbine Applications, USDOE, Wind Energy Tech. Division, REP-3387, UC-60, February 1982.

[16] Mikhail, A.S., Wind Power For Developing Nations, USDOE, Wind Tech. Division, SERI/TR-762-966, UC Catagory:60, July 1981.

[17] Ta'ani, R., Amr, M., and Saleh, I., "Water Pumping From Deep Wells By Using Aeroman 12.5/14 Wind Energy Converter," 6th International Sonnenforum, Berlin, Vol.2, DGS-Sonnenenergie Verlag GmbH, Muenchen, Germany, Aug. 22nd-Sep. 2nd 1988.

[18] Jensen, P.H., "Static Test of Wind Turbine Blades," Test Station For Wind mills, Risoe National Laboratory, Roskilde, Denmark, April 1986.

[19] Moment, R., and Pastore, J.,"Wind Energy Conversion," A short Seminar Presented to the Royal Scientific Society by Rocky Flats Wind Energy Research Center, Rockwell International Corporation, USAID, March 10-14, 1984.

[20] Habali, S.M., and Saleh, I.A., "Pitch Control Criteria For Small Wind Turbines," Proceedings of the 1992 International Renewable Energy Conference, Vol.II, University of Jordan, Amman, Jordan, June 1992 ,pp. 459-559.

[21] Hansen, A.C., and Cui, X., "A Summary of Experiences in the Analysis of Rigid- Rotor Yaw Control Systems," Ninth ASME Wind Energy Symposiom, SED-Vol.9, ASME, NY, NY, January 1990, pp. 181-187.

[22] Aries Technology, Inc., Finite Element Modeling Reference Manual, P/N2806301, Aries Technology, Inc., 600 Suffolk Street, Lowel, Massachusetts 01854, February 1993.

[23] Popov, E.P., Mechanics of Materials, 2nd Ed., Prentice-Hall, Inc., Englewood Clifs, New Jersey, 1976.

[24] Royal Scientific Society, Development of A Testing Procedure, WP Report, RSS, Amman, Jordan, February 1986.

[25] Risoe National Laboratory, Wind Turbine Test Vestas V27-225 kW, Risoe-M-2861, Roskilde, Denmark, October 1990.

[26] Risoe National Laboratory, Contributions From the Department of Meteorology and Wind Energy to the ECWEC'93 conference in Travemuende, Germany, Risoe-R-683(EN), Roskilde, Denmark, March 1993.

[27] Royal Scientific Society, Testing and Evaluation of the Small Stand Alone Wind Farm For Water Pumping, WP Report, RSS, Amman, Joradn, November 1988.

Appendix

ORIGINAL DATA OF THE RSS WEC TEST

ROYAL SCIENTIFIC SOCIETY
RENEWABLE ENERGY RESEARCH CENTER
AMMAN TEST SITE

TYPE OF CONVERTER : RSS TYPE-1
ORIGINAL DATA

WIND SPEED CLASS 4 - 5

EVENT NO.	10 MINUTES AVER. WIND SPEED (M/S)	U-L1 VOLT. VOLT	POWER KW	FREQ. HZ
1	4.97	95.16	.22	21.47
2	4.30	47.86	.01	10.56
3	4.66	84.69	.14	18.92
4	4.91	94.87	.33	21.36
5	4.72	40.32	.08	8.90
6	4.99	157.80	.44	35.27
MEAN	4.76	86.78	.20	19.41
STANDARD DEVIATION	.26	42.09	.16	9.47
CONFIDENCE LIMIT	.202 +/-	.932		

ROYAL SCIENTIFIC SOCIETY
RENEWABLE ENERGY RESEARCH CENTER
AMMAN TEST SITE

TYPE OF CONVERTER : RSS TYPE-1
ORIGINAL DATA

WIND SPEED CLASS 5 - 6

EVENT NO.	10 MINUTES AVER. WIND SPEED (M/S)	U-L1 VOLT. VOLT	POWER KW	FREQ. HZ
1	5.72	215.51	2.47	48.58
2	5.27	216.80	.70	48.77
3	5.85	217.24	1.47	49.45
4	5.50	217.16	.99	49.20
5	5.31	215.01	.85	48.51
6	5.12	40.03	.05	8.84
7	5.69	131.88	1.51	29.94
8	5.63	18.45	.05	4.12
9	5.73	214.63	1.07	48.32
10	5.86	174.08	.76	39.05
11	5.19	121.11	.16	27.02
12	5.89	215.16	1.75	48.56
13	5.88	47.74	.24	10.69
14	5.78	217.10	1.20	49.11
15	5.96	216.39	1.67	48.86
16	5.30	214.99	.12	47.88
17	5.46	217.48	.58	48.83
18	5.53	216.33	.33	48.60
19	5.29	215.04	.34	48.27
20	5.80	216.36	1.11	48.97
21	5.94	215.69	1.16	48.63
22	5.77	143.46	.76	32.65
23	5.92	217.39	.93	49.29
24	5.39	71.58	.16	16.05
25	5.83	216.01	1.25	49.10
26	5.86	217.77	1.68	49.58
27	5.98	76.72	.98	17.39
28	5.72	217.10	1.14	49.13
29	5.80	215.25	1.15	48.91
30	5.92	216.66	2.29	49.21
31	5.29	88.65	.17	19.78
32	5.55	43.26	.28	9.76
33	5.42	117.48	.57	26.41
34	5.56	147.42	1.39	33.40
35	5.54	63.78	.42	14.52
36	5.44	70.62	.38	16.11
37	5.96	206.07	1.53	46.55
38	5.93	163.11	2.40	37.01
39	5.43	64.05	.50	14.35

ROYAL SCIENTIFIC SOCIETY
RENEWABLE ENERGY RESEARCH CENTER
AMMAN TEST SITE

TYPE OF CONVERTER : RSS TYPE-1
ORIGINAL DATA

WIND SPEED CLASS 5 - 6

EVENT NO.	10 MINUTES AVER. WIND SPEED (M/S)	U-L1 VOLT. VOLT	POWER KW	FREQ. HZ
40	5.48	146.72	.42	32.81
41	5.69	78.12	.99	17.84
42	5.99	216.83	2.15	49.25
43	5.63	215.60	1.35	48.79
44	5.39	217.54	.78	48.95
45	5.43	216.10	1.11	48.67
46	5.38	216.57	.84	48.80
47	5.07	201.14	.09	44.60
48	5.87	147.92	1.55	33.35
49	5.87	39.62	.20	8.88
50	5.70	216.22	.86	48.53
51	5.29	170.35	.09	38.31
MEAN	5.63	164.98	.93	37.22
STANDARD DEVIATION	.26	66.56	.64	15.04
CONFIDENCE LIMIT	.927 +/-	.975		

ROYAL SCIENTIFIC SOCIETY
RENEWABLE ENERGY RESEARCH CENTER
AMMAN TEST SITE

TYPE OF CONVERTER : RSS TYPE-1
ORIGINAL DATA

WIND SPEED CLASS 6 - 7

EVENT NO.	10 MINUTES AVER. WIND SPEED (M/S)	U-L1 VOLT. VOLT	POWER KW	FREQ. HZ
1	6.31	123.78	1.56	28.00
2	6.01	216.16	3.55	49.24
3	6.65	218.74	3.56	50.44
4	6.94	218.48	4.36	50.14
5	6.59	218.45	3.37	49.89
6	6.18	218.24	2.40	50.10
7	6.50	43.81	.70	9.87
8	6.69	205.13	2.18	46.12
9	6.30	216.01	1.65	49.31
10	6.25	129.27	.79	29.13
11	6.83	58.59	.59	13.31
12	6.78	217.77	8.03	49.31
13	6.81	218.42	7.07	49.59
14	6.42	217.48	2.50	49.34
15	6.44	216.77	2.16	49.35
16	6.38	216.30	2.31	48.77
17	6.02	216.95	1.41	49.22
18	6.32	218.56	2.28	49.89
19	6.37	217.21	2.15	49.33
20	6.18	217.95	1.75	49.67
21	6.18	217.86	1.83	49.37
22	6.82	216.13	3.69	49.05
23	6.54	218.86	2.70	50.05
24	6.64	218.48	2.62	49.97
25	6.54	217.60	2.50	49.35
26	6.94	218.80	3.07	50.20
27	6.97	218.39	3.60	49.80
28	6.95	217.51	3.51	49.26
29	6.15	216.19	1.83	48.91
30	6.19	217.18	1.93	49.10
31	6.23	217.36	1.66	49.19
32	6.88	116.69	1.04	26.48
33	6.50	138.33	.80	31.20
34	6.78	216.04	2.26	49.21
35	6.73	216.92	2.94	49.09
36	6.20	137.98	.87	30.96
37	6.95	144.78	.72	32.63
38	6.49	217.01	3.07	49.22
39	6.71	218.80	3.45	50.04

ROYAL SCIENTIFIC SOCIETY
RENEWABLE ENERGY RESEARCH CENTER
AMMAN TEST SITE

TYPE OF CONVERTER : RSS TYPE-1
ORIGINAL DATA

WIND SPEED CLASS 6 - 7

EVENT NO.	10 MINUTES AVER. WIND SPEED (M/S)	U-L1 VOLT. VOLT	POWER KW	FREQ. HZ
40	6.18	218.39	2.13	49.54
41	6.75	182.61	4.40	41.35
42	6.94	216.48	3.99	49.27
43	6.89	219.00	4.40	50.11
44	6.48	217.21	3.48	49.47
45	6.88	217.71	3.63	49.38
46	6.91	216.83	4.18	49.35
47	6.60	217.01	3.90	49.16
48	6.85	217.65	3.94	49.46
49	6.60	217.01	3.61	49.30
50	6.43	217.77	3.05	49.58
51	6.16	217.33	2.54	49.41
52	6.76	218.71	4.02	49.97
53	6.71	216.57	4.88	49.04
54	6.08	218.36	2.83	49.41
55	6.07	217.36	1.73	49.30
56	6.49	187.13	2.10	42.74
57	6.32	190.23	1.32	43.21
58	6.55	189.30	1.49	43.01
59	6.15	216.16	1.51	48.87
60	6.48	162.14	1.62	36.90
61	6.11	42.46	.16	9.56
62	6.21	23.61	.07	5.26
63	6.98	96.63	2.50	22.14
64	6.84	217.24	3.92	49.65
65	6.70	122.82	1.76	27.99
66	6.04	218.33	1.79	49.60
67	6.86	218.21	3.83	49.64
68	6.99	218.04	4.67	49.40
69	6.13	216.45	2.19	49.15
70	6.42	217.80	2.60	49.44
71	6.37	61.14	.15	13.57
72	6.44	36.89	.08	8.15
73	6.92	152.49	2.51	34.84
74	6.42	103.17	.99	23.26
75	6.23	142.99	1.12	32.51
76	6.32	216.48	2.09	48.92
77	6.90	216.13	4.73	49.02
78	6.90	218.48	4.34	49.98

ROYAL SCIENTIFIC SOCIETY
RENEWABLE ENERGY RESEARCH CENTER
AMMAN TEST SITE

TYPE OF CONVERTER : RSS TYPE-1
ORIGINAL DATA

WIND SPEED CLASS 6 - 7

EVENT NO.	10 MINUTES AVER. WIND SPEED (M/S)	U-L1 VOLT. VOLT	POWER KW	FREQ. HZ
79	6.56	218.53	4.05	50.00
80	6.71	217.07	4.11	49.43
81	6.92	217.16	4.89	49.24
82	6.85	215.78	5.50	49.03
83	6.91	218.15	4.93	50.00
84	6.68	218.18	4.09	49.60
85	6.41	217.62	3.49	49.41
86	6.13	218.36	3.30	49.79
87	6.97	218.04	6.29	49.28
88	6.38	218.18	3.83	49.45
89	6.78	217.16	4.68	49.22
90	6.72	218.27	4.40	49.87
91	6.44	217.10	3.20	49.28
92	6.80	217.04	3.89	49.54
93	6.58	144.63	1.26	32.63
94	6.55	218.68	3.07	49.86
95	6.67	216.33	3.15	49.22
96	6.04	214.05	2.21	48.05
97	6.69	66.01	.56	15.05
98	6.94	216.42	3.98	48.86
99	6.68	215.48	4.38	48.86
MEAN	6.55	192.86	2.85	43.82
STANDARD DEVIATION	.29	50.19	1.51	11.46
CONFIDENCE LIMIT	2.848 +/-	.973		

ROYAL SCIENTIFIC SOCIETY
RENEWABLE ENERGY RESEARCH CENTER
AMMAN TEST SITE

TYPE OF CONVERTER : RSS TYPE-1
ORIGINAL DATA

WIND SPEED CLASS 7 - 8

EVENT NO.	10 MINUTES AVER. WIND SPEED (M/S)	U-L1 VOLT. VOLT	POWER KW	FREQ. HZ
1	7.47	218.74	11.49	50.34
2	7.48	164.43	10.21	37.49
3	7.63	178.89	5.23	40.69
4	7.99	217.57	7.92	49.49
5	7.51	218.39	7.68	49.54
6	7.41	218.12	6.95	49.57
7	7.08	46.28	.85	10.66
8	7.98	218.09	7.10	49.93
9	7.68	20.56	.45	4.77
10	7.83	195.89	4.85	44.50
11	7.21	217.21	4.88	49.39
12	7.10	217.60	4.83	49.74
13	7.56	205.01	5.95	46.89
14	7.84	217.80	9.89	49.43
15	7.06	108.33	.87	24.70
16	7.89	218.45	7.01	49.50
17	7.26	218.36	5.00	49.82
18	7.05	119.41	2.01	27.08
19	7.53	218.27	6.10	49.82
20	7.30	217.77	4.07	49.73
21	7.31	219.71	3.20	50.62
22	7.79	218.27	6.58	49.45
23	7.68	219.30	6.01	50.12
24	7.73	218.89	4.66	50.25
25	7.48	218.56	4.92	50.01
26	7.62	218.09	4.29	49.94
27	7.35	218.42	4.19	49.93
28	7.24	217.01	2.50	49.20
29	7.18	218.89	5.26	50.15
30	7.69	217.39	6.47	49.10
31	7.01	217.60	3.06	49.45
32	7.41	218.24	5.47	49.91
33	7.10	217.71	4.99	49.71
34	7.04	215.69	3.87	48.86
35	7.71	216.39	7.56	49.29
36	7.51	216.42	6.72	49.08
37	7.97	215.43	8.31	48.51
38	7.08	217.89	4.96	49.95
39	7.41	219.03	5.45	50.20

ROYAL SCIENTIFIC SOCIETY
RENEWABLE ENERGY RESEARCH CENTER
AMMAN TEST SITE

TYPE OF CONVERTER : RSS TYPE-1
ORIGINAL DATA

WIND SPEED CLASS 7 - 8

EVENT NO.	10 MINUTES AVER. WIND SPEED (M/S)	U-L1 VOLT. VOLT	POWER KW	FREQ. HZ
40	7.93	218.42	7.67	49.79
41	7.19	119.41	1.60	27.20
42	7.03	217.80	3.36	50.04
43	7.69	217.71	7.26	49.47
44	7.79	217.48	6.17	49.53
45	7.56	218.42	5.70	49.84
46	7.72	33.87	.37	7.69
47	7.46	218.18	6.77	49.53
48	7.70	217.80	7.10	49.38
49	7.08	217.04	4.99	49.27
50	7.84	218.15	7.71	49.55
51	7.02	217.07	5.18	49.20
52	7.30	217.86	4.83	49.47
53	7.08	216.72	4.65	48.99
54	7.11	216.86	2.93	49.38
55	7.03	87.21	.73	19.72
56	7.10	52.32	.99	12.04
57	7.68	218.12	7.69	49.39
58	7.35	217.33	6.05	49.29
59	7.45	217.18	6.63	49.25
60	7.37	218.27	5.23	49.91
61	7.46	217.48	6.18	48.89
62	7.97	208.59	6.45	47.66
63	7.22	186.92	2.92	42.61
64	7.48	217.83	4.61	50.00
65	7.57	165.75	4.40	37.57
66	7.71	140.12	3.34	32.31
67	7.01	162.87	2.57	37.17
68	7.94	218.04	6.60	49.76
69	7.75	218.45	5.91	49.78
70	7.89	218.01	6.98	49.61
71	7.90	217.74	7.07	49.50
72	8.00	217.68	8.59	49.51
73	7.41	217.92	6.03	49.25
74	7.07	216.72	5.05	49.54
75	7.08	217.16	5.28	49.58
76	7.08	217.16	5.28	49.58
77	7.23	218.65	4.76	50.02
78	7.08	217.80	4.24	50.02

ROYAL SCIENTIFIC SOCIETY
RENEWABLE ENERGY RESEARCH CENTER
AMMAN TEST SITE

TYPE OF CONVERTER : RSS TYPE-1
ORIGINAL DATA

WIND SPEED CLASS 7 - 8

EVENT NO.	10 MINUTES AVER. WIND SPEED (M/S)	U-L1 VOLT. VOLT	POWER KW	FREQ. HZ
79	7.14	217.18	5.30	49.22
80	7.70	216.69	7.99	49.04
81	7.46	216.92	6.94	49.09
82	7.58	218.33	7.43	49.23
83	7.48	216.66	7.22	48.98
84	7.03	217.48	5.69	49.36
85	7.12	217.92	4.75	49.75
86	7.75	217.89	8.17	49.17
87	7.60	216.95	7.50	48.35
88	7.50	49.47	.55	11.16
89	7.70	218.33	7.26	49.56
90	7.90	218.06	7.38	49.56
91	7.65	218.27	6.14	49.46
92	7.99	218.18	6.95	49.37
93	7.49	218.30	6.15	49.61
94	7.04	217.30	4.41	49.42
95	7.61	216.36	6.63	48.68
96	7.48	215.98	6.97	48.10
97	7.48	215.28	6.96	48.14
98	7.71	215.81	7.15	48.14
99	7.37	215.51	5.78	48.65
100	7.04	216.86	5.08	49.12
101	7.67	217.74	7.04	49.08
MEAN	7.47	201.09	5.52	45.72
STANDARD DEVIATION	.30	44.26	2.14	10.05
CONFIDENCE LIMIT	5.516 +/-	.963		

ROYAL SCIENTIFIC SOCIETY
RENEWABLE ENERGY RESEARCH CENTER
AMMAN TEST SITE

TYPE OF CONVERTER : RSS TYPE-1
ORIGINAL DATA

WIND SPEED CLASS 8 - 9

EVENT NO.	10 MINUTES AVER. WIND SPEED (M/S)	U-L1 VOLT. VOLT	POWER KW	FREQ. HZ
1	8.36	32.67	.50	7.46
2	8.08	218.89	8.01	49.80
3	8.15	217.86	6.88	49.72
4	8.05	188.48	2.69	43.20
5	8.37	217.95	11.37	49.58
6	8.37	218.09	7.95	50.10
7	8.75	217.95	10.33	49.49
8	8.36	217.57	7.24	49.86
9	8.12	218.74	6.32	50.28
10	8.34	219.35	8.61	49.96
11	8.13	217.42	7.74	49.36
12	8.89	218.86	8.40	49.93
13	8.41	218.30	7.48	49.74
14	8.65	217.86	7.85	49.49
15	8.12	218.45	7.73	49.68
16	8.44	217.95	8.09	49.42
17	8.81	216.36	7.71	49.37
18	8.91	218.21	10.41	49.18
19	8.50	216.92	8.47	48.93
20	8.52	217.45	8.39	49.16
21	8.78	219.00	7.66	50.08
22	8.26	218.45	6.54	49.71
23	8.78	217.80	8.26	49.73
24	8.93	218.18	10.24	49.70
25	8.32	216.72	7.35	49.08
26	8.66	218.50	8.38	49.75
27	8.11	218.27	8.01	49.62
28	8.16	217.01	9.04	48.74
29	8.32	217.51	9.03	49.04
30	8.04	218.33	8.72	49.23
31	8.92	218.77	11.14	49.46
32	8.14	217.24	9.16	49.01
33	8.27	218.01	8.77	49.36
34	8.26	217.51	10.04	49.15
35	8.09	217.48	8.52	49.31
36	8.91	219.33	9.14	49.99
37	8.14	218.09	7.49	49.69
38	8.89	218.74	8.81	49.89
39	8.10	218.18	7.49	49.62

ROYAL SCIENTIFIC SOCIETY
RENEWABLE ENERGY RESEARCH CENTER
AMMAN TEST SITE

TYPE OF CONVERTER : RSS TYPE-1
ORIGINAL DATA

WIND SPEED CLASS 8 - 9

EVENT NO.	10 MINUTES AVER. WIND SPEED (M/S)	U-L1 VOLT. VOLT	POWER KW	FREQ. HZ
40	8.33	218.06	8.74	49.48
41	8.30	218.56	7.97	49.63
42	8.20	106.45	2.97	24.13
43	8.92	203.37	5.98	46.68
44	8.89	217.95	8.94	49.56
45	8.63	217.60	9.43	49.41
46	8.35	217.16	8.18	49.35
47	8.90	216.69	10.26	49.01
48	8.85	218.36	11.87	49.18
49	8.60	218.12	9.80	49.39
50	8.20	216.83	7.78	48.97
51	8.54	216.95	9.13	48.88
52	8.54	216.69	10.72	48.75
53	8.81	216.89	11.36	48.61
54	8.62	217.95	10.01	49.30
55	8.45	217.86	9.49	49.11
56	8.86	217.83	12.00	48.91
57	8.70	219.56	10.74	49.80
58	8.48	218.68	11.24	49.50
59	8.81	219.09	9.36	49.74
60	8.43	124.05	4.67	28.09
61	8.29	219.27	7.54	49.93
62	8.11	36.80	.40	8.24
63	8.21	79.59	.88	17.99
64	8.48	197.18	4.70	45.32
65	8.03	218.18	5.05	50.26
66	8.37	218.48	6.34	50.08
67	8.34	217.39	7.96	49.64
68	8.37	217.92	8.79	49.74
69	8.18	218.33	6.44	50.06
70	8.05	218.45	5.78	49.96
71	8.06	217.45	7.68	49.52
72	8.26	218.74	8.02	49.87
73	8.64	218.15	10.55	49.48
74	8.53	216.95	10.18	49.04
75	8.66	218.01	8.29	49.67
76	8.16	217.60	9.11	49.16
77	8.43	218.15	11.15	49.20
78	8.62	217.62	10.94	49.17

ROYAL SCIENTIFIC SOCIETY
RENEWABLE ENERGY RESEARCH CENTER
AMMAN TEST SITE

TYPE OF CONVERTER : RSS TYPE-1
ORIGINAL DATA

WIND SPEED CLASS 8 - 9

EVENT NO.	10 MINUTES AVER. WIND SPEED (M/S)	U-L1 VOLT. VOLT	POWER KW	FREQ. HZ
79	8.54	218.59	10.72	49.20
80	8.64	217.92	11.67	49.28
81	8.55	218.56	8.86	49.86
82	8.94	219.62	9.41	50.02
83	8.70	218.94	8.77	49.73
84	8.55	45.34	.94	10.21
85	8.10	30.82	.45	7.03
86	8.75	218.21	9.76	49.56
87	8.81	219.03	8.19	50.03
88	8.63	218.80	7.97	49.81
89	8.35	219.00	8.19	49.84
90	8.44	218.62	9.07	49.78
91	8.39	219.00	8.92	49.81
92	8.47	217.80	9.15	49.36
93	8.24	219.00	8.09	49.89
94	8.80	218.89	8.62	49.90
95	8.97	219.47	9.62	49.99
96	8.90	217.80	9.31	49.45
97	8.77	216.77	12.28	48.39
98	8.52	217.86	9.92	49.13
99	8.19	215.87	9.25	48.06
MEAN	8.47	206.60	8.24	46.91
STANDARD DEVIATION	.28	40.55	2.48	9.22
CONFIDENCE LIMIT	8.238 +/-	.956		

ROYAL SCIENTIFIC SOCIETY
RENEWABLE ENERGY RESEARCH CENTER
AMMAN TEST SITE

TYPE OF CONVERTER : RSS TYPE-1
ORIGINAL DATA

WIND SPEED CLASS 9 -10

EVENT NO.	10 MINUTES AVER. WIND SPEED (M/S)	U-L1 VOLT. VOLT	POWER KW	FREQ. HZ
1	9.15	219.21	12.79	49.57
2	9.16	218.15	10.09	49.45
3	9.52	218.62	12.94	49.21
4	9.28	217.21	11.84	48.86
5	9.64	218.12	12.40	49.27
6	9.85	217.80	10.42	49.35
7	9.03	218.18	8.93	49.58
8	9.25	218.94	9.34	49.95
9	9.50	218.91	9.77	49.76
10	9.40	218.39	10.12	49.48
11	9.72	218.15	11.23	49.51
12	9.43	219.24	12.55	49.63
13	9.32	218.56	12.64	49.29
14	9.76	218.89	12.73	49.42
15	9.69	219.85	13.29	49.93
16	9.69	219.85	13.29	49.93
17	9.29	217.80	12.45	48.91
18	9.27	218.65	11.82	49.35
19	9.37	218.65	13.32	49.35
20	9.17	218.06	13.17	49.08
21	9.57	219.33	14.65	49.35
22	9.86	219.56	14.83	49.59
23	9.30	218.15	14.19	49.00
24	9.92	218.71	13.37	49.45
25	9.81	219.68	11.66	49.86
26	9.61	219.09	12.24	49.42
27	9.58	218.77	10.63	49.73
28	9.18	218.06	11.65	49.37
29	9.02	218.53	9.34	49.79
30	9.33	218.71	11.78	49.45
31	9.55	218.21	10.39	49.76
32	9.46	218.59	11.22	49.65
33	9.21	218.36	9.91	49.80
34	9.39	218.56	11.39	49.56
35	9.31	218.36	11.77	49.26
36	9.21	217.98	10.34	49.52
37	9.38	219.18	9.92	49.87
38	9.31	217.98	12.37	49.04
39	9.00	216.98	11.76	48.61

ROYAL SCIENTIFIC SOCIETY
RENEWABLE ENERGY RESEARCH CENTER
AMMAN TEST SITE

TYPE OF CONVERTER : RSS TYPE-1
ORIGINAL DATA

WIND SPEED CLASS 9 -10

EVENT NO.	10 MINUTES AVER. WIND SPEED (M/S)	U-L1 VOLT. VOLT	POWER KW	FREQ. HZ
40	9.63	219.38	10.67	49.86
41	9.34	218.50	11.86	49.42
42	9.20	218.48	10.90	49.54
43	9.00	218.83	9.89	49.86
44	9.75	218.65	13.94	49.31
45	9.69	219.79	13.48	49.80
46	9.63	218.68	14.66	49.29
47	9.82	218.04	13.19	49.30
48	9.80	218.42	14.23	49.42
49	9.81	218.36	11.31	49.46
50	9.84	219.27	11.50	49.71
51	9.39	219.03	10.85	49.60
52	9.25	218.89	11.91	49.46
53	9.09	219.38	6.72	50.39
54	9.48	219.30	11.10	49.74
55	9.31	218.56	11.27	49.37
56	9.38	218.56	11.59	49.51
57	9.19	219.21	9.98	49.89
58	9.16	218.83	9.37	49.91
59	9.01	218.30	8.38	49.63
60	9.93	218.86	13.37	49.35
61	9.34	218.42	10.25	49.64
62	9.41	219.27	12.25	49.71
63	9.49	218.74	11.90	49.49
64	9.25	218.21	11.35	49.39
65	9.44	218.21	12.65	49.23
66	9.18	218.50	11.59	49.38
MEAN	9.43	218.65	11.65	49.51
STANDARD DEVIATION	.25	.58	1.61	.30
CONFIDENCE LIMIT	11.647 +/-	.954		

ROYAL SCIENTIFIC SOCIETY
RENEWABLE ENERGY RESEARCH CENTER
AMMAN TEST SITE

TYPE OF CONVERTER : RSS TYPE-1
ORIGINAL DATA

WIND SPEED CLASS 10 -11

EVENT NO.	10 MINUTES AVER. WIND SPEED (M/S)	U-L1 VOLT. VOLT	POWER KW	FREQ. HZ
1	10.73	218.59	13.35	49.45
2	10.38	219.30	13.04	49.76
3	10.22	218.83	12.59	49.34
4	10.25	219.44	14.60	49.48
5	10.63	219.91	15.71	49.64
6	10.83	220.41	15.92	49.95
7	10.15	219.91	15.61	49.68
8	10.83	220.00	15.29	49.79
9	10.79	220.44	15.92	49.99
10	10.70	220.38	15.74	49.72
11	10.50	219.71	14.73	49.66
12	10.33	219.77	15.17	49.69
13	10.47	220.12	15.16	49.74
14	10.08	218.89	14.96	49.43
15	10.60	220.00	15.49	49.79
16	10.92	219.62	15.14	49.66
17	10.49	220.09	14.98	49.83
18	10.55	219.85	14.49	49.81
19	10.93	220.09	15.20	49.83
20	10.50	219.65	14.49	49.61
21	10.45	219.33	14.05	49.47
22	10.54	220.12	14.99	49.75
23	10.02	219.15	8.46	50.08
24	10.39	219.56	10.45	50.13
25	10.43	218.65	11.20	49.81
26	10.25	218.45	12.61	49.52
27	10.59	220.15	16.05	49.89
28	10.09	218.53	14.11	49.35
29	10.46	219.56	15.56	49.68
30	10.61	220.00	15.82	49.89
31	10.21	219.12	14.90	49.53
32	10.34	219.94	15.55	49.61
33	10.14	219.33	13.74	49.48
34	10.29	219.09	12.18	49.67
35	10.22	218.94	13.69	49.30
36	10.86	220.12	13.66	49.87
37	10.12	219.21	12.61	49.66
38	10.41	219.77	14.98	49.62
39	10.79	220.50	15.43	49.82

ROYAL SCIENTIFIC SOCIETY
RENEWABLE ENERGY RESEARCH CENTER
AMMAN TEST SITE

TYPE OF CONVERTER : RSS TYPE-1
ORIGINAL DATA

WIND SPEED CLASS 10 -11

EVENT NO.	10 MINUTES AVER. WIND SPEED (M/S)	U-L1 VOLT. VOLT	POWER KW	FREQ. HZ
40	10.94	219.94	15.68	49.61
41	10.43	220.35	15.94	49.80
42	10.39	220.06	15.47	49.57
43	10.34	220.12	16.05	49.98
44	10.78	219.89	15.63	49.97
45	10.11	220.00	15.82	50.02
46	10.49	220.23	15.74	49.88
47	10.89	219.79	15.14	49.81
48	10.79	220.10	15.92	50.01
49	10.91	220.34	15.78	50.01
50	10.72	220.42	15.95	49.99
51	10.99	220.11	15.23	49.88
52	10.67	220.45	15.93	50.21
53	10.77	220.22	16.03	50.04
54	10.82	220.30	16.00	50.00
55	10.79	220.14	16.01	49.99
56	10.86	220.18	16.03	50.23
57	10.11	220.32	16.00	49.90
58	10.89	220.46	16.06	50.43
59	10.55	220.35	16.03	50.33
60	10.87	220.22	16.00	50.32
61	10.59	220.11	16.03	50.12
62	10.71	220.19	16.02	50.00
63	10.55	219.22	14.96	49.88
64	10.22	218.99	14.35	49.39
65	10.76	219.88	15.18	50.10
66	10.49	220.21	15.39	50.05
67	10.44	220.01	14.22	50.22
68	10.98	219.33	15.66	50.31
69	10.59	218.99	14.96	50.21
70	10.48	219.78	15.20	50.11
71	10.75	219.48	15.48	50.35
72	10.74	220.22	15.17	50.05
MEAN	10.55	219.79	14.90	49.84
STANDARD DEVIATION	.26	.54	1.42	.27
CONFIDENCE LIMIT	14.899 +/-	.963		

ROYAL SCIENTIFIC SOCIETY
RENEWABLE ENERGY RESEARCH CENTER
AMMAN TEST SITE

TYPE OF CONVERTER : RSS TYPE-1
ORIGINAL DATA

WIND SPEED CLASS 11 -12

EVENT NO.	10 MINUTES AVER. WIND SPEED (M/S)	U-L1 VOLT. VOLT	POWER KW	FREQ. HZ
1	11.93	220.35	15.94	50.01
2	11.03	220.06	15.23	49.93
3	11.07	219.88	14.59	49.85
4	11.49	220.15	14.85	49.93
5	11.46	220.03	15.48	49.87
6	11.82	219.47	14.00	49.86
7	11.00	220.15	15.66	49.75
8	11.19	220.47	15.86	49.94
9	11.17	220.26	15.85	49.89
10	11.55	220.44	15.93	50.01
11	11.49	220.41	15.92	49.99
12	11.55	220.38	15.81	49.95
13	11.02	219.91	14.89	49.77
14	11.05	220.21	15.70	49.80
15	11.64	220.18	15.28	49.93
16	11.49	219.94	14.62	49.71
17	11.09	219.59	13.17	49.86
18	11.63	220.06	14.92	49.79
19	11.62	220.32	15.48	49.79
20	11.90	219.82	16.00	49.82
21	11.17	219.38	15.08	49.64
22	11.55	220.47	15.48	49.96
23	11.82	220.38	15.89	49.74
24	11.51	219.85	15.50	49.69
25	11.41	220.35	15.44	49.99
26	11.04	220.12	15.80	49.60
27	11.74	220.18	15.67	49.83
28	11.88	220.47	16.06	49.97
29	11.20	220.47	16.00	49.87
30	11.74	220.50	16.04	49.94
31	11.02	220.26	15.71	49.85
32	11.36	220.41	16.02	49.91
33	11.38	219.79	15.81	49.56
34	11.58	220.30	15.64	50.03
35	11.48	220.41	15.94	49.99
36	11.39	218.97	15.72	49.69
37	11.46	218.98	15.07	49.89
38	11.33	220.18	14.85	49.19
39	11.58	220.31	13.88	49.77

ROYAL SCIENTIFIC SOCIETY
RENEWABLE ENERGY RESEARCH CENTER
AMMAN TEST SITE

TYPE OF CONVERTER : RSS TYPE-1
ORIGINAL DATA

WIND SPEED CLASS 11 -12

EVENT NO.	10 MINUTES AVER. WIND SPEED (M/S)	U-L1 VOLT. VOLT	POWER KW	FREQ. HZ
40	11.23	218.77	14.13	48.59
41	11.46	220.11	14.72	49.89
42	11.78	220.33	14.49	50.01
43	11.77	219.79	14.30	50.70
44	11.71	219.99	14.21	49.88
45	11.55	220.11	14.42	50.03
MEAN	11.45	220.07	15.27	49.84
STANDARD DEVIATION	.27	.41	.71	.28
CONFIDENCE LIMIT	15.267 +/-	.969		

ROYAL SCIENTIFIC SOCIETY
RENEWABLE ENERGY RESEARCH CENTER
AMMAN TEST SITE

TYPE OF CONVERTER : RSS TYPE-1
ORIGINAL DATA

WIND SPEED CLASS 12 -13

EVENT NO.	10 MINUTES AVER. WIND SPEED (M/S)	U-L1 VOLT. VOLT	POWER KW	FREQ. HZ
1	12.46	106.30	6.26	24.21
2	12.04	220.29	15.62	50.02
3	12.98	220.50	15.85	50.04
4	12.22	220.26	15.69	50.02
5	12.04	220.41	15.95	50.01
6	12.61	220.32	15.69	49.88
7	12.03	220.32	14.98	50.00
8	12.00	220.53	15.92	49.90
9	12.96	220.38	15.93	49.73
10	12.70	220.20	14.99	50.01
11	12.34	220.13	15.41	50.21
12	12.98	220.34	15.56	49.89
13	12.31	220.41	15.92	50.10
14	12.81	220.11	15.48	50.21
15	12.48	220.19	14.87	50.00
16	12.64	220.07	15.65	50.14
17	12.79	220.00	15.82	50.21
18	12.49	220.22	15.92	50.21
19	12.15	220.35	15.92	49.98
20	12.78	220.18	15.92	50.01
21	12.34	220.26	15.69	50.04
22	12.20	220.35	16.01	50.22
23	12.13	220.29	15.92	50.30
24	12.17	220.32	16.00	49.99
25	12.45	220.11	15.99	49.89
26	12.89	220.23	16.00	50.22
27	12.66	220.17	15.99	50.04
28	12.39	220.10	16.01	50.22
29	12.87	220.45	16.02	50.32
30	12.97	220.13	16.06	50.42
31	12.48	220.11	15.24	50.31
32	12.35	220.22	15.31	49.77
33	12.59	220.18	15.07	50.32
34	12.68	219.69	15.14	50.21
35	12.69	220.29	15.17	50.22
36	12.59	220.01	15.57	49.94
37	12.68	219.69	15.15	50.09
38	12.47	219.98	15.81	50.10
39	12.68	220.32	15.56	49.88

ROYAL SCIENTIFIC SOCIETY
RENEWABLE ENERGY RESEARCH CENTER
AMMAN TEST SITE

TYPE OF CONVERTER : RSS TYPE-1
ORIGINAL DATA

WIND SPEED CLASS 12 -13

EVENT NO.	10 MINUTES AVER. WIND SPEED (M/S)	U-L1 VOLT. VOLT	POWER KW	FREQ. HZ
40	12.82	220.11	15.19	50.33
41	12.29	220.04	15.57	49.89
42	12.58	219.29	14.87	49.89
43	12.55	220.22	15.17	50.11
MEAN	12.52	217.54	15.39	49.48
STANDARD DEVIATION	.28	17.37	1.47	3.95
CONFIDENCE LIMIT	15.392 +/- .932			

ROYAL SCIENTIFIC SOCIETY
RENEWABLE ENERGY RESEARCH CENTER
AMMAN TEST SITE

TYPE OF CONVERTER : RSS TYPE-1
ORIGINAL DATA

WIND SPEED CLASS 13 -14

EVENT NO.	10 MINUTES AVER. WIND SPEED (M/S)	U-L1 VOLT. VOLT	POWER KW	FREQ. HZ
1	13.84	220.38	15.91	50.12
2	13.79	220.41	15.76	50.07
3	13.34	220.38	15.98	50.06
4	13.04	220.41	15.95	49.99
5	13.22	220.38	15.96	50.02
6	13.17	220.44	15.95	49.96
7	13.63	220.50	15.94	49.94
8	13.97	220.41	15.98	50.01
9	13.42	220.47	15.94	49.95
10	13.89	220.47	15.95	49.94
11	13.87	220.50	15.95	49.96
12	13.38	220.47	15.92	49.91
13	13.54	220.44	16.11	49.95
14	13.70	220.47	16.04	49.90
15	13.19	220.26	15.95	49.77
16	13.14	220.41	16.03	49.85
17	13.29	220.44	16.00	49.80
18	13.85	220.44	16.06	49.92
19	13.47	220.50	15.93	49.88
20	13.38	220.51	16.03	50.05
21	13.09	220.03	16.06	49.97
22	13.66	220.11	16.04	50.00
23	13.87	220.45	16.00	50.20
24	13.69	220.45	16.01	50.14
25	13.89	220.16	16.03	50.19
26	13.33	220.39	16.02	49.94
27	13.71	220.39	16.00	50.00
28	13.50	220.47	16.06	50.22
29	13.81	220.51	15.25	48.90
30	13.44	220.12	15.06	49.99
31	13.69	220.11	15.16	50.11
32	13.79	219.59	15.07	48.89
33	13.18	218.59	14.64	48.69
34	13.38	220.32	15.41	49.87
35	13.59	220.43	15.41	50.11
36	13.65	220.51	14.97	50.33
37	13.44	220.45	14.79	50.11
38	13.19	220.21	14.78	48.99
MEAN	13.53	220.32	15.74	49.89
STANDARD DEVIATION	.27	.34	.44	.37
CONFIDENCE LIMIT	15.739 +/- .977			

ROYAL SCIENTIFIC SOCIETY
RENEWABLE ENERGY RESEARCH CENTER
AMMAN TEST SITE

TYPE OF CONVERTER : RSS TYPE-1
ORIGINAL DATA

WIND SPEED CLASS 14 -15

436615

EVENT NO.	10 MINUTES AVER. WIND SPEED (M/S)	U-L1 VOLT. VOLT	POWER KW	FREQ. HZ
1	14.70	220.48	16.00	50.00
2	14.59	220.30	16.04	50.22
3	14.80	220.41	16.08	50.11
4	14.67	220.23	16.17	50.21
5	14.89	220.41	16.08	50.32
6	14.83	220.00	16.01	50.11
7	14.85	220.35	15.99	50.05
8	14.81	220.36	16.03	50.08
9	14.58	220.36	15.98	50.32
10	14.53	220.22	16.00	50.12
11	14.46	220.32	16.04	50.08
12	14.70	220.41	15.85	50.07
13	14.15	220.47	15.85	50.05
14	14.39	220.44	15.96	49.97
15	14.79	220.47	15.98	50.02
16	14.54	220.41	15.97	49.98
17	14.35	220.47	15.94	49.94
18	14.12	220.50	16.04	49.90
19	14.24	220.47	16.06	49.88
20	14.76	220.44	16.06	49.89
21	14.80	220.44	16.03	49.86
22	14.95	220.41	16.03	49.87
23	14.87	220.47	16.04	49.87
24	14.51	220.53	15.95	49.84
25	14.76	220.53	16.01	49.93
26	14.56	220.54	15.81	50.15
27	14.68	220.15	15.17	49.88
28	14.69	219.88	15.14	50.22
29	14.58	220.11	15.57	49.82
30	14.69	220.34	15.84	49.87
31	14.69	220.18	14.80	48.87
32	14.62	220.45	15.05	49.97
33	14.39	220.33	15.78	50.44
34	14.58	220.10	14.87	49.88
35	14.55	220.38	14.87	49.83
MEAN	14.62	220.35	15.80	49.99
STANDARD DEVIATION	.20	.16	.40	.25
CONFIDENCE LIMIT	15.803 +/- .977			

ROYAL SCIENTIFIC SOCIETY
RENEWABLE ENERGY RESEARCH CENTER
AMMAN TEST SITE

TYPE OF CONVERTER : RSS TYPE-1
ORIGINAL DATA

WIND SPEED CLASS 15 -16

EVENT NO.	10 MINUTES AVER. WIND SPEED (M/S)	U-L1 VOLT. VOLT	POWER KW	FREQ. HZ
1	15.50	220.40	15.56	50.01
2	15.08	220.30	15.99	50.01
3	15.89	220.27	15.97	49.99
4	15.10	220.49	16.00	50.12
5	15.69	220.89	16.08	50.12
6	15.16	220.23	15.57	50.01
7	15.79	220.38	15.92	50.21
8	15.52	220.04	15.97	50.00
9	15.17	220.51	16.04	50.02
10	15.15	220.48	15.92	49.98
11	15.78	220.34	15.92	49.88
12	15.91	220.52	15.95	50.03
13	15.05	220.38	15.99	50.07
14	15.33	220.44	16.02	49.86
15	15.09	220.41	16.04	49.87
16	15.91	220.38	16.04	49.88
17	15.37	220.47	16.02	49.84
18	15.53	220.47	16.06	49.90
19	15.62	220.59	15.97	49.86
20	15.83	220.59	15.98	49.87
21	15.66	220.29	15.81	50.33
22	15.29	220.23	15.17	50.32
23	15.84	220.19	15.19	50.22
24	15.66	220.04	0.00	50.32
25	15.49	220.15	14.59	50.45
26	15.67	219.75	14.90	48.94
27	15.61	220.36	15.74	50.23
28	15.62	220.43	14.80	49.78
29	15.69	220.41	15.41	49.92
30	15.29	220.33	15.44	49.22
MEAN	15.51	220.36	15.20	49.98
STANDARD DEVIATION	.28	.20	2.90	.30
CONFIDENCE LIMIT	15.202 +/-	.802		

ROYAL SCIENTIFIC SOCIETY
RENEWABLE ENERGY RESEARCH CENTER
AMMAN TEST SITE

TYPE OF CONVERTER : RSS TYPE-1
ORIGINAL DATA

WIND SPEED CLASS 16 -17

EVENT NO.	10 MINUTES AVER. WIND SPEED (M/S)	U-L1 VOLT. VOLT	POWER KW	FREQ. HZ
1	16.77	220.34	15.95	50.02
2	16.24	220.21	16.00	50.12
3	16.16	220.56	16.10	50.23
4	16.76	220.49	15.95	50.13
5	16.78	220.37	15.94	50.05
6	16.56	220.45	15.90	49.09
7	16.77	220.60	16.00	50.09
8	16.65	220.12	16.01	49.98
9	16.39	220.51	16.03	50.11
10	16.38	220.48	16.18	50.32
11	16.88	220.44	16.09	50.29
12	16.66	220.48	15.94	50.04
13	16.79	220.41	16.16	50.39
14	16.09	220.44	16.04	49.89
15	16.80	220.47	16.01	49.84
16	16.40	220.53	15.99	49.90
17	16.55	220.56	15.97	49.86
18	16.96	220.53	15.96	49.84
19	16.60	220.50	16.00	49.92
20	16.58	220.53	16.02	49.94
21	16.55	220.22	15.53	50.03
22	16.77	220.54	15.65	50.59
23	16.94	220.40	15.53	50.33
24	16.49	220.44	15.45	49.99
25	16.92	220.43	15.67	50.01
26	16.41	220.44	15.16	50.34
27	16.81	220.04	15.55	50.22
28	16.78	220.46	15.14	48.94
29	16.49	220.00	15.20	50.22
30	16.43	220.58	15.44	50.29
MEAN	16.61	220.42	15.82	50.03
STANDARD DEVIATION	.23	.15	.30	.33
CONFIDENCE LIMIT	15.819 +/- .979			

ROYAL SCIENTIFIC SOCIETY
RENEWABLE ENERGY RESEARCH CENTER
AMMAN TEST SITE

TYPE OF CONVERTER : RSS TYPE-1
ORIGINAL DATA

WIND SPEED CLASS 17 -18

EVENT NO.	10 MINUTES AVER. WIND SPEED (M/S)	U-L1 VOLT. VOLT	POWER KW	FREQ. HZ
1	17.71	220.39	16.01	50.33
2	17.39	220.21	16.09	50.20
3	17.89	220.49	16.00	50.01
4	17.57	220.22	16.09	50.29
5	17.88	220.33	16.17	50.31
6	17.91	220.28	16.10	50.09
7	17.48	220.42	16.11	50.13
8	17.04	220.27	16.00	50.00
9	17.39	220.26	16.19	50.27
10	17.14	220.25	16.09	50.21
11	17.77	220.33	16.19	50.19
12	17.88	220.49	16.03	50.21
13	17.35	220.28	16.08	50.11
14	17.89	220.46	16.14	50.02
15	17.13	220.00	16.09	50.01
16	17.50	220.56	15.97	49.87
17	17.96	220.56	15.93	49.78
18	17.55	220.59	15.96	49.85
19	17.56	220.56	15.93	49.80
20	17.49	220.37	15.90	50.04
21	17.88	220.59	15.65	50.03
22	17.91	220.44	15.57	50.66
23	17.88	220.41	15.65	50.09
24	17.81	220.22	15.81	49.88
25	17.49	220.31	15.81	50.33
26	17.33	220.11	15.34	50.12
27	17.77	220.51	15.62	50.09
28	17.82	220.32	15.90	50.22
29	17.75	220.30	15.83	50.28
MEAN	17.62	220.36	15.94	50.12
STANDARD DEVIATION	.27	.15	.21	.19
CONFIDENCE LIMIT	15.940 +/- .985			

ROYAL SCIENTIFIC SOCIETY
RENEWABLE ENERGY RESEARCH CENTER
AMMAN TEST SITE

TYPE OF CONVERTER : RSS TYPE-1
ORIGINAL DATA

WIND SPEED CLASS 18 -19

EVENT NO.	10 MINUTES AVER. WIND SPEED (M/S)	U-L1 VOLT. VOLT	POWER KW	FREQ. HZ
1	18.66	220.59	15.97	49.87
2	18.70	220.56	15.96	49.84
3	18.76	220.55	15.93	49.80
4	18.91	220.49	16.01	50.01
5	18.49	220.29	16.03	49.91
6	18.59	220.22	15.94	50.01
7	18.77	220.33	15.93	50.00
8	18.72	220.42	16.01	50.21
9	18.88	220.30	16.08	50.03
10	18.90	220.29	16.03	50.11
11	18.92	220.21	15.99	49.98
12	18.59	220.49	16.06	50.02
13	18.51	220.14	16.03	50.23
14	18.37	220.18	15.94	49.87
15	18.66	220.59	15.97	49.87
16	18.70	220.56	15.96	49.84
17	18.76	220.56	15.93	49.80
18	18.59	220.27	15.92	50.20
19	18.88	220.22	15.65	50.22
20	18.11	220.33	15.56	50.10
21	18.36	220.31	15.55	49.99
22	18.22	220.48	15.17	49.86
23	18.29	220.48	15.19	50.05
24	18.49	220.49	15.81	50.41
25	18.91	220.44	15.16	50.32
26	18.35	220.09	15.24	49.78
27	18.39	220.22	15.75	50.21
28	18.46	220.01	15.93	50.22
MEAN	18.61	220.36	15.81	50.03
STANDARD DEVIATION	.23	.16	.29	.17
CONFIDENCE LIMIT	15.811 +/-	.979		

ROYAL SCIENTIFIC SOCIETY
RENEWABLE ENERGY RESEARCH CENTER
AMMAN TEST SITE

TYPE OF CONVERTER : RSS TYPE-1
ORIGINAL DATA

WIND SPEED CLASS 19 -20

EVENT NO.	10 MINUTES AVER. WIND SPEED (M/S)	U-L1 VOLT. VOLT	POWER KW	FREQ. HZ
1	19.20	220.21	16.01	50.02
2	19.19	220.09	16.08	50.21
3	19.49	220.39	16.07	50.22
4	19.31	220.33	16.08	50.09
5	19.10	220.38	16.17	50.11
6	19.79	220.10	15.96	49.99
7	19.21	220.37	16.10	50.41
8	19.89	220.21	16.08	50.33
9	19.47	220.32	16.03	50.04
10	19.81	220.11	15.93	49.99
11	19.11	220.49	16.09	50.42
12	19.24	220.41	16.01	50.33
13	19.01	220.48	16.11	50.00
14	19.82	220.34	16.04	50.05
15	19.36	220.32	16.11	50.22
16	19.52	220.10	16.08	50.34
17	19.79	220.31	16.03	50.02
18	20.00	220.20	16.02	50.12
19	20.00	220.04	16.08	50.22
20	20.00	220.39	16.08	49.99
21	20.00	219.89	15.89	49.89
22	20.00	220.01	16.01	50.02
23	20.00	220.33	16.08	50.21
24	20.00	220.43	16.03	50.30
25	20.00	220.49	16.08	50.41
26	20.00	220.22	16.06	50.42
27	20.00	220.48	16.09	50.51
28	20.00	220.23	16.10	50.45
29	20.00	220.46	16.07	50.32
30	20.00	220.24	16.02	49.98
31	20.00	220.11	15.99	49.99
32	20.00	220.00	16.01	50.03
33	20.00	220.48	16.08	50.03
34	19.12	220.59	15.95	49.83
35	19.04	220.53	15.97	49.84
36	19.81	220.53	15.93	49.78
37	19.87	220.37	15.90	50.00
38	19.59	220.44	15.53	50.22
39	19.35	220.32	15.45	49.88

ROYAL SCIENTIFIC SOCIETY
RENEWABLE ENERGY RESEARCH CENTER
AMMAN TEST SITE

TYPE OF CONVERTER : RSS TYPE-1
ORIGINAL DATA

WIND SPEED CLASS 19 -20

EVENT NO.	10 MINUTES AVER. WIND SPEED (M/S)	U-L1 VOLT. VOLT	POWER KW	FREQ. HZ
40	19.59	220.71	15.81	50.33
41	19.22	220.43	15.53	49.78
42	19.23	220.11	15.57	49.87
43	19.41	220.49	15.82	48.78
44	19.77	220.59	15.92	49.98
45	19.44	220.38	15.81	50.22
46	19.24	220.58	15.90	49.39
47	19.18	220.61	15.84	49.39
48	19.49	220.32	15.48	50.31
49	19.89	220.11	15.50	50.11
MEAN	19.62	220.33	15.95	50.07
STANDARD DEVIATION	.35	.18	.19	.30
CONFIDENCE LIMIT	15.951 +/- .992			

«فحص واداء عنفة توربينية هوائية مصنعة محليا مـن الالياف الزجاجية»

اعداد : اسحق علي صالح
اشراف : د. سعد الحبالي

لقد جلبت طاقة الرياح في السنوات الاخيرة اهتماما كبيرا كواحد من البدائل لمصادر الطاقة في الاردن. ولقد كانت معظم نشاطات البحث والتطوير المحليين في هذا المجال موجهة لاستكشاف وتطوير او تحسين اداء انظمة طاقة الرياح المستورده. وعند الاطلاع على الابحاث السابقة والتي بمجملها نظرية فقد حان الوقت لوضع الاسس العملية لربط العمل العلمي المحلي بالصناعة المحلية وذلك لخلق تكنولوجيا يمكن الاستفادة منها لزيادة حجم المشاركة في صناعة طاقة الرياح الناشئة في الاردن لا محالة .

من اجل قيام صناعة لطاقة الرياح في الاردن فلا بد من وجود قاعدة صناعية تتعامل مع هذه التكنولوجيا. ويوجد في الاردن مئات من الصناعات المختلفة ولكن لا يوجد مصنع واحد متخصص او يتعامل بمكونات انظمة طاقة الرياح. لذا فان هنالك حاجة ملحة وسوف تعالج من خلال هذه الدراسة لوضع الاسس لطريقة التصنيع والقدرات المحلية لانتاج عنفات المراوح المصنوعة من الالياف الزجاجية المقواه بالغراء البلاستيكي بالاضافة الى تحديد وتعريف العناصر الرئيسية لهذه التكنولوجيا والتي ستكون مطلوبه من السوق المحلي.

تم في سياق هذه الدراسة اعطاء لمحة موجزة عن الديناميكا الهوائية لعنفات المراوح لتعريف وتحديد المتغيرات المختلفة التي تتحكم في تصميم العنفات. وبمساعدة برنامج كمبيوتر متخصص، تم اجراء معالجة وحسابات ديناميكية هوائية كاملة للتصميم المقترح. وتم ايضا وبمساعدة برنامج وكمبيوتر متطورين عمل نموذج بالابعاد الثلاثة ومن ثم اجراء حسابات الاجهاد وقدرة التحمل باستخدام طريقة العنصر المحدود والتي بواسطتها امكن عمل محاكاة حقيقية للعنفات وتصرفها تحت الاحمال المختلفة. ونتيجة لذلك تم تحديد الشكل النهائي للعنفات ومن ثم بناء نموذج خشبي بالحجم الكامل .

وقد تم اثناء هذه الدراسة تحديد شركة صناعية اردنية لهذا الغرض بحيث نجحت في التعامل مع هذه التكنولوجيا وحسب الطريقة التي وضعت قامت الشركة بانتاج عنفة متطورة ذو جودة عالية من الالياف الزجاجية بطول خمسة امتار. وقد اجتازت العنفة فحص الاجهاد حسب برنامج معد مسبقا، وعند تركيب ثلاثة من العنفات على مروحة لتوليد الطاقة الكهربائية ومربوطه على شبكة الكهرباء الرئيسية فقد عملت العنفات باداء جيد وبقدرة عالية وحققت كفاءة وصلت الى ٢ر٤١٪ .